The University of Edinburgh
Student Rocketry Team

Darwin II: The Supersonic Endeavour

Team 9 Project Technical Report to the 2021 EuRoC

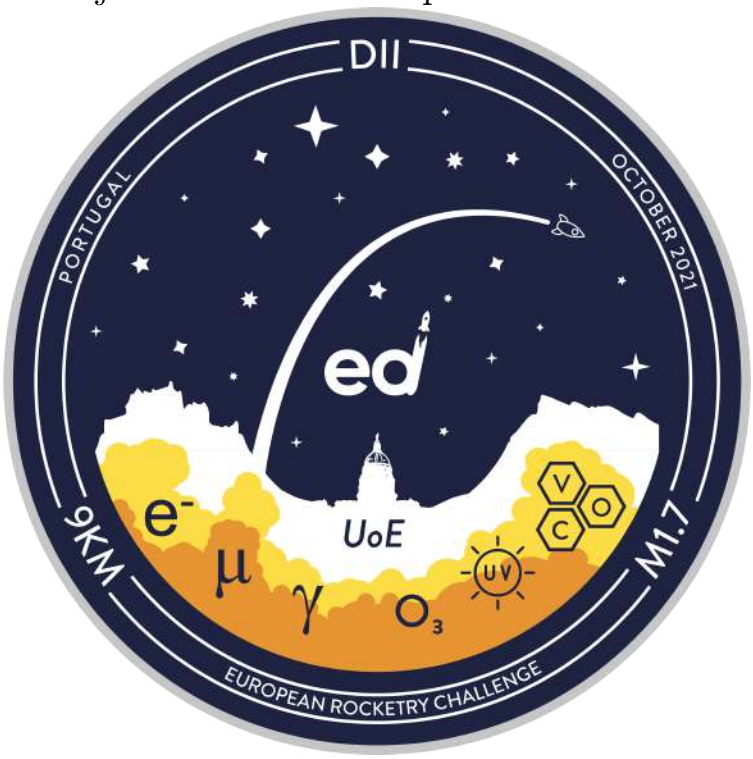

September 5, 2021

Abstract

The aim of this technical report is to describe the design, validation, optimization, and key system implementation of Darwin II (DII) from endeavour. DII will mark the first participation of the team in EuRoC and the first ever supersonic rocket made by the team. The rocket features innovative technologies which will help develop a solid platform to base our next rockets. Some of the key systems are: a carbon composite fuselage, active air brake recovery, modular avionics bay fuselage, and a deployable payload. This report introduces the structure of endeavour and Darwin project and outlines the main stakeholders. Then, the different system architectures are discussed, focusing on the propulsion, structure, recovery system, payload and airbrake. Each section describes the systems in more detail and highlights key features. Afterwards, a holistic view of the mission is given. Major milestones, improvements, and lessons learnt are discussed in conclusion.

Acknowledgements

We would like to thank The University of Edinburgh for their support. Their financial support enabled team activities, the mechanical lab manufactured vital components for Darwin II, and the advise of the staff members were very helpful in improving our design. We would like to specifically mention Dr. Francisca Martinez Hergueta, Dr. David Garcia Cava, Dr. Jeff Steynor, Kristina Tamane, the G.20 staff, the Student Led Initiatives Support committee, and Iain Gold for their advice and support for the team.

While not a part of the team, we would like to acknowledge and thank Liam Foley and Gustav Ramner for their hard work on the MEng project that we have referenced in this report. Their work has played a key role in design of Darwin II.

We are also very grateful for our sponsors; Cirrus Logic, RS Grass Roots, nTopology, Ansys, Dassault Systèmes, M-Carbo, The Institute for Research in Schools (IRIS), and playerdata for their support. Whether it was an in-kind or financial support, they have enabled us to design, simulate, and manufacture Darwin II. In particular, Charles Simpson from Alternum gave us unique insights and advice as an experienced rocketeer and helped us improve our design.

We would like to thank Portugal Space, Município de Ponte de Sor, and the wonderful team at EuRoC for hosting and organising this competition. It is an exciting event that gives us a chance to launch Darwin II and meet other rocketeers. We can't wait to be in Portugal!

Finally, and perhaps most importantly, we would like to thank our members for their dedication throughout the years. This rocket and the team wouldn't have happened without them.

Contents

List of Abbreviations

BP - Black Powder

CFD - Computational fluid dynamics

CFRP - Carbon fibre reinforced polymer

CNC - Computer numerical control

COTS - Commercial off the shelf

DoF - Degrees of freedom

EMC - Environmental Monitoring Cluster

FC - Flight computer

FEA - Finite element analysis

FoS - Factor of safety

GFRP - Glass fibre reinforced polymer

GPS - Global positioning system

HDPE - High-density polyethylene

LOS - Line of sight

PCB - Printed circuit boards

RF - Radio frequency

RFC - Recovery flight computer

SARA - Scottish Aeronautics and Rocketry Association

SHSS - Shoulder Head Socket Screw

SRAD - Student research and developed

STEM - Science, technology, engineering, and mathematics

TD - Tender descender

Nomenclature

ρ	Density [kg/m^3]
σ	Stress [Pa]
a	Acceleration [m/s^2]
C_D	Drag coefficient [-]
F	Force [N]
g	Gravitational acceleration [m/s^2]
m	Mass [kg]
P	Pressure [Pa]
R	Combustion Gas Constant [ft lbf/lbm°R]
r	Parachute area [m^2]
r	Parachute radius [m]
T	Combustion gas temperature [°R]
v	Velocity [m/s]

1. Introduction

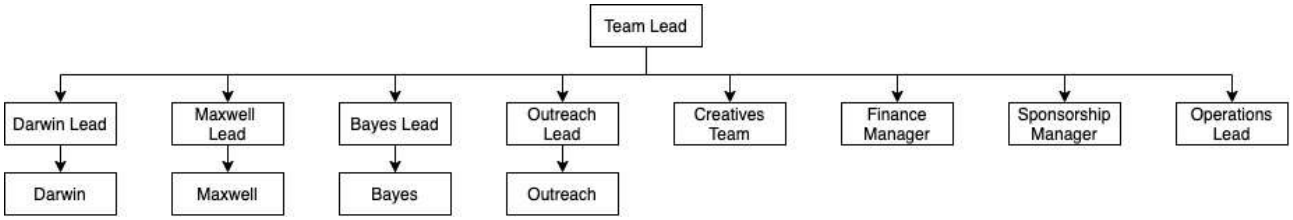

Figure 1.1: Endeavour team structure.

Endeavour is the student rocketry team at The University of Edinburgh. There are three technical projects: Darwin, the sounding rocket project, Maxwell, liquid engine project, and Bayes, thrust vector controlled vehicle project. In addition, there are two non-technical teams working on outreach and creatives. The outreach team goes to local high schools and wider audiences and does workshops on rocket science and STEM. The creatives team narrates the journey to space from the student's perspective through various mediums. The management team (team lead, finance manager, outreach lead, media and sponsorship lead, technical leads, operation lead) oversee the various aspects to lead the five projects and integrate them under the roof of endeavour. Through effective communication and teamwork, the team has grown exponentially over the past two years. There are 43 members with around half of the team dedicated to the Darwin team. Around 16% of the team is in the Maxwell team, and Bayes make up about 6% of the team. A similar percentage of the members are in the Outreach team, and 9% of our members are in the creatives team.

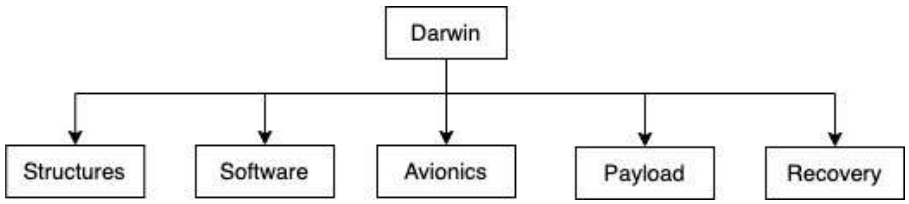

Figure 1.2: Darwin team structure.

Endeavour is composed of students from different degree programs in The University of Edinburgh. The majority of the team is from the School of Engineering and studies either mechanical engineering or electrical and electronics engineering. The team also have members from the School of Informatics, School of Physics, School of Chemistry, and School of Mathematics, with students studying computer science, physics, chemical engineering, and mathematics. In addition, some of these members are from Herriot-Watt University and Fife College, two local higher education institutions in Edinburgh, and one member has recently completed a modern apprenticeship in CNC machining.

With these team members from a variety of backgrounds, endeavour aspires to advance the British aerospace industry from the grassroots level and allow students to experience the aerospace industry during university, especially since The University of Edinburgh does not yet have an active aerospace department.

Our biggest supporters are The University of Edinburgh and various industry partners. In addition to financial support, the advice from experienced staff and technicians from the University has been invaluable in improving the design of Darwin II. The industry partners offer financial support and provide access technologies and other industry players that would not otherwise be available. The United Kingdom Rocketry Association (UKRA) and the Scottish Aeronautics and Rocketry Association (SARA) were also able to offer support with advice on various regulations and matters surrounding amateur rocketry in the UK.

All CFRP components were gifted to the team by M-Carbo Composites, who are based in Belarus. This allowed us to have industry-standard composite components that ensured the structural integrity of the rocket. nTopology, Ansys, and Dassault Systemes allowed us to design, simulate, and optimise our design through valuable software. RS GrassRoots supported the manufacturing and assembly process with various tool kits, and Cirrus Logic gave financial support that enabled various technical and logistical activities. IRIS has gifted a particle detector to use in Darwin II's payload, and playerdata have offered advice and support to the payload team. While the support from various stakeholders and sponsors has been helpful, there were many challenges faced during the design and manufacture of Darwin II. COVID-19 has brought many logistical challenges and restrictions in meetings and manufacturing of the vehicle. It caused significant delays and longer lead times in machining, acquiring components, and assembly. The team has therefore spent the past year improving the rocket's design, ensuring that all necessary health and safety regulations are met whilst planning the manufacturing processes.

Figure 1.3: Team sponsors.

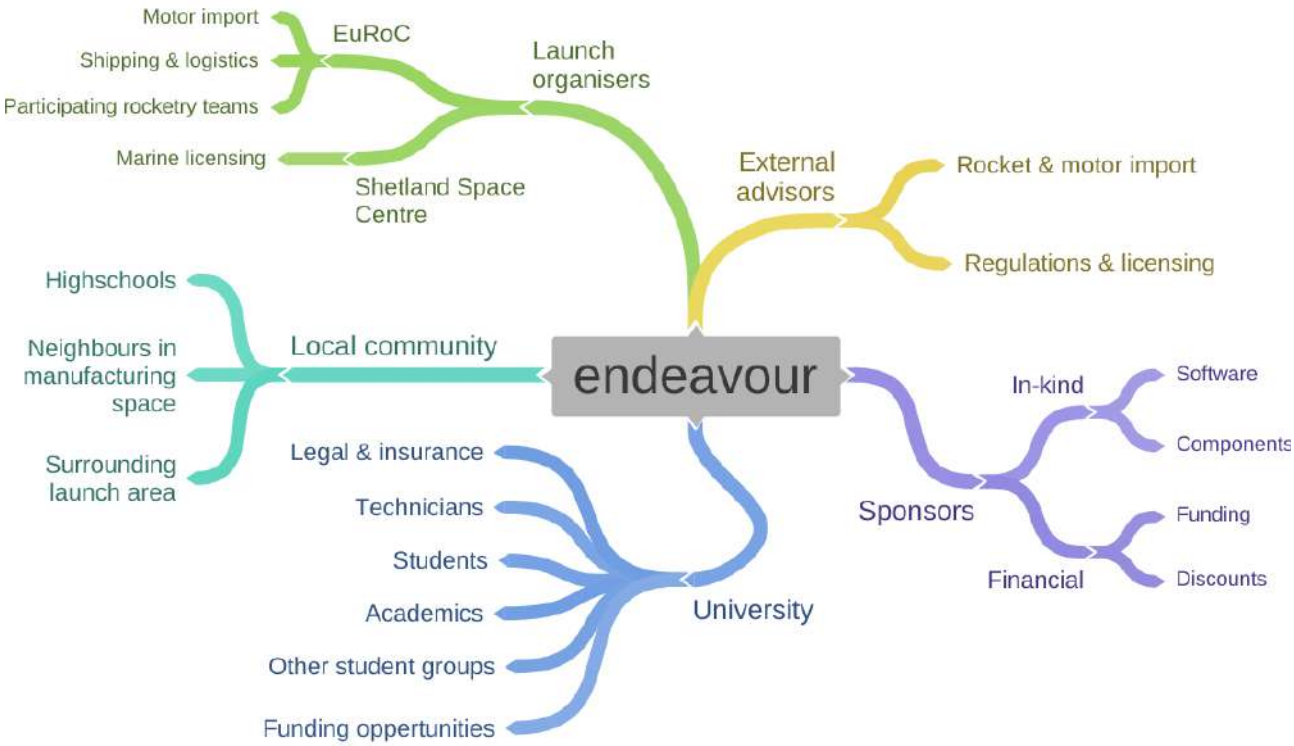

Figure 1.4: Team stakeholders.

2. System Architecture

2.1 Overview

Darwin II is endeavour's second sounding rocket design. It is designed for a 9 km apogee, and travels in the supersonic flight regime. The final length of the vehicle is 2.66 m, with a total mass including motors of 35.5 kg and a 156.4 mm (6 inch) outer-diameter with 2 mm wall thickness. The fuselage is made up of carbon-fibre-reinforced polymer (CFRP), except for the radio frequency (RF) windows located at the avionics bay and the nose cone, which are made out of glass-fibre-reinforced polymer (GFRP). The aft cone is additively manufactured from 3D printed continuous carbon fibre. The bulkheads are aluminium 6082-T6 and many non-structural components are 3D-printed with PLA. A student research and developed (SRAD) airbrake system made up of aluminium and high-density polyethylene (HDPE) allows for the manipulation of the drag generated after motor burnout and better target the predicted apogee. Darwin II employs a dual deployment system, where separation and drogue chute deployment occur at apogee at the nose cone using CO_2 charges, and the main parachute is deployed at an altitude of 500 m using a tender descender. The recovery system will be described in more detail in Section 2.4.

The flight computer (FC) of Darwin II, named Major Tom, is comprised of three PCBs. The first board, as shown in Figure J.2, holds the two Raspberry Pi's for two cameras. The second board (Figure J.3) acts as a SRAD flight computer and holds the sensors, switches, outputs for the airbrake and recovery, and sensory status indicators. The third board (Figure J.4) is used to mount the telemetry components, a GPS module, commercial off the shelf (COTS) redundancies, and the camera that will be recording the outside during flight. Major Tom communicates with the ground control over RF for initialisation at launch and data transmission during flight and recovery. The sensors communicate with the central microcontroller (Teensy 4.0) through SPI protocol and measurements are filtered with a Kalman filter for more accurate data. See Figure I.1 for a detailed software architecture, the different phases, and the conditions that defines each of the phases.

Darwin II's scientific payload is a deployable body that ejects at apogee and houses its own recovery system. It takes the form of a CANSat, housing the scientific instruments and a 1U CUBESat structure housing telemetry and recovery subsystems. The CANSat collects environmental data as well as the incidence of high-energy particle activity throughout the atmospheric column. Section 2.5 covers the detailed structure, avionics, and other relevant information related to the payload.

2.2 Propulsion Subsystem

Engine Design

The first major step in Darwin II's design process was in selecting an appropriate motor: this decision prescribes the thrust available throughout the flight, and therefore imposes restrictions on the rocket's overall mass, aerodynamic properties and structural integrity, which are required in order for the rocket to reach its target apogee of 9 km. Since Darwin II is being entered into the COTS Solid Propellant category, only motors of this type were considered in the design process. For additional simplicity, only motors easily obtainable through the EuRoC competition were considered, and thus various motors from Cesaroni's Pro98 line of reloadable rocket motors were looked at. Figure 3.1 shows a cross-sectional view of the Cesaroni's Pro98 21062O3400-6GXL rocket motor casing, for which Darwin II's lower body is designed to integrate with.

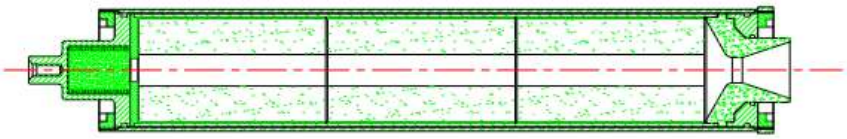

Figure 2.1: Rocket motor casing cross-section.

Propellant

The motor selected (21062O3400-6GXL) uses the Imax propellant, which packs the maximum total impulse in a given motor envelope (hence the name). The total impulse of Imax reloads is around 10-1%5 higher than that of any other reload in the same motor hardware. Imax reloads feature a large flame with a hint of green and a large volume of dense smoke. Despite not having the highest specific impulse on the market, it has a higher density compared to other propellants available. Therefore, the O3400 has a considerable total impulse.

Impulse

Following simple OpenRocket analysis during the early stages of design, and based on existing similar rocket designs, it quickly became clear that a high thrust, high impulse motor, from either the top range of the N class (total impulse of 10,240.01–20,480 Ns) or low range of the O class (total impulse of 20,480.01–40,960 Ns) was required. Figure 2.2 shows a comparison between the thrust curves of two such motors: Cesaroni's 21062O3400-P and 20146N5800-P, both of which provide sufficient thrust for Darwin II's design to exceed its target apogee under simulated conditions.

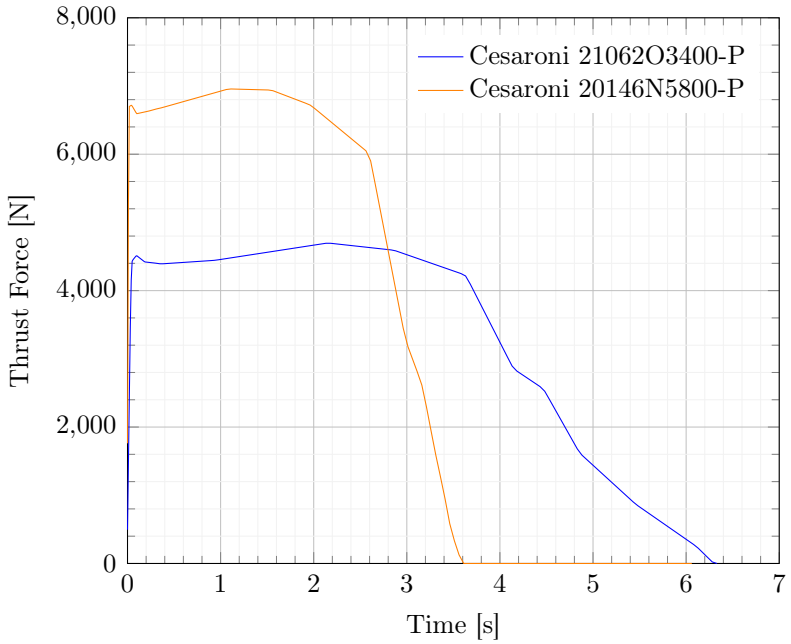

Figure 2.2: Rocket motor thrust curve comparison.

Ultimately, the Cesaroni 2106203400-P has been selected as Darwin II's first choice motor. Its lower peak thrust compared to the 20146N5800-P results in a reduced risk of failure caused by stresses on the motor mounting assembly due to this load. The chosen motor also takes longer to reach this peak force, resulting in less of a shock load being applied, and ultimately lower inertial forces on the rocket's body due to the lower acceleration caused by the reduced thrust force.

Arming and Ignition

As a COTS motor, no special arming and ignition sequence is necessary. The manufacturer introduces the use of an e-match connected at the bottom of the motor (nozzle), which can then be ignited remotely once everyone is within a safe range from the rocket, as per EuRoC's launch system layout. Once the e-match is activated by an electrical signal, the solid propellant of the rocket engine starts its combustion, accelerating the air and propelling the rocket to the sky.

2.3 Aerostructure Subsystem

2.3.1 External

Carbon Fibre Components

Early on in the design process, the decision was made to use CFRP as the primary material in the rocket's airframe. CFRP's high strength-weight ratio make it an obvious candidate for use in the rocket's airframe. Following the in-house manufacture of a roll-wrapped CFRP tube for endeavour's first sounding rocket design, Darwin I, and the various challenges that this presented without access to suitable industrial equipment, the decision was made to outsource the manufacture of Darwin II's CFRP components. The manufacture of the CFRP airframe and motor-mount sleeve used in Darwin II was carried out using state-of-the-art filament winding technology, with a winding angle of 15° as per manufacturers' recommendations, to provide the best compromise between strength under axial and bending loads.

All flat CFRP components (fins and their relevant connectors) have been manufactured using sheets of CFRP consisting of a 3k tow, which have then been precision manufactured using a CNC cutting process. The resulting components from these processes are shown in Figure 2.3.

(a) (b)

Figure 2.3: Filament wound CFRP (a) motor mount tube and (b) body tube alongside sheet CFRP fins, images courtesy of M-Carbo.

RF Transparent Sections

One of the biggest disadvantages of using a CFRP fuselage is the lack of radio frequency transparency: the carbon fibres in the matrix conduct electricity and cause the fuselage to act as a Faraday cage, thus preventing the passage of radio waves through it. To solve this issue, the parts of the fuselage that contain radio frequency transmitters, or signal emitters, are made of GFRP. Glass fiber does not conduct electricity and therefore allows RF signals to pass through. The sections with RF transparency can be seen in Figure 2.4. The RF transparent sections make up a 3-sided fuselage, used in the

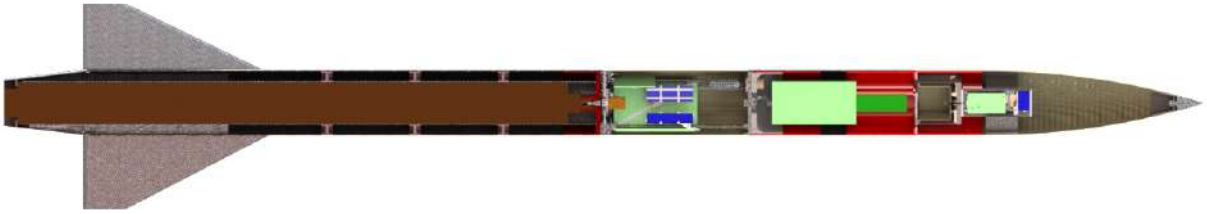

Figure 2.4: Cross section of Darwin II, black fuselage representing CFRP and the yellow one for GFRP (RF transparent)

electronics bay, manufactured using wet layup glass fibre, and the nose cone, manufactured using a continuous fibre 3D print with a blend of kevlar and glass fibre. To ensure there is no interference, both RF transparent sections are at least two body diameters in length.

2.3.2 Internal

Section Interfaces

The rocket can be divided into three main sections:

- A lower section containing the motor, fins, aft cone, motor sleeve, centering rings and motor bulkhead.
- An electronics bay: which holds all electronics components, the air brakes system, the fuselage (including three rods for structural strength), recovery bulkhead and recovery activation systems.
- Nose cone and payload.

The three main interfaces are highlighted in red in Figure 2.5. Starting from the aft end of the rocket, there is the motor bulkhead, a machined part from aluminum 6082-T6, optimized for weight reduction and stiffness. It interfaces with half of a body-diameter of the lower fuselage and is secured to the fuselage through 12 M3 bolts. A machined groove for the attachment and centering of the motor sleeve is included, as well as a shoulder for the top of the motor.

Figure 2.5: Render of Darwin II with transparent fuselage. The three interfaces are highlighted in red.

Figure 2.6: Avionics bay and nose cone assemblies. Highlighted in red are the interfaces. The two green cylinders in the middle represent the parachutes.

There are three threaded steel rods screwed to the motor bulkhead that carry the rocket's structural loads through the avionics section, as shown in Figure 2.6. Moving forwards, the three rods are bolted to the machined aluminum 6082-T6 recovery bulkhead. A body-diameter long coupling tube is glued to the bulkhead for additional interference. It also includes a 3D printed extension to increase the bonded surface between the bulkhead and the coupling tube. The recovery fuselage, where the parachutes and lines are stored, is glued permanently to this bulkhead assembly and reinforced with 6 M3 bolts.

The last interface is between the recovery fuselage and the nose cone-payload assembly. As this is the only section of the rocket that separates for recovery deployment, the stiffness and integrity of this is a priority for the safety of launch and a successful recovery. For this reason a conventional coupling tube has been employed here, extending a full body-diameter to either side of the separation point. This coupling tube can be seen on the right of Figure 2.6. It is bonded with epoxy to the CFRP recovery fuselage, making a solid piece with the recovery bulkhead which is also glued to the fuselage. The coupling tube is held to the nose cone with 4 M2 Nylon shear pins, which will break once the CO_2 canisters have been fired, separating the nose cone and deploying the drogue parachute. More detail about the interfaces between the Payload and the Nosecone can be found in Section 2.5.

Motor Retention and Load Transfer

The motor has a positive retention mechanism to prevent failure and release from the rocket. A 3/8" Shoulder Head Socket Screw (SHSS) screws into the motor through a centre hole in the motor bulkhead. The SHSS is used to locate and secure the motor, and is not responsible for the transfer of the thrust force to the motor bulkhead. The motor also has a relatively snug fit inside the motor sleeve which will help to stop unwanted rotation of the motor when being handled.

The motor must be secured in place using a motor casing. The casing is made from filament-wound CFRP to provide a strong, lightweight part. There are 3 equispaced centering rings located across the motor sleeve to keep the casing in line with the outer body of the rocket, as seen in Figure 2.7. These will help distribute the lateral forces on the airframe as well as the motor bulkhead by keeping the motor centered. There are also three sets of connectors on the motor sleeve for fin attachment, and will pass through the body tube to lock the rotation of the motor sleeve. These connectors will then be further strengthened by laying up GFRP on the connectors and the interfaces with the outer tube to ensure no movement of the fin root. In addition, the fins and fin attachments also help with centring the motor as the fins pass through the lower body. The combination of these securing techniques provides a solid mount for the motor as it is fixed axially, laterally and vertically.

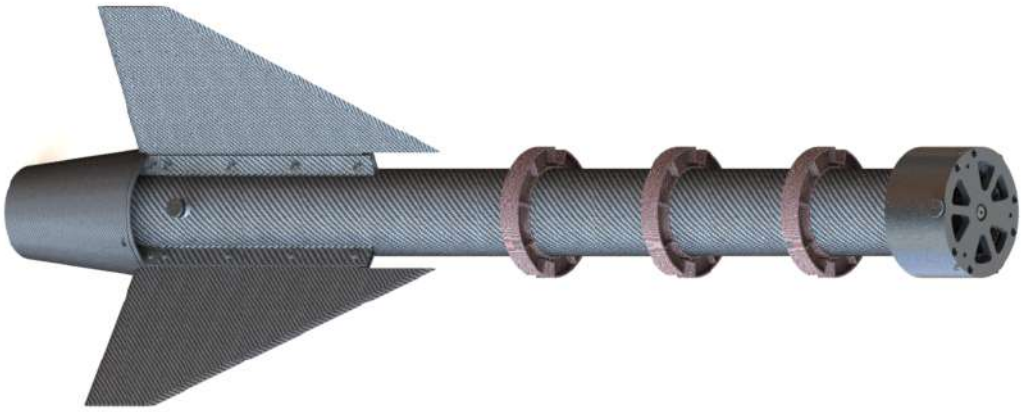

Figure 2.7: Render of the lower section of Darwin II with the fuselage being suppressed to see the internal structure

Near the bottom of the motor there is a 'lip' which has a larger diameter compared to the rest. This lip will provide a surface for the thrust to be transferred. The motor sleeve extends all the way from the lip to the motor bulkhead to allow thrust transfer. This single continuous part will distribute the loads over a large area of the motor bulkhead and take away the loads from the SHSS.

Mechanical connections

Motor SHSS: the motor SHSS is not a structural connection and is only there to retain the motor and to stop it falling from the rocket. It is 3/8" in diameter and secured through the motor bulkhead.

Recovery/motor bulkhead structural rod connections: there are three 8mm rods that run from the motor bulkhead through the avionics bay to the recovery bulkhead. They are 120 degrees apart, as shown in Figure 2.8. The rods screw into the motor bulkhead, secured using brackets that tighten onto the the rods, and bolted with nylon lock nuts that secure the rods to the recovery bulkhead. These structural rods are used to transfer some the thrust of the rocket rather than relying on just the fuselage of the rocket to handle these large thrust forces.

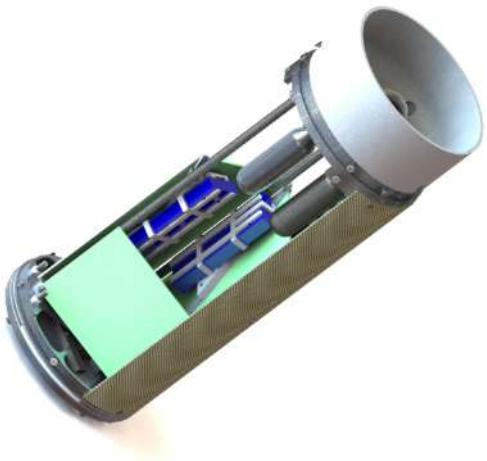

Figure 2.8: Render of the avionics bay. Motor bulkhead on the bottom, one of the avionics bay fuselage section in between, and the recovery bulkhead on top. Light green components represents the PCBs, blue for batteries, and dark grey for CO_2 canisters

Recovery bay eyebolt: the recovery bay eyebolt will have to withstand the force of a sudden decelerating rocket at apogee. It should slow the descent of the rocket from 30 m/s to 7 m/s in a short amount of time. The recovery bulkhead is 8 mm thick, but if a small diameter connection is used, then the force would be concentrated onto a small area and cause failure. Therefore, an M10 eyebolt is used as it provides a greater area for the force to act over.

Rail guides: the rail guides are secured tangentially to the body tube. The upper rail guide attaches to the motor bulkhead, and the lower rail guide uses a small block inside the body tube to mount onto. The lower guide will have to rely on the strength of the body tube and it transfer of loads to the motor sleeve, motor bulkhead and rest of the rocket. The upper guide has a more secure attachment compared to the lower guide as some of the forces will be directed to the bulkhead. However, the lower rail guide does not need as solid of a connection since lower rail guides typically have less forces acting on them.

Flanges: the flanges are used to give extra material for the screws to embed into, as well as an overlap for connecting coupling tubes and body tubes. The flanges allow the potential lateral forces on the tubes to be spread over a larger area. If they are too short, the body/coupling tubes can act as a lever and introduce large stresses into the airframe. In the motor bulkhead there is a large flange projected to the aft end that allows two rows of offset screws to be placed to secure body tube in place. If no flange were to be used, the bulkhead would have to be thickened to allow for a suitable mounting points for the screws. However, the flange allows the thickness of the bulkhead to be reduced and only extend the perimeter that comes into contact directly with the fuselage.

Another benefit that flanges has is that it provides a suitable surface to line up the body tube. For example, the body tube for the upper section of the rocket will slip over the flange and will then be screwed into position. The extra surface area that the flange provides for the body tube helps to spread any forces more evenly over the body tube interface, as well as providing a greater seal for the recovery sequence.

2.3.3 Numerical Analysis

Trajectory simulations

To validate that Darwin II's design is capable of exceeding its target apogee with the chosen motor and airframe design described above (including budgeted masses for payload, recovery and avionics subsystems), flight trajectory simulations were performed and compared using two pieces of software: OpenRocket and RASAero II. OpenRocket beneftis from a superior UI and integration of optimisation features, which were utilised throughout the design process. However, in the supersonic regime, which Darwin II is expected to reach, OpenRocket suffers from poorer accuracy as a result of various simplifying assumptions used in its calculation of drag.

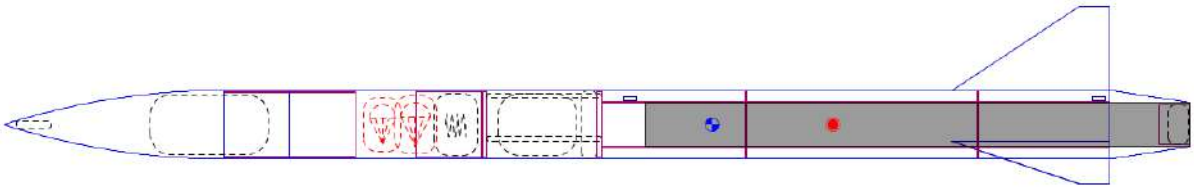

(a)

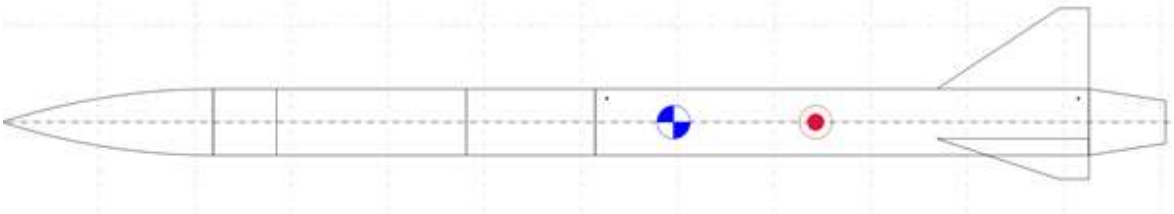

(b)

Figure 2.9: Darwin II schematic in (a) OpenRocket and (b) RASAero II.

Compounded with other factors, such as little previous launch experience within the team, as well as high sensitivity of the simulations to factors such as surface finish and centre of gravity, it is clear that there is going to be a considerable inherent level of error in any simulations carried out in both OpenRocket and RASAero II. As such, the results of these simulations are used merely as a guide for predicting the rocket's apogee, with the aim of "fine-tuning" this prediction actively throughout the rocket's flight using an actively controlled airbrake system, discussed in more detail in Section 2.6.

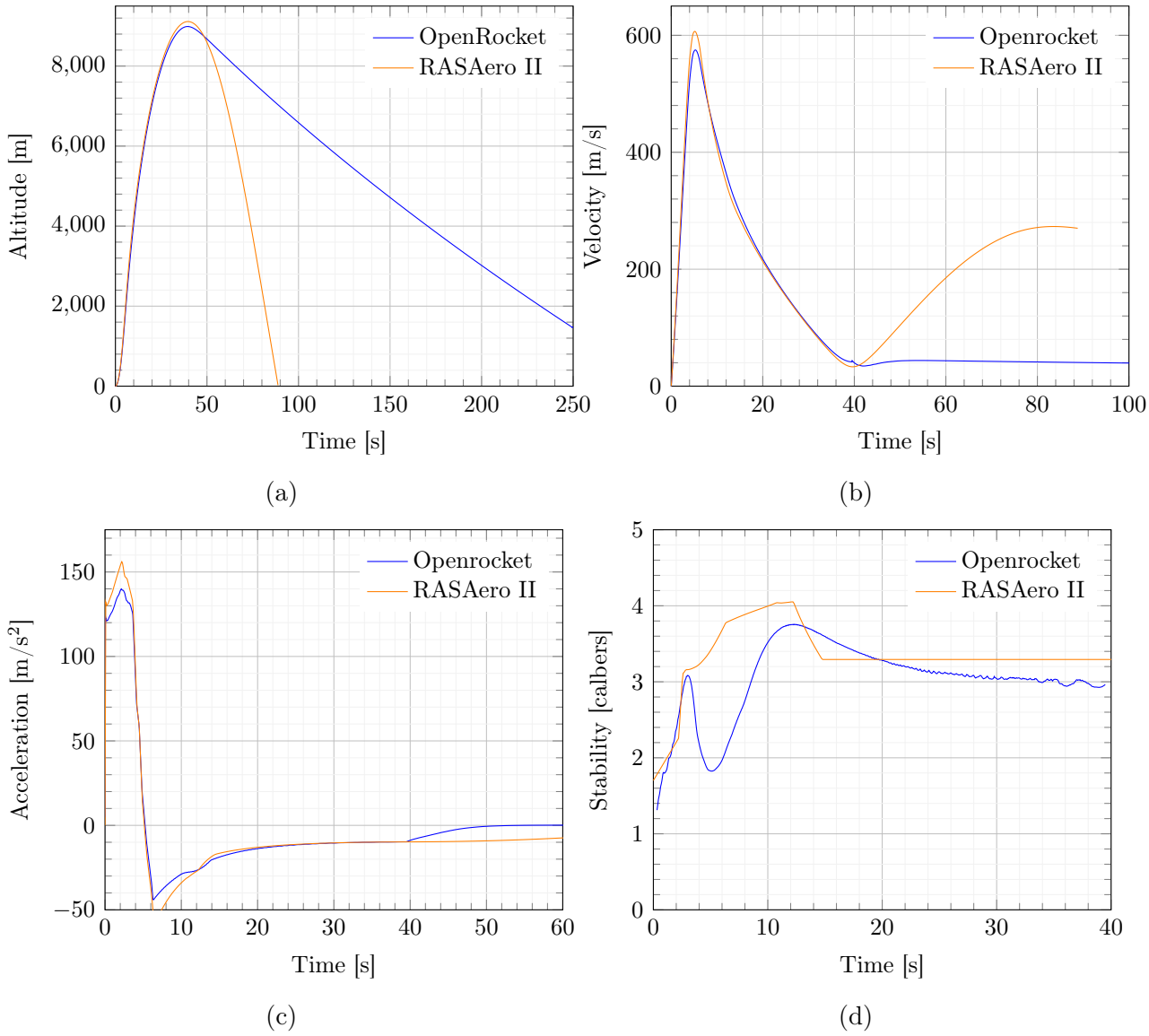

Figure 2.10: Comparison between OpenRocket and RASAero II simulated (a) altitude, (b) velocity, (c) acceleration and (d) stability over duration of flight. Note, RASAero II does not include recovery system, hence the large discrepancy in results following apogee.

A summary of the key results of these simulations are given in Table 2.1.

Table 2.1: Key trajectory simulation results.

Parameter	**OpenRocket**	**RASAeroII**	**Units**
Apogee	9,044	9,112	m
Max. velocity	575	604	m/s
Max. acceleration	141	156	m/s^2
Stability off rail	1.8	2.0	-

The above simulations are carried out assuming the rocket is launched at an angle of 84° pointing upwards from the horizontal. They also incorporate a simple wind model, assuming an average wind speed of approximately 3 m/s, a reasonable value for October in Ponte de Sôr, with a standard deviation of 0.3 m/s and a wind direction that is parallel to the horizontal. However, in order to better understand the influence of wind speed on the overall trajectory of the rocket, a simple sensitivity

analysis was carried out in OpenRocket for a range of wind speeds, ranging from 0 to 6 m/s, the results of which are presented in Figure 2.11

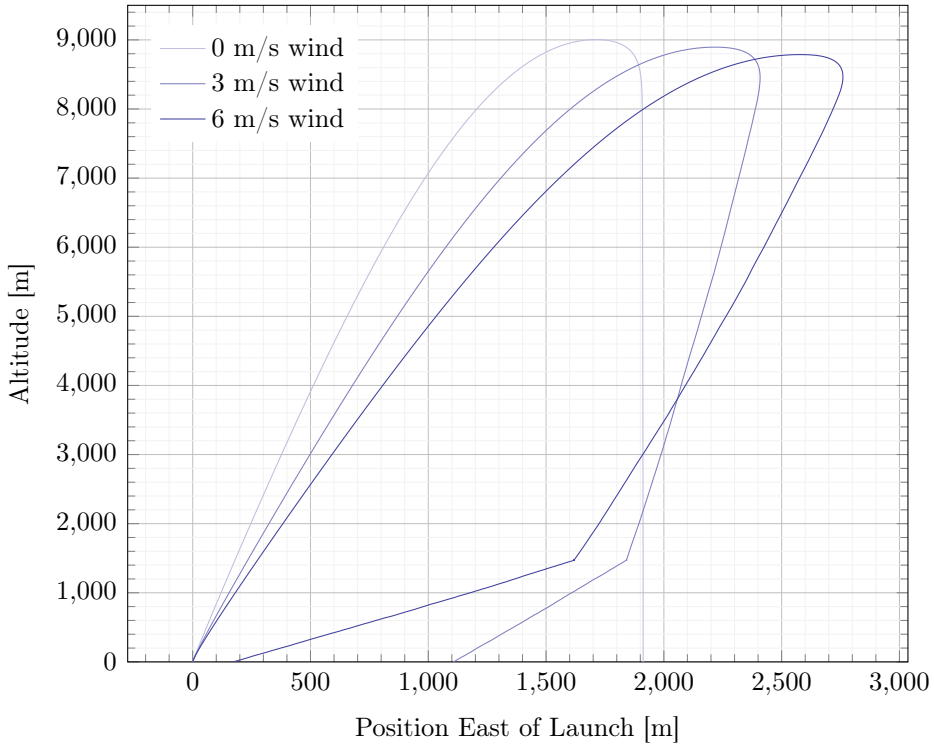

Figure 2.11: OpenRocket wind sensitivity analysis.

From this it can be seen that, whilst not having a major impact on the predicted apogee, increasing wind speed does have significant effect on the rocket's drift during descent. Note, the results shown here are for an upwind launch, and therefore should the rocket be launched downwind the resutls would be reversed, and the rocket would drift further East of launch during its descent.

In addition to the use of OpenRocket and RASAero, a simple in-house trajectory simulation software was developed in the MATLAB-based graphical programming environment Simulink. This software was developed with the intention of using the same equations of motion as those used in OpenRocket, but with added model interactivity which incorporates calculation of drag provided by the airbrake subsystem, as well as simulation of the recovery of a deployable payload.

Detailed Aerodynamic Analysis

With the aim of going supersonic with Darwin II, it is vital that all of the vehicle's aerodynamic surfaces are well understood prior to launch and that the chances of achieving a successful flight are maximised through ensuring the chosen design is sufficiently stable and efficient. Due to the complexity involved in accurately modelling supersonic flow, endeavour enlisted the help of a final-year MEng student at The University of Edinburgh, Liam Foley, who undertook a year-long research project focusing on this challenge. All subsequent methodology and results outlined in this section are credited to Liam.

The focus of this work was divided into two main stages: performing initial analytical simulations to be used for verification, and a numerical analysis of a full 3D model of the rocket. For the purpose of keeping this section concise, the focus will be on the latter of the two stages, in which Darwin II's geometry was imported into the commercial Computational Fluid Dynamics based simulation software, StarCCM+. Within StarCCM+, the the solver conditions, surfaces, and boundary conditions of the domain were defined. In simulating Darwin II, a steady-state, three-dimensional, inviscid ideal gas flow solver was used. A coupled implicit method was chosen and a Courant number of 1.0 was used.

- Steady-state: due to the rocket's aerodynamic profile, there will be relatively low drag force and therefore it can be assumed that the deceleration experienced will be slow. As such, quasi-steady-state analysis is suitable.
- Inviscid: viscous effects are generally negligible compared to pressure effects, therefore assuming that the flow is inviscid will give an accurate result.
- Three-dimensional: due to the geometry of the rocket, a 2D simplification is unrealistic. Simulation time has been reduced by sectioning the smallest repeating symmetrical section on of the rocket, a length-wise 60° section from the nose cone tip to the end of the aft cone.

A summary of the initial conditions used in the simulation of Darwin II are summarised in Table 2.2.

Table 2.2: Initial conditions used in CFD simulations.

Flow property	**Initial conditions**	**Units**
Altitude	10,000	m
Flow velocity	1.8	Mach
Local speed of sound	299.8	m/s
Velocity	539.64	m/s
Freestream density	0.414	kg/m^3
Freestream pressure	26,500	Pa
Freestream temperature	223.3	K

The results of the computational simulation can be seen in Figure 2.12, which shows the velocity distribution and Mach number. In Figures 2.13 and 2.14 show the Mach distribution in more detail and the temperature around the fins. The results of the simulations were validated analytically. This analysis help the design of the aerodynamic surfaces of the rocket, implementing a front and rear taper in the fins to reduce the stagnation zone behind the fins for reduction in drag and temperature. Another change from this analysis was the reduction of the leading edge angle of the fins. This will reduce the effect of the shock waves traveling along the span of the fin, which will increase the effects of the shock waves towards the tip. This will increase the pressure on the main surface of the fin, which will pull the CoP further towards the aft of the rocket at supersonic speeds, increasing the stability.

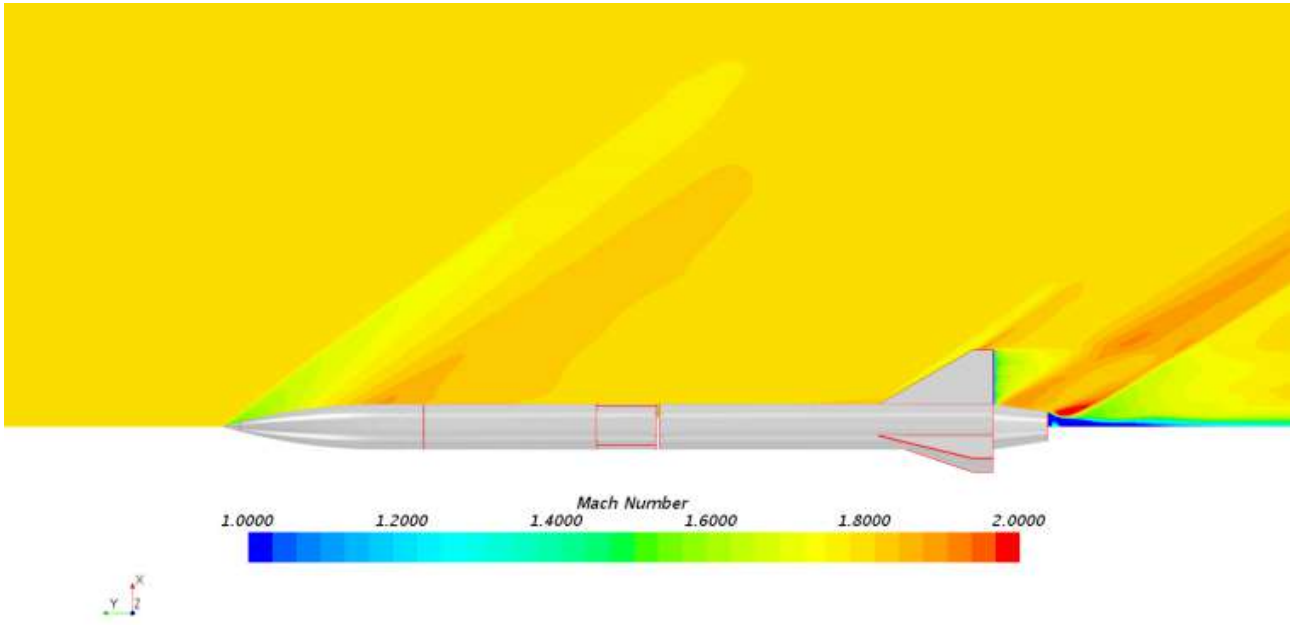

Figure 2.12: A side-on view of the Darwin II rocket simulation showing the velocity of the flow around the rocket.

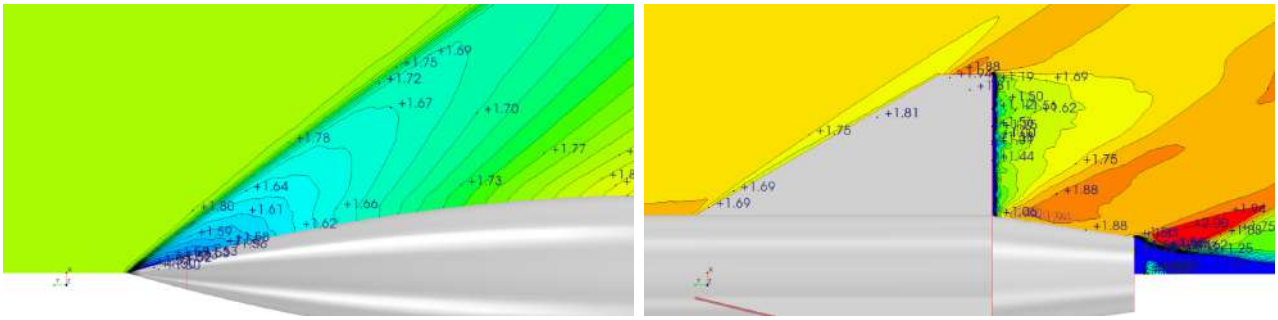

Figure 2.13: Plots of Mach number of air-flow around (a) the tip of the nose cone and (b) the fins and tail of the rocket.

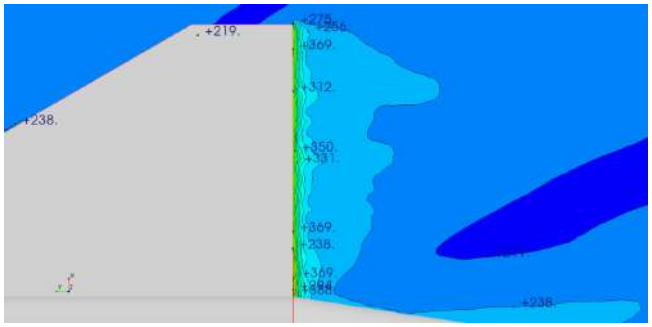

Figure 2.14: Plot of air-flow temperature around the fins.

To add to the analysis carried out in the previous section, a summary of the positions of the Centre of Pressure and Centre of Gravity during the ascent are given in Figure 2.16, which compares the values obtained in OpenRocket with those obtained through the above described CFD simulations.

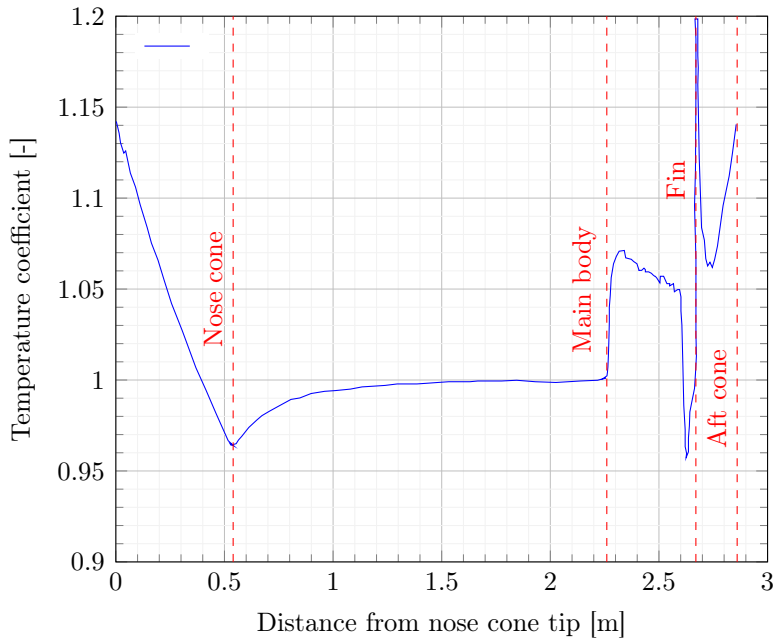

(a)

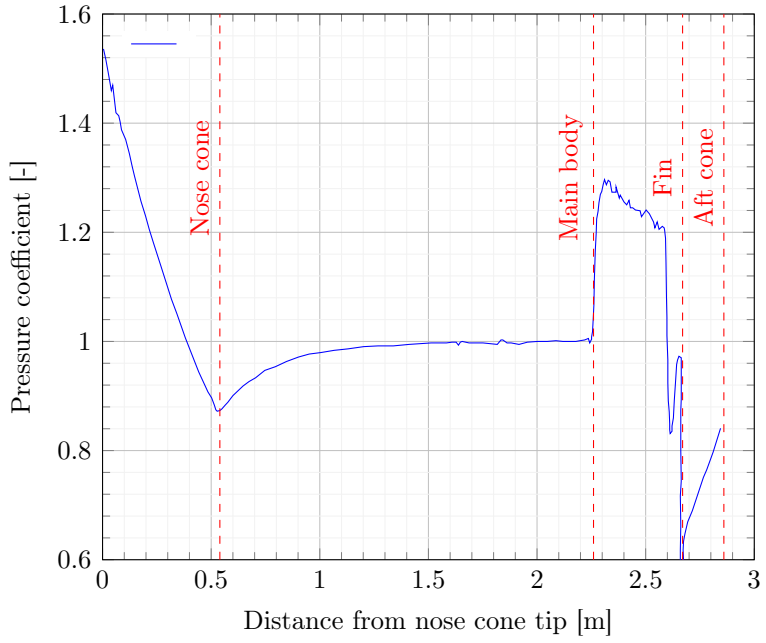

(b)

Figure 2.15: Distribution of (a) temperature and (b) pressure along the length of the rocket.

Figure 2.16: Schematic veiw of Darwin II showing Centre of Gravity at beginning (Orange) and end (Black) of the boost phase, along with Centre of Pressure calculated using OpenRocket at subsonic velocities (Blue) and supersonic velocities (Red), and from CFD simulations (Black).

Expected Loading

To ensure the safety and structural strength of Darwin II's airframe and its connections, an understanding of the magnitude of structural loads that will be encountered throughout its flight is essential. As endeavour's first attempt at performing a detailed structural analysis of a rocket design, the approach taken for estimating the loads the rocket's airframe is subjected to is a simple one: for the determination of axial loads, the rocket is treated as a 1-D rigid beam, with the axial load at any point along the rocket's length, at any instant during the flight, calculated by summing the axial forces acting at this point. Such an approach requires dividing the rocket into segments, along which the acting drag force is assumed to be a constant and the mass is assumed to increase linearly along the length of the segment. Figure 2.17 details the various segments chosen for this simplified approach, and the loads acting on each.

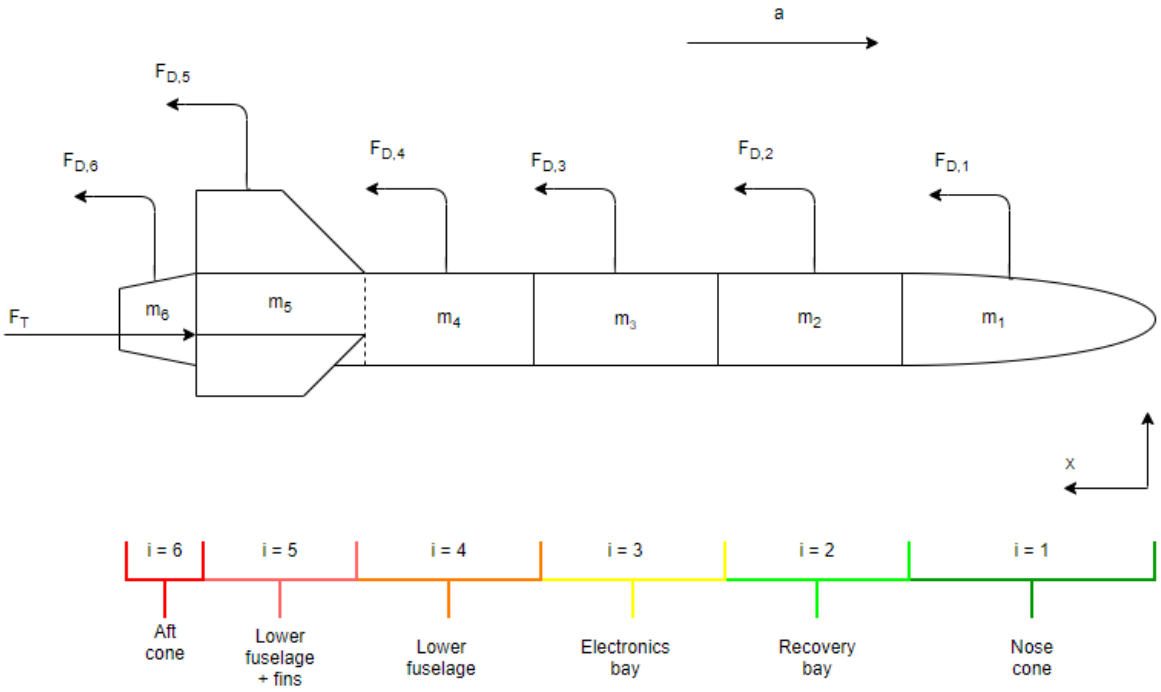

Figure 2.17: Treatment of axial loads on rocket's airframe structure.

This method can then be used to calculate the expected axial load at any point along the rocket's length using the following equation:

$$F_a(x,t) = \sum_{i=1}^{i=6} [F_{a,i-1}(t) + F_{T,i}(t) - a_x(t) \cdot m_i(x) - F_{D,i}(t)] \tag{2.1}$$

where F_a is the axial force acting at the chosen point at a distance x from the nose cone tip at a time t into the duration of the rocket's ascent. $F_{a,i-1}$ is the total axial force acting on all segments in the forward direction of the chosen point and F_T is the motor's thrust force. The inertial force due to the rocket's acceleration is accounted for through the term $a_x \cdot m_i$ where a_x is the rocket's acceleration in the x-direction and m_i is the total mass of all rocket segments in the forward direction of the chosen point, as well as the total forward mass of that particular segment at the chosen point. Finally, the drag force acting on each segment is accounted for through the term F_D.

For a full, detailed analysis and explanation of these various loads, see Appendix H. Using the above approach, a plot detailing the axial force along the length of the rocket throughout the duration of the motor's burn is obtained, shown in Figure 2.18. From this, it is then possible to extract the time at which the maximum axial loads are experienced, shown in Figure 2.19.

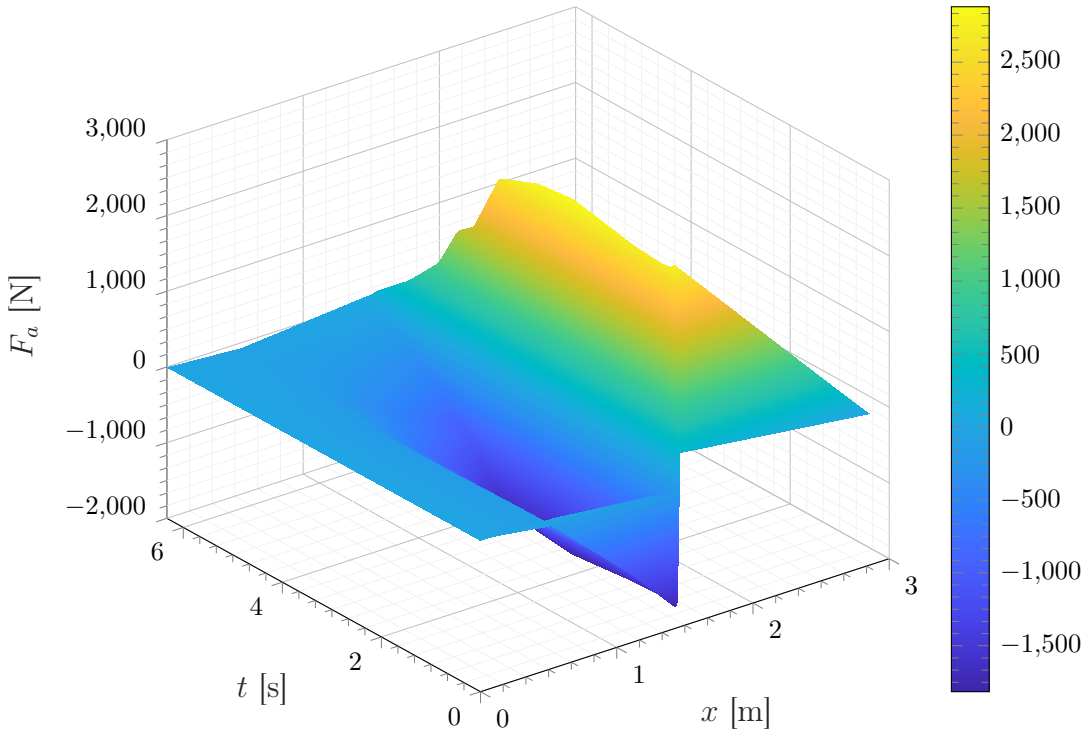

Figure 2.18: 3-D plot showing the variation in axial forces on the rocket's airframe along its length during the motor's burn time.

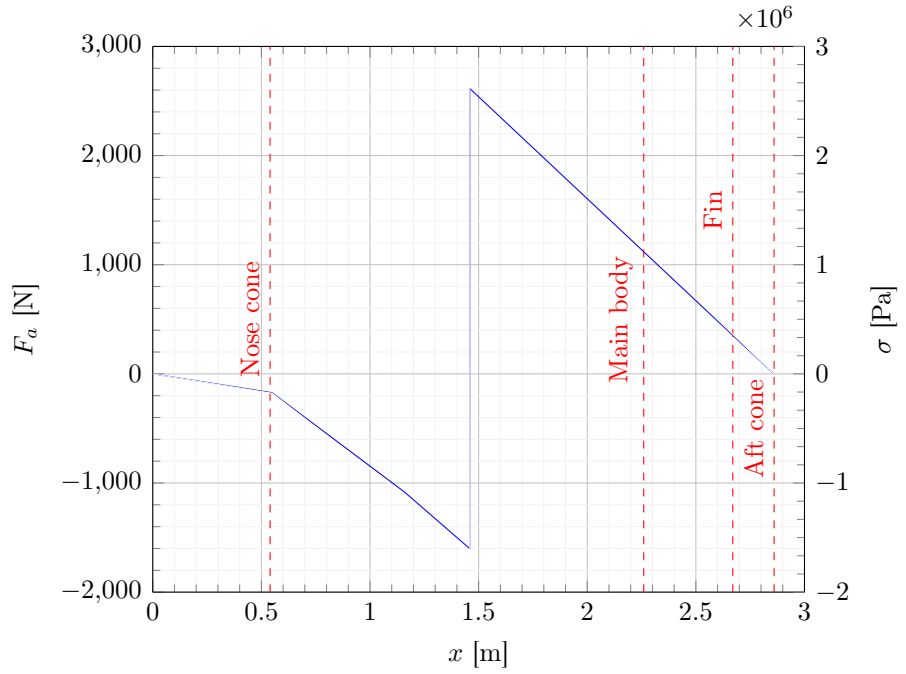

Figure 2.19: Maximum axial force and axial stress acting along the length of the airframe.

From this analysis, it is clear that the stresses experienced by the vehicle's airframe are low in comparison to the yield strength of both CFRP and GFRP, with a more detailed analysis of the critical loads and their effect being looked at in the following section.

Critical Loading Analysis

To ensure that the critical load bearing parts of Darwin II are sufficiently strong, static stress analysis using FEM was performed on the aft cone cap, the motor bulkhead, and the recovery bulkhead using a software called nTopology.

The first part analysed is the aft cone cap. This part is responsible for transferring the thrust of the motor to the motor sleeve, which then transfers it to the motor bulkhead. As this part is directly responsible for transferring the thrust of the motor to the rest of the rocket, the force acting on it is due to the inertia of the rocket minus the motor. With the mass of the rocket (not including the motor) is constant during ascend, the largest force this part experiences is when the vehicle is undergoing peak acceleration. The magnitude of this force is calculated using the following equation:

$$F = (m_{total} - m_{motor}) \cdot a_{peak} \tag{2.2}$$

Where F is the inertia force on the aft cone cap, m_{total} is the total mass of the rocket (about 34.6 kg), m_{motor} is the mass of the motor at launch (about 16.8 kg) and a_{peak} is the peak acceleration (expected to be about 15 g). Using the equation above, a maximum force of 2619.3 N is expected, but for this simulation a peak acceleration of 22.5 g is used for a high FoS, which raises the maximum force to 3928.9 N. This force acts along the small lip of the motor casing and then transferred through the aft cone cap into the motor sleeve's bottom face. These faces were used as boundaries, with the lip of the motor being the surface where the inertia force is acting, and the motor sleeve's bottom face being a displacement constraint. The results of the analysis are shown in Figure 2.20.

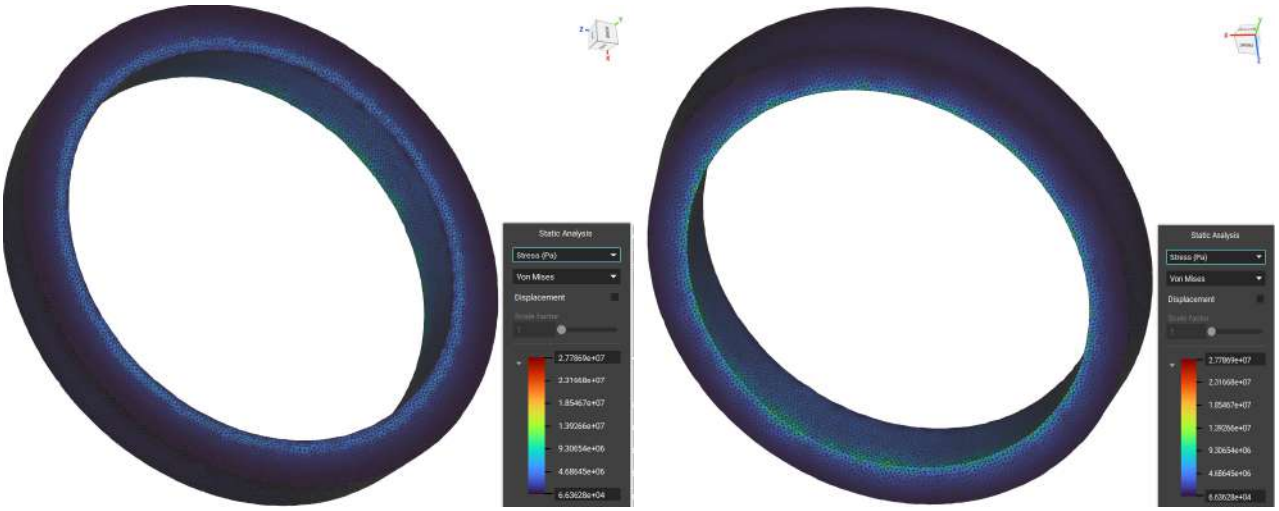

(a) (b)

Figure 2.20: Results of the static analysis of the (a) top and (b) bottom faces of the aft cone cap

According to the analysis, the largest stress on the cap is about 28 MPa. This part is manufactured out of Al 6082-T6, which has a yield stress of about 260 MPa. With the yield stress of this alloy being 9.3 times larger than the maximal stress experienced, the part is deemed safe. Using an acceleration in the analysis that is 1.5 times larger than the expected peak further confirms the safety of this part.

Analysis the motor bulkhead was done in a similar manner. This part is responsible for transferring the thrust from the lower body, through avionics bay, and to the upper body. Using equation 2.2 with a peak acceleration of 22.5 g (for the same reason as before), total mass of 34.6 kg, and replacing m_{motor} with m_{lower}, where m_{lower} is the mass of the lower body (about 21.5 kg), gives a maximum inertia force of 2891.5 N. Technically the lower body's skin is also connected to the bulkhead, but it

is screwed into the bulkhead's outer radius, and as its mass is negligible to the rest of the rocket that is being accelerated by the bulkhead, it is not included in the analysis. The maximum inertia force of 2891.5 N acts along the groove the motor sleeve and is transferred to the three rods that form the structure of the avionics bay. Taking these into consideration, the groove's horizontal surface (where the surface on the top face of the motor sleeve touches) is the surface at which the inertia force acts, and as the rods are screwed into the tapped holes of the bulkhead, the displacement restraint is the cylindrical surface of the tapped holes. The results of the analysis are shown in Figure 2.21.

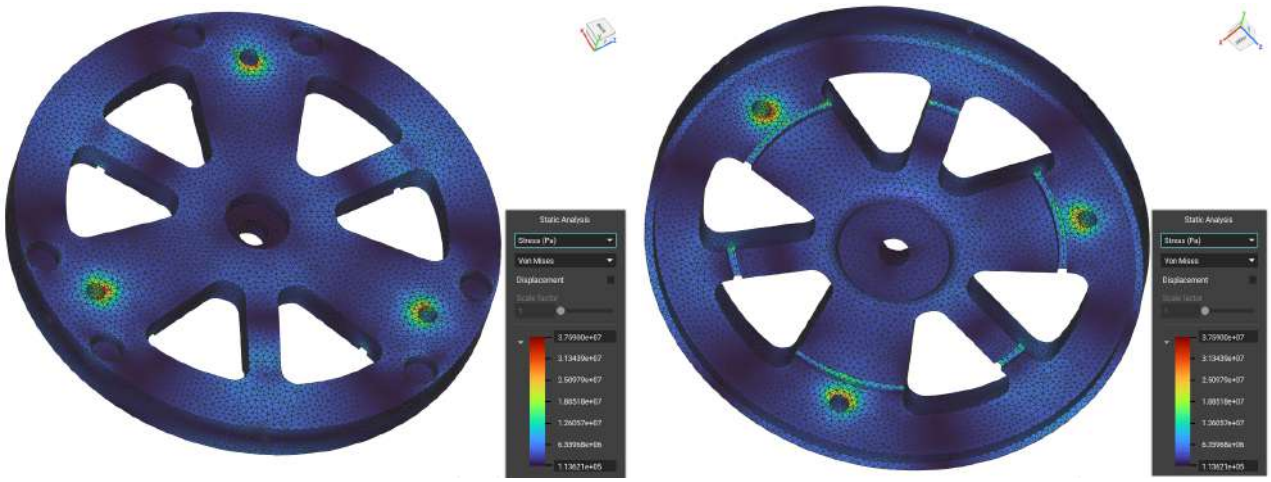

(a) (b)

Figure 2.21: Results of the static analysis of the (a) top and (b) bottom faces of the motor bulkhead. To reduce computation, the shoulder that adds extra stability to the skin connection was shortened during the analysis as the thrust is not transferred through it.

The analysis shows that the largest stress on the bulkhead is 37.5 MPa. Like the aft cone cap, this part is also Al 6082-T6, with a yield stress of 260 MPa. With the yield stress of this alloy being 6.9 times larger than the maximal stress experienced, the part is deemed safe. Using an acceleration in the analysis that is 1.5 times larger than the expected peak further confirms the safety of this part.

The recovery bulkhead is connected to the upper body through a large surface, which reduces stress accumulations during ascent. However, when the main chute opens during descent, all the inertia force is transferred through the eye bolt and then through the three rods of the avionics bay that are secured to the recovery bulkhead. This can create stress accumulation at the eyebolt and the the area where the three rods are secured, which can lead to failure. The analysis used a peak force of 2000 N, while 1300 N was expected to be the maximum force on the eyebolt. Since the time of the analysis, the payload area underwent a slight change which resulted in the maximal force being smaller than 1300 N. A new analysis was not done because if the part is suitable for 2000 N, then decreasing the force acting on it makes it more safe. Calculating the expected force is done using equation 2.8 that is described in section 2.4.3. As the chute is attached to the eyebolt, the force is transferred to the bulkhead through the tapped hole of the bolt and then the into the three rods of the avionics bay through the securing nuts. As a result, the cylindrical surface of the eyebolt's hole is where the 2000 N acts, and the top surface of the bulkhead where the nuts are secured is the displacement restraint. The results of the analysis are shown in Figure 2.22 below.

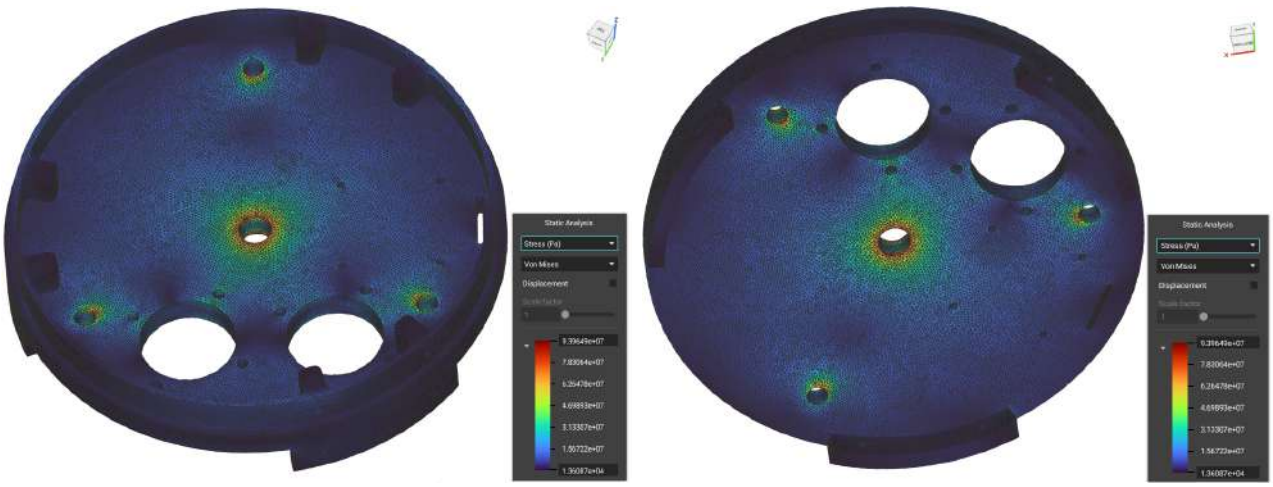

(a) (b)

Figure 2.22: Results of the static analysis of the (a) top and (b) bottom faces of the recovery bulkhead.

The analysis shows that the largest stress on the bulkhead is 94 MPa. Like the two previous parts, this bulkhead is also Al 6082-T6, with a yield stress of 260 MPa. With the yield stress of this alloy being 2.8 times larger than the maximal stress experienced, the part is deemed safe. Using a force for the analysis that is much larger than the expected one further confirms the safety of this part.

2.4 Recovery Subsystem

2.4.1 Introduction

The Darwin II recovery system is a dual deployment two-chute system consisting of a 24-inch drogue parachute, a 96-inch main parachute, a CO_2 canister powered ejection mechanism and a pyrotechnic staging system.

2.4.2 Components and Specifications

The components of the DII recovery system are as follows:

1. Rocketman 96-inch High Performance Parachute, 1x – Main Parachute
2. Rocketman 24-inch Elliptical Parachute, 1x – Drogue Parachute
3. Tinder Rocketry RAPTOR CO_2 Ejection System, 2x
4. Rocketman Shock Cord, 1x
5. Rocketman Y-harness, 3x
6. Eye Bolt M8 x 18mm, 2x
7. 25 x 0.3m E-match, 1x
8. 23g CO_2 Canister, 2x
9. Fruity Chutes L2 Recovery Tether, 1x

The parachute specifications are as given in Table A.2.

2.4.3 Recovery Subsystem Calculations

The parachute sizes were calculated from solving the drag equation 2.3 as follows:

$$F_d = \frac{C_d \pi \rho r^2 v^2}{2} \tag{2.3}$$

Where the symbols correspond to the following physical parameters:

- F_d - Drag force acting on the rocket measured in Newtons (N)
- C_d - Drag Coefficient
- ρ - Air Density for a given altitude in kilogrammes per cubic metre (kg/m^3)
- r - Radius of the parachute in metres (m)
- v - Descent speed of the rocket in metres per second (m/s)

Equating the drag force to the rocket's weight and rearranging for r, we have that:

$$r = \sqrt{\frac{2mg}{\pi C_d \rho v}} \tag{2.4}$$

Where:

- m - Mass of the rocket in kilogrammes (kg)
- g - Acceleration due to gravity in metres per square second (m/s^2)

The results are given in Table 2.3 below:

Table 2.3: Range of radii of drogue and main for successful recovery

	Chute		
Parameter	Drogue	Main	Unit
Deployment Altitude	~10	0.5	km
Range of $C_D Values$	1.6<C_D < 2.2		
Air Density	0.4135	1.225	kg/m^3
Target Speed Range	23<v<46	v<9	m/s
Calculated Range of Radii	**0.42<r<0.94**	**1.14<r<1.54**	**m**

*The range of C_D values was based upon what was quoted in commercially available parachutes.

From the results in Table 2.3, a shortlist of suitable commercially available parachutes was written up from which the Rocketman 96-inch, high performance toroidal parachute and 24-inch, elliptical parachute were selected in order to give a high speed of descent while minimising wind drift.

In order for the recovery system to deploy, the CO_2 gas has to exert enough pressure given in equation 2.5.

$$Pressure(lb/in^2) = \frac{Force(lb)}{Area(in^2)} \tag{2.5}$$

The volume of the recovery bay is given in equation 2.6:

$$Volume(in^3) = \frac{\pi \times (diameter(in))^2 \times length(in)}{4} \tag{2.6}$$

If we know the pressure required to deploy the recovery system, then the mass of BP we require is given by equation 2.7, and the mass of CO_2 is simply five times the required mass of BP.

$$m_{BP} = \frac{PV}{RT} \tag{2.7}$$

Where:

- m_{BP} - Mass of BP in grammes, (g)
- P - Pressure required to eject the nose cone and drogue chute in (lb/in^2)
- V - Volume of Free Recovery Bay in (in^3)
- R - Combustion Gas Constant of FFFF BP $R_{BP} = 22.16 ftlbf/lbm°\text{R}$
- T - Combustion Gas Temperature, for FFFF BP, $T_{BP} = 3307°\text{R}$

The results of our calculations are given in Table A.2 in Appendix A.

At the centre, an M10 eyebolt is anchored in with an M10 hex nut, which should provide a large area to dissipate the jerking force of the parachute deployment. With a bad case scenario of a 1560N force, from a sudden opening of 0.5s, from 32m/s to 6m/s at 30kg. Using SolidWorks simulations, it came to a factor of safety of 4.3 before yield stress is reached.

$$F = \frac{m\delta V}{t} \tag{2.8}$$

Where:

- F - Force in N
- m - Mass of the rocket in kg
- δV - Change in velocity from deployment in m/s
- t - Time for the main parachute to deploy in s

2.4.4 Recovery Simulation

The descent of the rocket was simulated using a combination of analytical and computational tools. First we analyse the time and velocity of the recovery using the equations described in section 2.4.3. We validated these results with the OpenRocket one, showed in Figure 2.10. Finally we created the MATLAB Simulink code so we could analyse the recovery distance, time and area of recovery in a home-developed software. This analysis shows that even with high wind conditions for a safety launch (no more than 20 km/h wind-speed) the recovery Area will be within 1km of the launch pad.

2.4.5 Recovery sequence

For the recovery of the rocket, a dual deployment system will be implemented. This will involve a jettison of the payload and nosecone that will fall separately to the main body of the rocket. At apogee, the RAPTOR CO_2 ejection system will activate, releasing the gas from two 23 g CO_2 canisters. The expansion of the CO_2 will result in shear pins holding the nose cone in place to break. This will allow the drogue chute to be released and inflate at apogee, bringing the main body descent speed to a predicted 28 m/s. The main body should descend at this speed until it reaches an altitude of 500 m, where the main parachute will be released. This will be done by using a Tender Descender L2, which once activated, will allow the drogue to pull the main parachute bag up, which will release the main parachute, slowing the rocket body to 6 m/s until it lands.

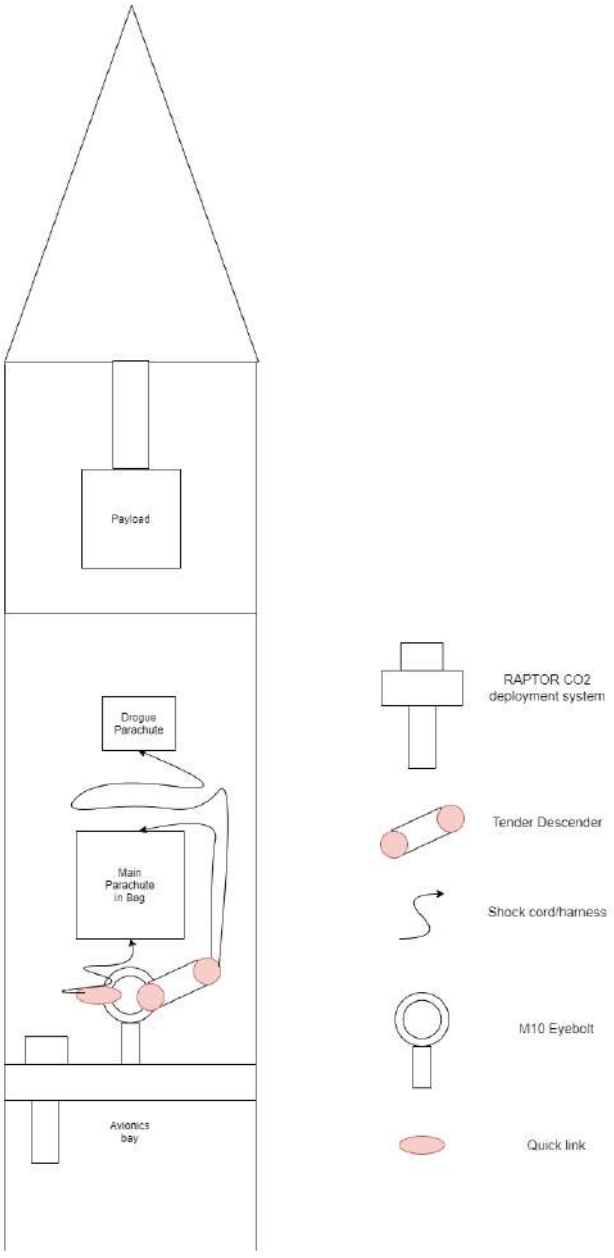

Figure 2.23: Diagram showing the connections present at the launch stage in the recovery system

The main parachute and TD (Tender Descender) will be anchored to the eyebolt in the centre of the recovery bulkhead using quicklinks. The body of the TD is then attached to the eyebolt using a kevlar lanyard to prevent it escaping once activated. The drogue parachute will be connected to the top

quicklink on the TD using a shock cord. A seprate kevlar Y-harness will connect the main parachute bag to the top TD quicklink to stop the bag from moving up the recovery bay. Both the RAPTOR and TD have redundant ignition charges, in the event that there is a failure on one of the charges in either system.

2.5 Payload Subsystem

Introduction

Endeavour's Payload for this edition of EuRoC was designed to be modular and able to fly on several different types of missions. Its first mission was at Mach 21, a payload competition taking place at Machrihanish AFB, which required us to use a CANSat format with a 350g mass limit. Following EuRoC, we are scheduled to fly aboard of Darwin I, the Team's 3000 ft, subsonic launcher. We created an "Advanced Mission's Pack" to operate our Payload even aboard Darwin II, with greater accelerations and lower temperatures. The Pack augments the CANSat capabilities and introduces telemetry and dual-event recovery systems housed in a CUBESat structure, allowing us to control our descent and capture atmospheric and radiation data more reliably.

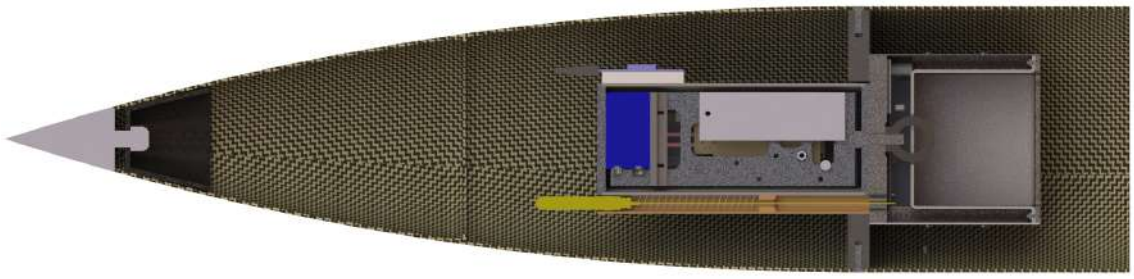

Figure 2.24: Cross Section view of the Nosecone, the CANSat and the CUBESat after separation from the main body.

Mass and Form Factor

Re-usability and modularity across a variety of missions was a critical mission requirement. Most of the sensing electronics - including the radiation sensing instrumentation - reside within a standard CANSat enclosure (66 mm in diameter and 160 mm in height). The recovery hardware and the relevant recovery and telemetry electronics are housed in a 1U CUBESat enclosure (100mm x 100mm x 100mm). The two modules are fully independent electrically, with their own power supplies, and are coupled mechanically through an M6 Eye Bolt, placed to allow the loads from the mission's most violent event (Main Chute deployment) to optimally traverse the craft and prevent catastrophic failure. Following separation, the Nosecone and Payload remain coupled, descending as an unit, independent from the main body tube. In the following points we dig deeper into the specifics of each module. Detailed mass budgets are given in Appendix G, Figures G.1 and G.2.

CANSat form factor: For this section, we were restricted by the Mach 21 regulations to a maximum of 350g. The structure is composed of two modular, lightweight aluminium vertical plates which support

all of the electronics. The plates are secured to an upper and lower poly-carbonate bulkheads. The CNC machines at the student Maker Space could not handle metals, and poly-carbonate was the natural choice, representing the intersection of low cost, low mass and manufacturability. The plates are bolted on to the bulkheads such that the SRBF composite external shell is clamped and held in place thanks to lips carved in the bulkheads.

CUBESat form factor: Darwin II can launch up to 4kg, putting a limit on the mass of the CUBESat at 3.65kg - more than sufficient. The frame is constructed from a lightweight aluminium plate, strong stainless steel corner rails, and GFRP faces all around. An important factor to consider is the effect of an extended descent-time on the down-range drift. While it is desirable to *minimise* the mass at liftoff to increase our chances of reaching apogee at 9000m, it is also desirable to *descend rapidly*, so that cross-winds do not make ground recovery efforts too lengthy. It was decided to couple the system to the nosecone so that they could descend as a single body. This design change allowed us to increase the mass being supported by the Payload parachutes *without* adding any mass to the lift-off weight of Darwin II. The aluminium and steel structure is enclosed in GFRP sheets on the four lateral faces, in order to ensure RF transparency necessary for the GPS Ceramic Patch Receiver. The upper face of the cube is open and exposes the custom-made GRFP recovery bay, which houses the main 30" parachute, the Tender Descender pyrotechnic device and the relevant shock-cords. This bay includes two small, separate compartments for the batteries and the pyrotechnic device, mitigating the risks of damaging or catching the lines or the parachute. All the electronics to handle GPS tracking, telemetry and downlink communications, as well as our COTS flight computer, are housed below the recovery bay. The 868MHz omni-directional stub antenna for ground communications is held within a 3D-printed housing epoxied to the outer shell of the CANSat to maximise the chances of perfect Line of Sight (LOS) communication with the ground station. Similarly, the COTS EggTimer GPS Mini Transmitter mandated by the Altitude Logging and Transmission Addendum is epoxied to the side of the CANSat through a 3D printed adapter.

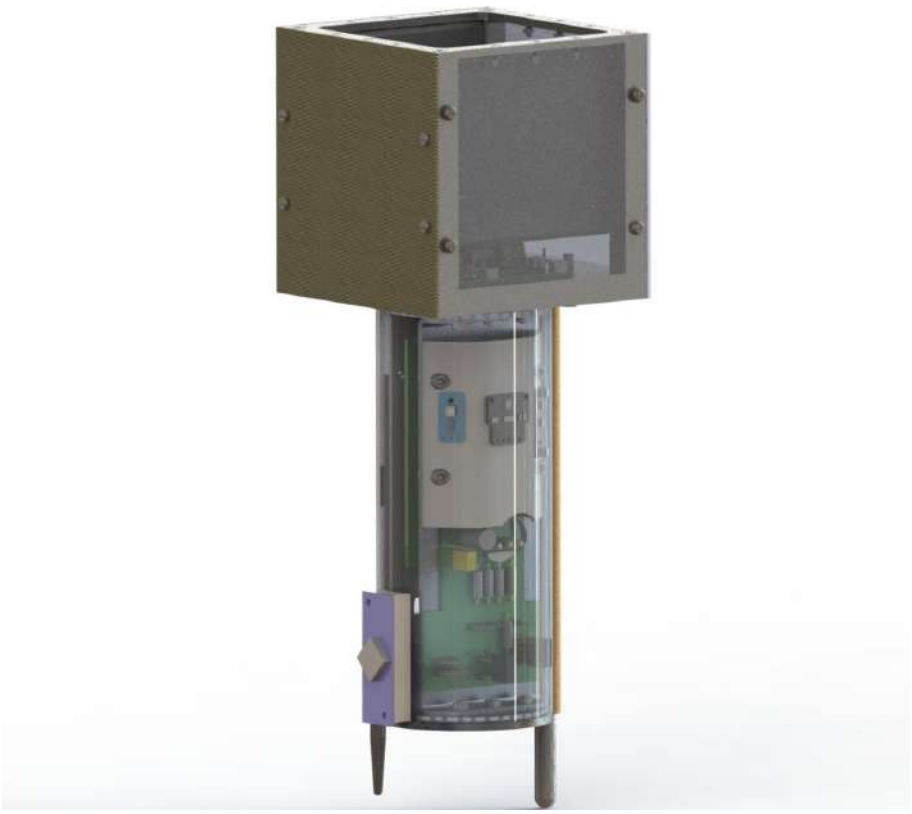

Figure 2.25: Render showing the CUBESat and CANSat ready to be integrated. Note that the transparency of the outer shells has been altered to facilitate grasp internal layout

Removal, Interface and Deployment

The payload is mounted "upside-down" during launch. After deployment, aerodynamic forces acting on the nosecone shell and drogue parachute will force the Payload+Nosecone system in a stable "nose-down" configuration. There are two key interfaces with the Upper Body of the rocket. Moving afterwards, the first of these interfaces is a GFRP ring epoxied to the inner diameter of the upper-body coupling tube, which supports a round GFRP pusher plate upon which one of the CUBESat's faces lay. During launch, this ring contributes to supporting the weight of the payload. Not being connected to its support ring by bolted connections or adhesives, during the CO_2 over-pressure event that initiates the recovery phase, the plate acts as a piston. The shear pins that connect the Nosecone to the body tube fail, and the assembly separates permanently.

There is a further interface connecting the Payload to the Nosecone, coupling the two for the whole mission, including descent. The 8mm thick Bulkhead is made of continuous carbon fiber reinforced nylon, selected for its excellent impact resistance and strength comparable to aluminium. It connects to the bottom face of the CUBESat and features a cutout for the CANSat to pass through. Reinforcing ribs housing threaded inserts extend to the inner face of the Nosecone, allowing for 6 short countersunk bolts to secure the Bulkhead to the Nosecone.

This coupling structure allows the payload to be easily worked on on launch day. After final electronics tests, the pusher plate is laid onto its support ring and the bulkhead is bolted onto the CUBESat lower face. The payload is then lowered into the Nosecone and the fasteners connecting the Bulkhead to the Nosecone can be screwed in. Finally, the Nosecone+Payload Assembly is slid onto the upper coupling tube, and the shear pins are inserted, completing the upper body integration.In Figure 2.26, the different elements of the assembly are distinguished based on colour: the Upper Coupling tube (yellow), the Pusher Plate (green), the Payload Bulkhead (red) and Nosecone (blue).

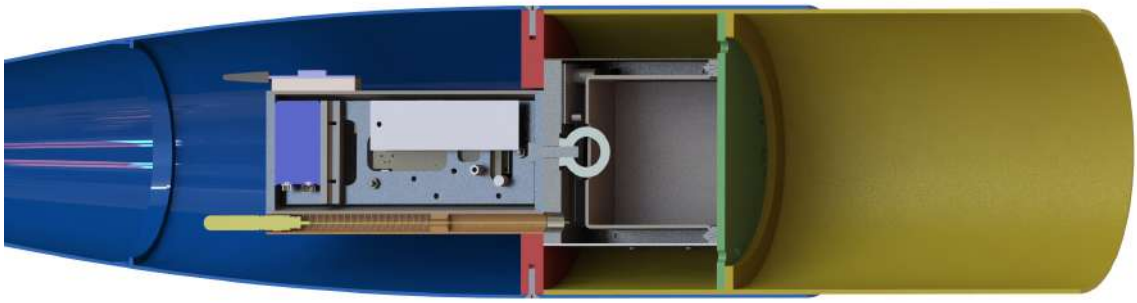

Figure 2.26: Colourised Cross Section of the Nosecone-Payload Assembly

Functionality

This payload accomplishes a series of main missions. It has its two scientific objectives, which are entirely performed by the CANSat:

1. To characterise the radiation environment at altitude by collecting snapshots of high-energy particles using a reverse-engineered RasPIX - a CERN-developed particle detector.

2. To collect atmospheric data from a collection of environmental monitoring sensors (EMC - Environmental Monitoring Cluster), and build a data bank that can be compared with previous and future flights.

In addition, it acts as an *engineering demonstrator* to experiment with deployable payloads and all the complexity of ejection sequences, dual event recovery and radio communications in extremely reduced dimensions. Experience from this campaign will facilitate the team's future deployable payloads that will be able to incorporate our 1U module for a turn-key recovery solution. All of the recovery electronics, hardware, and the Recovery Flight Computer (RFC) are housed in the CUBESat.

RASPix is a COTS particle detector for years and has flight heritage aboard the ISS. The system which we obtained, courtesy of a partnership with the Institute for Research in Schools, consists of an FPGA capable of recording 15 exposures per minute via a single, 300 µm thick silicon radiation imaging detector. The system will be used for radiation monitoring: its 256x256 sensor captures the trace of particles, each decaying and interacting with the silicon wafer according to specific patterns. Electrons, being the least massive, leave long, curly, thin traces (visible in Figure 2.27, while protons leave shorter, thicker traces. The counting and sorting of each type is handled by a Raspberry Pi B, which we stripped of all unnecessary components to minimise failure points, reduce mass and reduce the volume taken up by the board. The Pi logs radiation data, and creates a wireless network to remotely initiate data capture from the launch rail. The detector is powered by a 3.7V, 750mAh LiPo pouch-style battery.

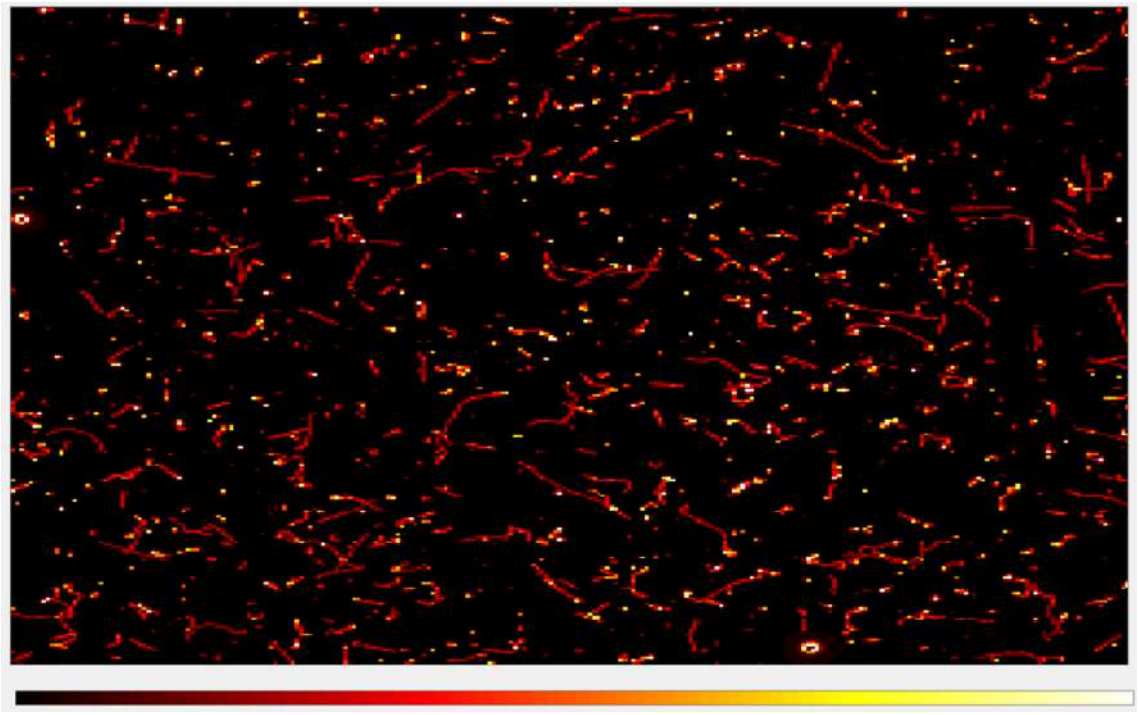

Figure 2.27: Example of Data Outputted by the RasPIX - from P. Burian et al 2017 (JINST)

EMC was developed in house - it is based around an Arduino Nano and features a number of sensors and peripherals. After breadboard tests, the design was moved to Altium Designer to formalise our schematics (available in the appendix) into robust CAD models. Upon ordering the first iteration of our PCB, we spotted some non-critical faults. The second version of the PCB features a more robust electronic design, thanks to wider traces, more efficient routing and better aligned pins and silkscreen. The unconventional shape of the board is due to the tight volumetric constraints in this section of the payload. The sensors are lifted off the board, and are supported by a 3D printed "bridge". This has the benefit of positioning the sensors up against the outer shell of the payload, improving the reliability of our sensors by exposing them more directly to the atmosphere.

Since our team is relatively new and does not have any high-altitude flight data from previous launches, we have no data describing the cooling or heating of the internal volumes of our vehicles as they traverse the stages of recovery. All components of the EMC and the descent computer were chosen to be able to operate at -40°C, but The RASPix and Eggtimer batteries are based on Lithium Polymers, which are notoriously sensitive to very low temperatures. Approximate calculations using a lumped capacitance thermal model, and assuming the worst case scenario (150% faster descent speed, assuming a uniform block of ABS, and ignoring the protection given by the nosecone structure) show that the temperature of the payload, if exposed to a -40C air-stream at 60m/s, would reach equilibrium with the environment in 30 seconds. A COTS 7.5W resistive patch heater was selected to work in conjunction with a simple thermistor mounted to the battery pouches. -10°C was deemed an acceptable operational temperature for the LiPo battery, and a PD controller was implemented on the Arduino Nano using Pulse Width Modulation (PWM).

The heating patch requires a 12V power supply, so a XL6009 boost converter was chosen to upscale the 9V provided by a Lithium PP3 battery from Energizer, which will be discussed further in the Power & Energy section. The electrical architecture of the CANSat is shown in 2.28

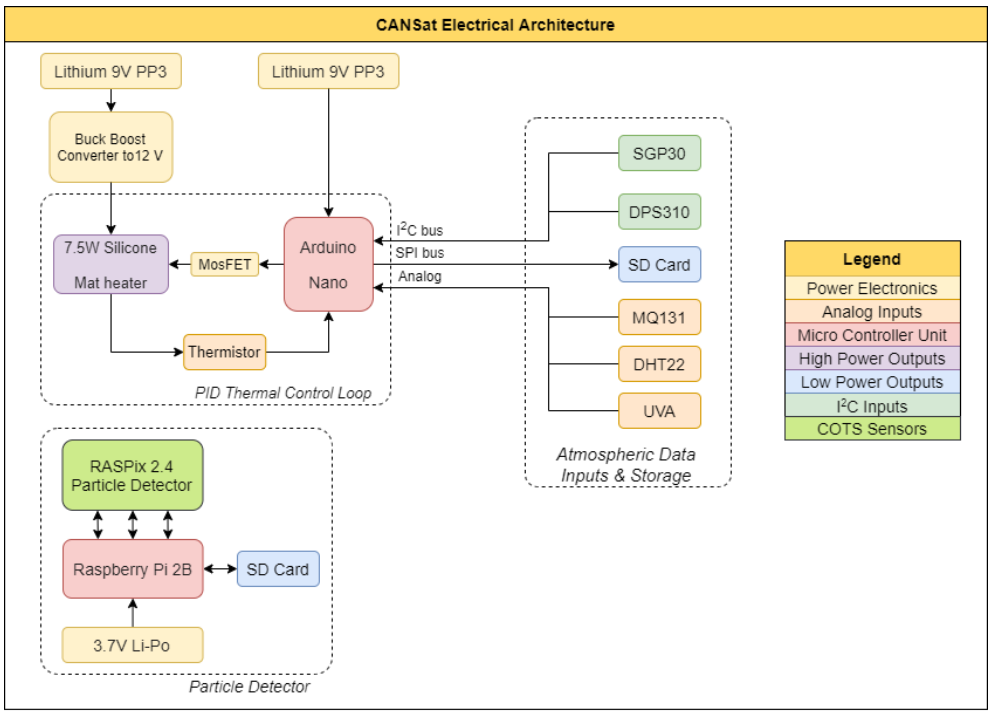

Figure 2.28: CANSat Electrical Architecture

Finally, the RFC, residing in the CUBE, handles all tasks concerning telemetry and recovery. It is powered by a Teensy 4.0, chosen for its fast clock speed and compact size. This allows us to run telemetry and recovery software tasks on separate virtual threads, isolating so that that if an unexpected critical fault occurred in either one of them, the other would not be affected. For example, if a fault occurred in the GPS tracking, that would not stop the program firing the chute from completing its task.

Recovery Task: Altitude is tracked using a high precision barometer from Bosch (BMP388) which offers a ±8 Pascal uncertainty (approximately of ±0.5 metres). The program starts off by saving a reading for the ground pressure at the launch site. Then it begins comparing the previously recorded altitude with the current altitude every 250ms. If the current altitude is found to be lower than the previously recorded one for three times in a row, the RFC assumes the payload has begun descending from apogee. It then starts monitoring when the altitude crosses the 500m above launch site level mark, at which point it triggers a BJT transistor switch, closing the high-current Pyro channel feeding

an e-match, which will ignite the black powder held in the Tender Descender chamber, deploying the main parachute.

Telemetry Task: GPS coordinates are received at a 1Hz frequency via serial communication from a passive Ceramic Patch antenna facing upwards. The sentences are decoded from the NMEA standard into a string showing latitude, longitude, altitude and number of satellites in view, and then transmitted via SPI to an RFM95W LoRa transceiver operating at 868MHz operating at a transmission power of +20dBm (100mW is the legal maximum transmission power). Due to our team being scattered around Europe to complete internships, it was not possible to conduct tests on the range of the system. Our calculations (equations 2.9 and 2.10) show that at a range of 9km we can expect a -116dBm signal at the ground station using the stock 2dBi RX/TX antennas and incorporating a 30dB loss due to humidity, which is sufficient for the RFM95W receiver given its low-end sensitivity of -148dBm.

$$P_{out}[dBm] = P_{tx} + G_{tx} - L_{freespace} - L_{misc} + G_{rx} \tag{2.9}$$

$$\text{where } L_{\text{free space}}[dBm] = 20log_{10}(\text{range [km]}) + 20log_{10}(\text{frequency [MHz]}) + 32.44 \tag{2.10}$$

Finding the Payload is a major criterion for mission success. Our base station features an omni-directional 3 dB-gain stub antenna for ground recovery, and a 8.5dB-gain, 6-element Yagi-Uda one, for live telemetry. According to the same calculations, this setup triples our range.

The complete CUBESat architecture is shown in Figure 2.29

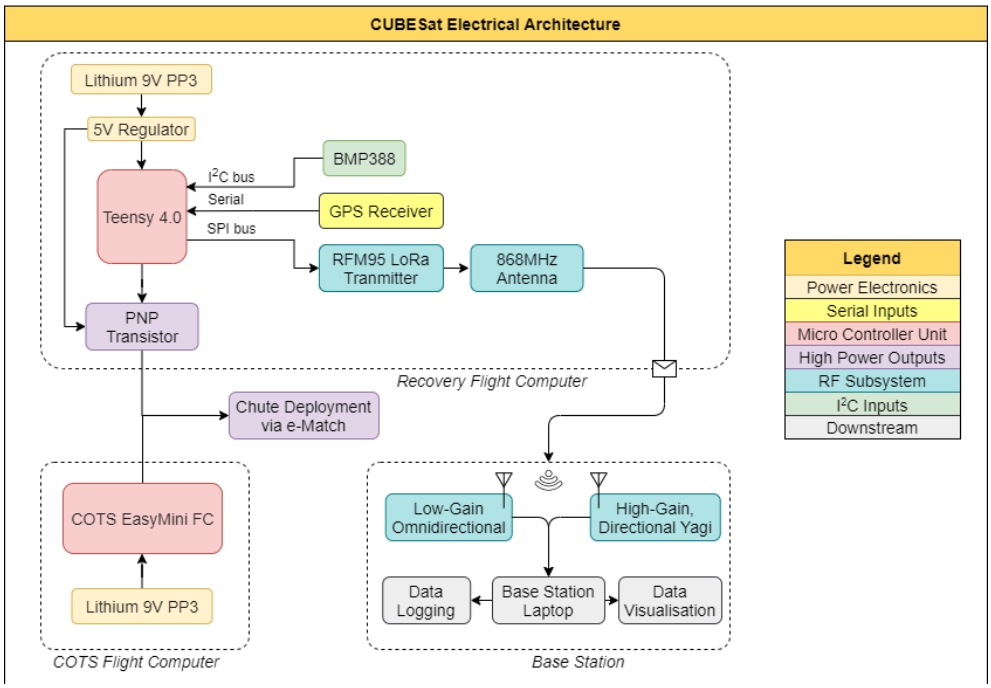

Figure 2.29: CUBESat Electrical Architecture

Power/Energy

In total, 4x 9V Energizer Lithium-Manganese Dioxide (Li/MnO2), PP3 format batteries were used throughout the entire payload, powering the EMC board, the Heater, the Recovery Flight Computer, and the EasyMini FC . These provide several advantages, being 1/3 of the mass of conventional alkaline equivalents, but most importantly being designed with extreme operating conditions in mind. Unlike LiPo's, they are equipped with vents to prevent pressure buildup when exposed to lower atmospheric pressures at apogee and are able to supply a constant current at lower temperatures. They support

a high burst discharge rate up to 1.5Amps, which is much more than the 500mA we found necessary for the correct operation of our e-matches. In terms of expected flight time, EMC's flight heritage shows that it is able to continuously log data while surviving off a single of the above mentioned 9V batteries for over 3 hours. Similarly, the RASPix has been tested in continuous logging mode for 57 minutes running off its 750mAh LiPo pack. Based on manufacturer specifications and data-sheets, the Recovery Flight Computer's (RFC) should consume no more than 300mA when running at 5V, so we expect the battery to last over 3 hours on the 750mAh 9V battery. The team has not yet tested the final configuration of the Recovery Flight Computer (RFC) and is eagerly awaiting to confirm this. If that proves not to be the case, another 9V battery will be added in parallel to double the battery life. The EasyMini has also proved to reliably survive in flight mode for over 1 hour on a 9V battery. The other form of stored energy on board is in the form of 0.2 grams of black powder held in the combustion chamber of the Tender Descender. In order to fire, the system has to be **armed** by manually flipping a slide switch on the main PCB (done on the launchpad through a small opening on the nose cone) and then **activated** by either the RFC or the COTS EasyMini FC, both relying on barometric data showing the vehicle has **BOTH** started descending **AND** crossed the 500m altitude mark.

Recovery

Dual event recovery is absolutely necessary for our payload. A drogue parachute enables a rapid but controlled descent from apogee to 500 metres, while limiting the terminal velocity of the system such that, at the instant of main chute deployment, the payload is not torn apart by excessive deceleration loads. The main criteria for Descent solution selection are reliability, practicality, and the reduction of deployment loads and landing energy. The payload relies on a 10" COTS Drogue Chute from Black Cat Rocketry in conjunction with a 30" COTS Main Chute from Fruity Chutes.

Recovery Sequence: Upon separation from Darwin's Lower Body, the drogue is immediately exposed to the air-stream. It will tension a 1m long shock cord secured to the CUBESat bulkhead by an M4 eye nut. This line is equipped with a Tender Descender (TD), a COTS pyrotechnic device redundantly controlled by our SRAD Recovery Flight Computer and COTS EasyMini Flight Computer. This line is bifurcated above the TD, with a short connection to the main chute bag. When the 500m mark is reached, the 0.2 gram black powder charge held in the Tender Descender is detonated by any 1 of 3 parallel e-matches, severing the line that previously transferred the drag force from the drogue to the bulkhead. The drogue, initially loose, will start pulling away, engaging the other end of the bifurcated line and pulling the Main Chute bag out of the Recovery Bay and into the free air-stream. The Bag is connected to a loop sewn to the crown of the Main, so as the Drogue engages the line, the Bag and Main are pulled apart, and the Main proceeds to inflate, transferring its drag force down through another 1 metre line of shock cord, through a swivel and finally into a separate M6 eye nut secured to the CUBESat Bulkhead. The sequence is shown in a simplified way in Figure 2.30:

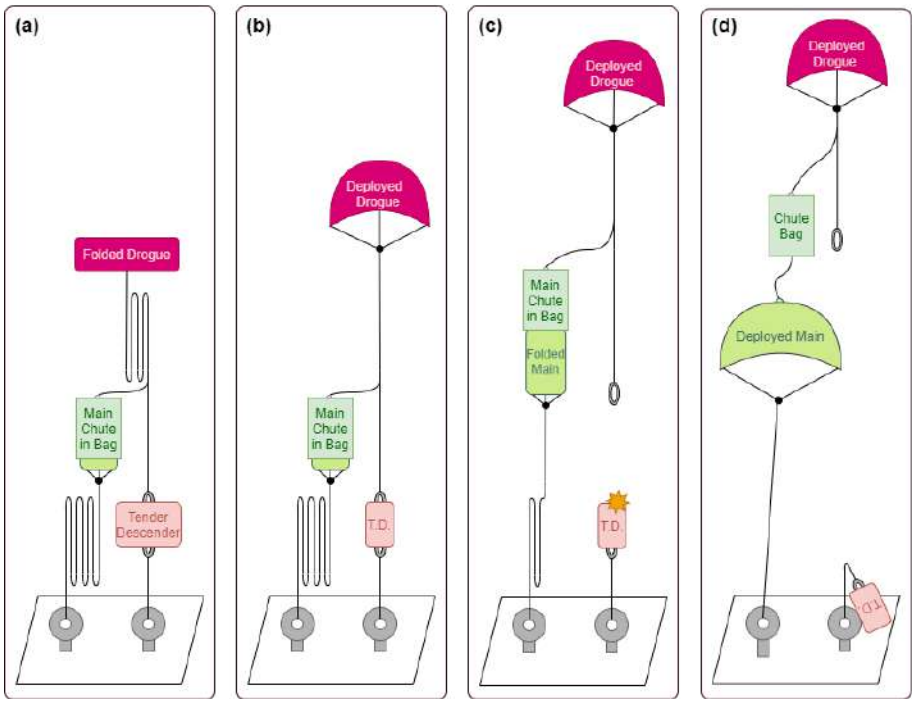

Figure 2.30: Payload Deployment Sequence

Knowing the mass of the Payload+Nosecone assembly is 3kg, the system specifications (Table A.2), and the terminal velocity formula (Equation 2.11), we can estimate the descent speed of the chutes, which allows us to obtain shock loading figures to input into FEM simulations of the structure.

$$v_t = \sqrt{\frac{2mg}{\rho A C_d}} \tag{2.11}$$

Fruity Chutes estimates the main chute should unfurl in 0.25 to 0.5 seconds. Using Formula 2.8, the the shock loading can be calculated to be between 154 and 308 N. Results of FEM analysis on the Payload Bulkhead subjected to a 600N are shown in Figure 2.31. It shows that the maximum stress in the part is 7.73MPa, well below the yield stress of the carbon reinforced nylon material (60MPa matrix, 540MPa fiber).

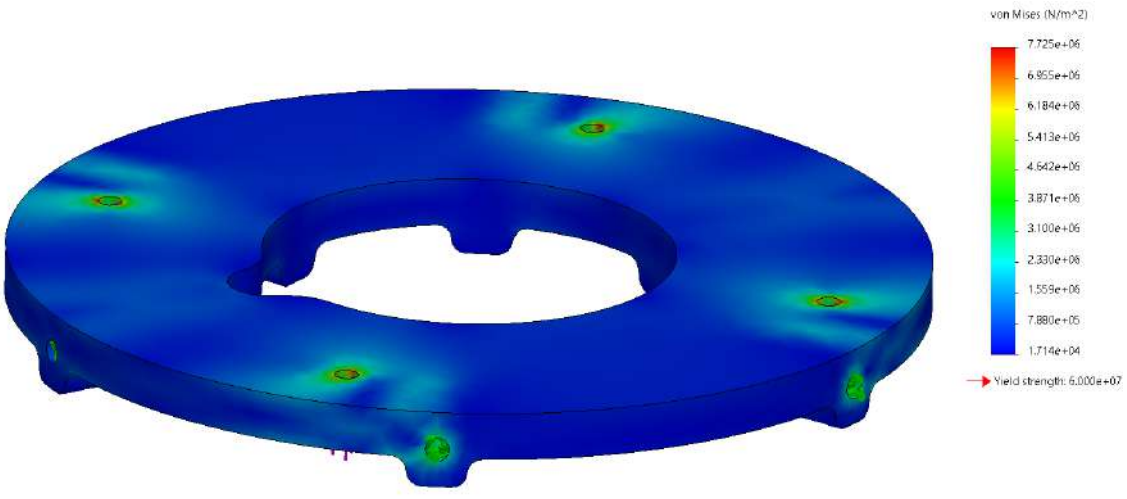

Figure 2.31: Payload Bulkhead Static Analysis - Main Chute Deployment

Table 2.4: Recovery system data of the Payload.

Assembly	Parameter	Value	Units
Drogue (Supplied by Black Cat Rocketry)	Coefficient of drag	0.7	-
	Diameter	10	inch
	Mass incl. hardware	21	g
	Packing Volume	25	cm^3
	Mass of black powder used	0.2	g
	Deployment altitude	9000	m
	Descent rate @ 9000m	57.3	m/s
	Descent rate @ 500m	32.9	m/s
Main (Supplied by Fruity Chutes)	Chute coefficient of drag	1.5	-
	Diameter	30	inch
	Mass incl. hardware	63	g
	Packing Volume	190	cm^3
	Mass of black powder used	0.2	g
	Chute deployment altitude	500	m
	Maximum stopping velocity	60	m/s
	Chute descent rate	8.4	m/s

At sea level, the descent speed for Drogue and Main chutes can be calculated easily as 31.3 and 8.4 m/s respectively. However, air density varies continuously and significantly (by a factor of 3, depending on atmospheric conditions) from the deployment altitude of 9000m to sea level. Thus, a Simulink model accounting for the variation was created, showing the following results shown in Figure 2.32. The model predicts the descent rate, showing both vertical speeds and altitude over time. The total descent time of 232 seconds is easily found as the instant the altitude crosses the zero mark. Crucially, it does not model horizontal wind loading, which affects the horizontal speed and ultimately determines the final landing spot of the payload.

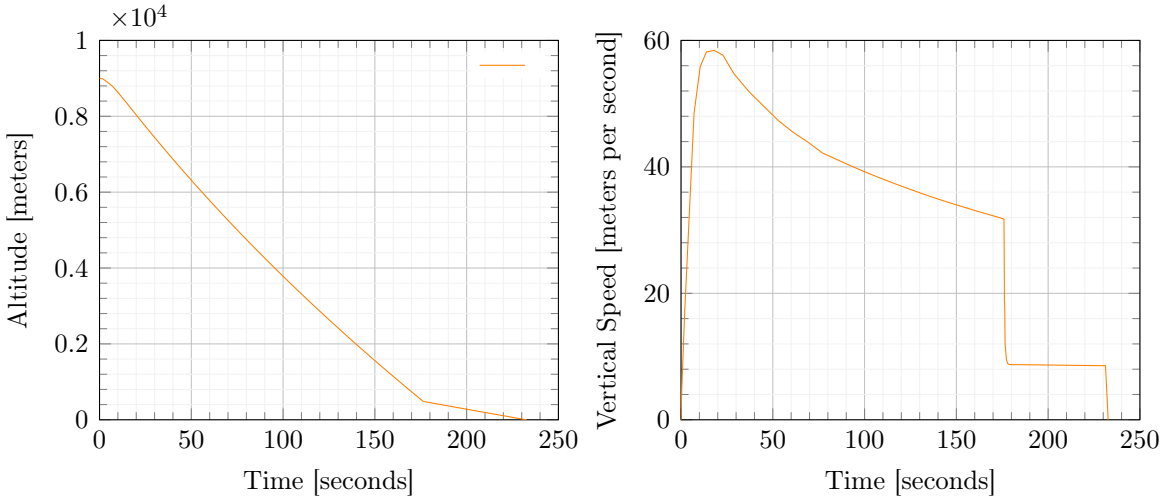

(a) Altitude vs Time

(b) Vertical Speed vs Time

Figure 2.32: Results of the Simulink Model

Data Ouput and Dissemination of Results

The Payload will produce a great deal of valuable data from the sensors in the CANSat section. The 9 data streams from the EMC will be logged as a .csv file to a 16GB SD card, while the frames from the radiation camera RASPix will be recorded on a separate card, within the Raspberry Pi OS. The data collected by the payload will go on to enrich our data bank and enable us to compare flight data and environmental conditions from our previous and future launches, including the already-flown mission at Machrihanish AFB, and our team's upcoming mission at the Shetland Islands, where our payload will fly once again aboard Darwin I, a subsonic version of the vehicle we are presenting at EuRoC. The reason why it is even possible for the team to fly such delicate and expensive hardware as the RASPix is because of a collaboration with the Institute for Research in Schools, who kindly donated the device. In exchange, Endeavour has planned and participated in a series of educational activities within the local high-schools of Edinburgh covering topics such the importance of space exploration technology, the fundamental physics of rocketry, and deep dives into how many of the sensors aboard Darwin actually work. Following EuRoC, we are scheduled to conduct programming workshops where, using Python together with popular libraries such as SciPy, Pandas and Matplotlib, students will manipulate, filter and visualise real flight data from our test campaigns and flights.

2.6 Active Flight Control Subsystem

Airbrake Design Overview

Darwin II features the ability to apply active braking during its ascent through the use of a servo-actuated, geared three-fin airbrake system, the final design for which is pictured in Figure 2.33. The purpose of such a system is to allow Darwin II to achieve a greater level of accuracy in reaching its target apogee: the logic is to design the rocket to overshoot the 9 km target, then, during the ascent phase, actively adjust the deployment of the airbrake fins based on live data measurements, such that sufficient drag is provided to allow the rocket to come to come to a stop as close to the target height as possible. This idea, whilst simple in concept, proved to be a complex challenge to execute in practice.

Figure 2.33: Render of the fully actuated airbrake system.

Safety

The Air-brakes are a critical feature of the rocket and its correct deployment (or lack thereof) can be the difference between a successful launch or expensive and dangerous fireworks. The first design feature that the need to have is to produce only axial forces; any other asymmetry could affect the rocket trajectory, deviating it from its parabolic path and potentially going sideways with the consequent risk. Thus, the system need to be completely symmetrical in the axial direction, both in design and

actuation. If one flap deploys sooner than the other, it will create a lateral force, deviating the rocket from its trajectory and making it going sideways. In order to achieve this, the 3 flaps are completely identical and all are actuated by the same central gear-rack system attached to the servo.

In order to ensure that the air brakes retract during failure mode, the system was originally planned to have three extension springs to retract upon failure. However, with issues fitting them into the assembly alternative options were explored. Spiral torsion springs were considered, but after contacting various spring manufacturers, the combination of size, force and rotational angle made this impossible. It was therefore decided that the failure mode retraction would be accomplished through a secondary redundant control system, which would control the servo to fully retract the brakes if the primary control system was lost.

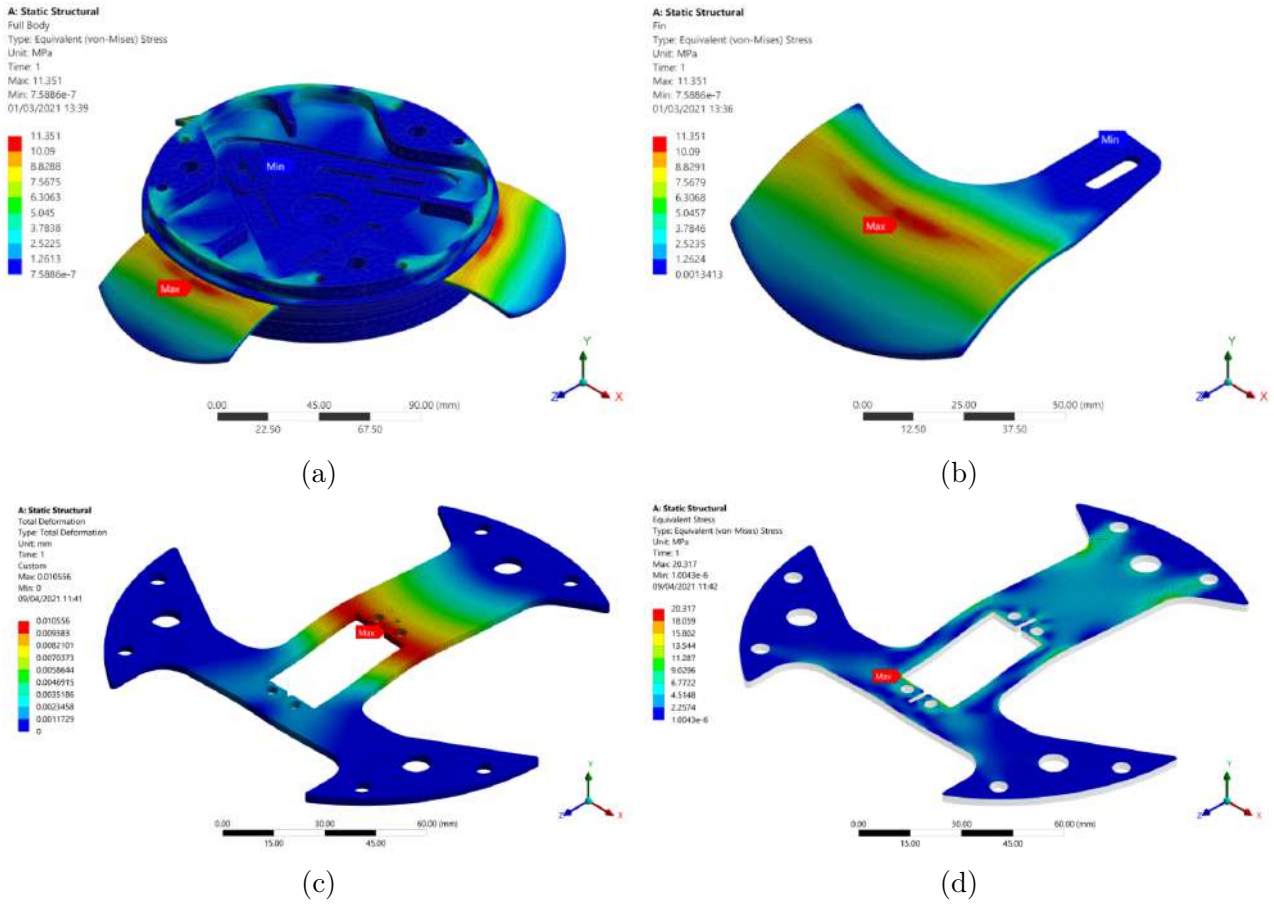

Figure 2.34: Airbrake system FEA key results: (a)

Finally, It is necessary to ensure that the flaps stiff enough for the application and the they do not jam and get stuck due to external loading. The later problem was solved by adding a layer of HDPE between the laser cut layers of aluminum and the flap. Due to it lubricant properties and low density the HDPE is perfect for this application. To ensure sufficient stiffness and structural integrity, several FEA using ANSIS and analytical calculation were made. The maximum deployment velocity of the Airbrakes is 200m/s, in order to avoid transonic effects. Thus we can calculate the maximum expected load for the biggest possible length (biggest area). The biggest uncertainty with this approach is that it is difficult to estimate the drag coefficient of a flap perpendicular to the flow attached to a surface. The literature estimates a Cd or around 1.1-1.2, but the load calculation a Cd of 1.6 was using, give a load per flap of 133N/flap. The results of this FEA analyses can be seen in figure 2.34. The maximum stress, as one intuitively guesses, is at the root of the flap. This is 11.3 MPa well below the 250 MPa of the yield stress of the aluminium 6086-T6 used, given a safety factor of around 23. Thus the second unknown to ask if the total deflection and stiffness of the flap. The analysis showed that only a maximal deflection of 0.1mm is expected in the worst case scenario. Then, it is safe to conclude that

the stack is structurally strong and stiff enough for this application, and the biggest focus should be on the control system and characterization of the system.

Active Control

Once the air brake design has been validated and there is confidence its mechanical integrity, the biggest problem to solve is how to control them. As mention previously the, the flaps are actuated by a gear-rack system controlled by a servo motor, thus, the output of our active control will be the angle of rotation of the servo. Since we now the length and number of teeth of the rack, it is easily shown that it is necessary 100 degrees of rotation to fully deploy the flaps.

One option to control the rotation of the serve would be estimate the drag force of the flaps using equation 2.3, but due to the uncertainties of drag coefficient this method is not reliable. Instead a combination of a model predictive and PID control have been used: First the ideal trajectory has been calculated using a 6-DOF model implemented in Simulink, predicting an apogee of 9Km, then a critically damped PID controller has been implemented into the FC. This critically damped PID control (not overshoot) compared the current velocity, acceleration and altitude (system inputs) with the previously calculated ideal path, then using a tabulate servo angle-drag table, it operated the flaps. So instead of being calculating every time step the whole trajectory, which will be very computationally expensive, the system is just compared the inputs with the ideal inputs, then actuated the servo to change the inputs and repeated until the ideal trajectory is reached.

3. Mission Concept of Operations Overview

For a nominal launch, the vehicle must be initialised successfully through the standard e-match procedure, launch with no structural failure, transmit data live to ground station, achieve apogee of 9 km exactly with payload and drogue chute deployment occurring, and main chute deployment at 500 m. Ideally both the vehicle and the payload is recovered successfully with GPS coordinates transmitting from both. See Figure 3.1 for more information on each phase of the rocket.

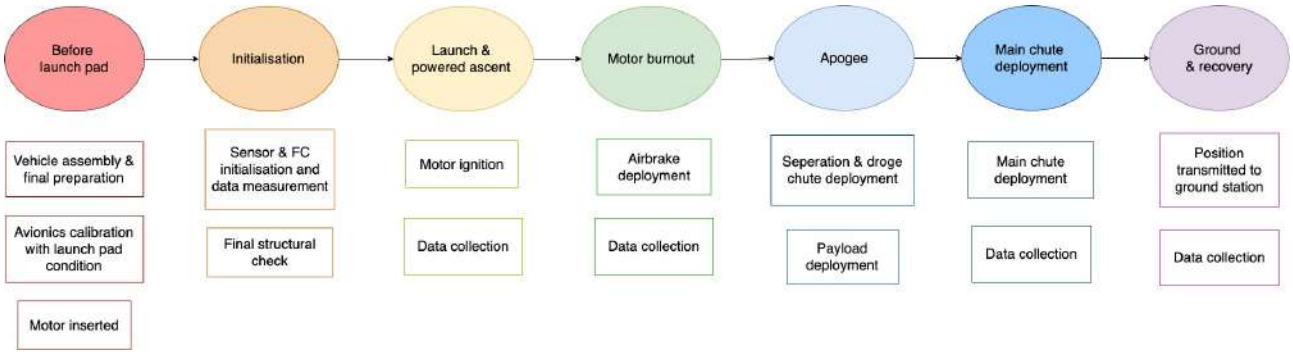

Figure 3.1: Rocket's stages

Before arriving at the launch pad, the vehicle and the payload should be fully assembled and motor loaded. While the structures, recovery, and payload teams work to prepare the vehicle and payload on the launch rail, avionics and software have to set the sensor 'initial' values for the launch area into the flight computer (on both vehicle and payload) for accurate measurements during flight. Once the structure is on the launch rail and sensors are calibrated, the initialisation sequence of the FC logic can be initiated on ground control with the software & avionics team. The GPS from both vehicle and payload should start transmitting. They will also ensure that sensors are collecting measurements and writing to the SD card with no issues, thus entering the armed state.

The motor should be ignited once everyone has cleared the launch pad. If the launch is successful, the rocket should enter the powered ascent phase where the motor propellant is burned. This is when the vehicle is under the highest acceleration and should fly without sustaining damage. The payload should begin collecting and logging data, although no meaningful data is expected as it is housed inside the nose cone. The FC logic should enter the powered ascent or 'Boosting phase' when the measured acceleration is positive (upwards). The Kalman filter should start filtering measurements for noise reduction and the FC boosting phase timer will be constantly extended until acceleration starts decreasing. This should signal the FC that the vehicle has entered the motor burnout phase, or 'Coasting phase'. The motor propellant has been exhausted and the FC should deploy the airbrake to adjust the projected apogee to exactly 9 km. The airbrake should operate with no failure and should generate enough drag to slow the rocket down for the target apogee along with the controller, which will be in charge of operate the Air brakes base on previous ground simulation and tabulated values. Alongside the controller, the FC should continue to collect, filter, and log data.

When the apogee is reached, the FC should enter 'DrogueDeployed State' by satisfying two of three conditions: 1. velocity passed a minimum threshold, 2. altitude starts dropping, or 3. pressure increases. During this state, the airbrake should be retracted and the recovery phase should begin. The recovery charges (CO_2 canisters) should be deployed with a digital signal from the FC activating the e-matches, causing the shear pins to shear off and the nose cone, coupled with the payload, is separated from the rest of the vehicle. This ejects the drogue chute and deploys it as well.

The separated nose cone and payload should start a different descent path down compared to the vehicle. The drogue chute should deploy automatically just after ejection and the sensor cluster in the CanSat should collect and log actual environmental data. The FC on the payload should also calculate

its altitude for deployment of the main chute and be transmitting GPS data to the ground station. During this face the Tender Descender will be connected to the drogue chute, carrying the load.

Meanwhile the vehicle should be coasting with the drogue chute deployed. The FC should be constantly measuring and comparing the altitude measurement to the defined main chute deployment altitude of 500 m. If the altitude is equal or below the stored value or if the time after drogue deployment surpasses the pre-set time limit of 315 sec, then the main chute should automatically deploy through the same separation as the drogue chute. The FC will activate the e-matched of the Tender Descender, breaking the plastic pin and releasing the main chute. After the main chute deploys, the FC enters 'MainDeployed State' with no additional recovery events in the vehicle. The vehicle will coast down until it reaches ground, and the FC should register touchdown when pressure and altitude is constant, and velocity is close to zero.

Throughout the different phases, the FC should be collecting and logging data onto the SD card on board, and transmit data to ground control. While the data collected after landing is irrelevant, the avionics bay should be functional as the most important data transmitted to the ground station after landing is the GPS coordinate for recovery. The avionics power source should last for 1.8 hours.

See Figure 2.10 for simulated flight trajectory, vertical velocity, acceleration, and stability of the vehicle during flight.

See Figure 2.2 for the thrust curve of our primary motor selection Cesaroni O3400 and secondary selection N5800.

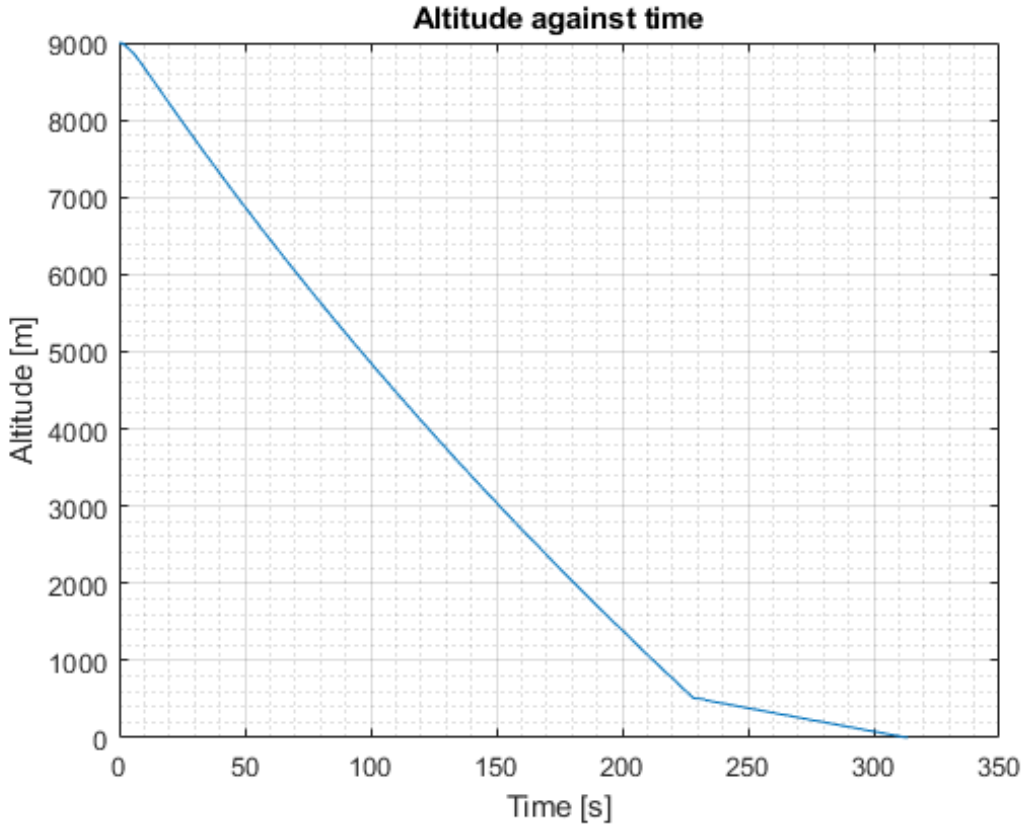

Figure 3.2: Altitude vs Time

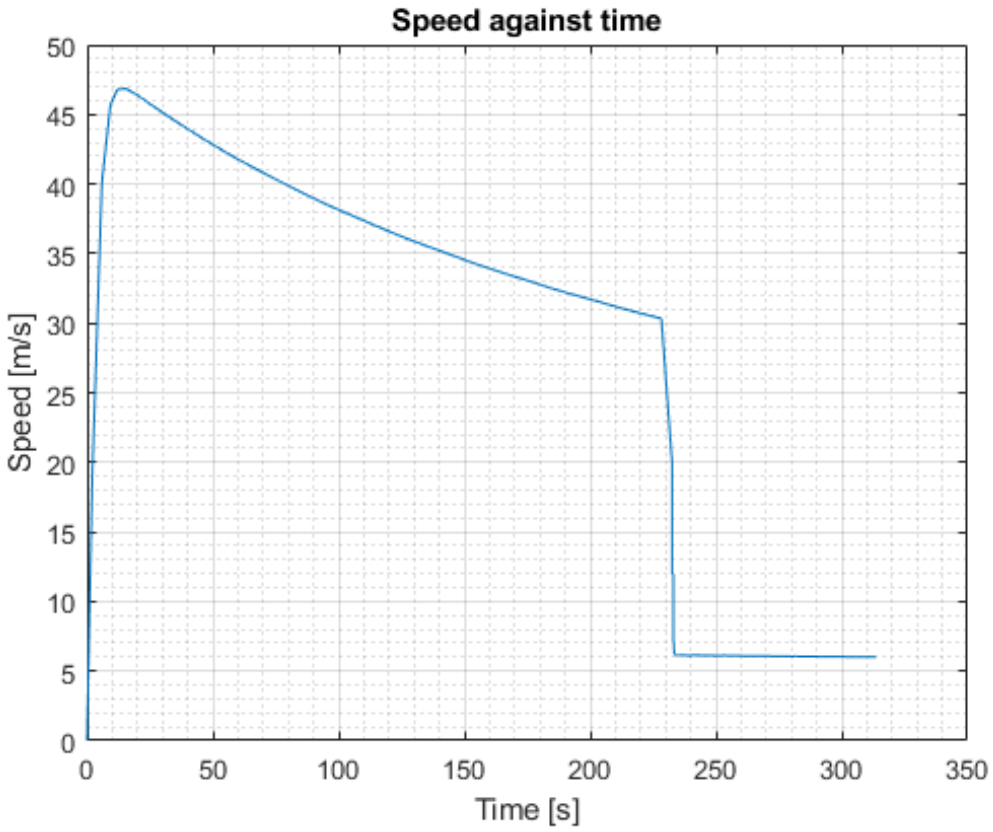

Figure 3.3: Speed vs Time

4. Conclusions and Outlook

We have successfully designed a vehicle with a deployable payload capable of surviving travel in the supersonic regime, control its apogee, transmit data real-time, and be recovered with minimal damage to vehicle and payload. We have also design and implemented an SRAD FC using Rust, and created simulation and numerical models in MATLAB and Simulink of the rocket, trajectory and expected loads. This is a huge milestone for the team, and it will the foundation for future projects.

Endeavour has accomplished major tasks through the pandemic. We have successfully designed and manufactured a new rocket from scratch when we had to do most of our work online and had restrictions on number of people that were allowed to meet. Even thought it is our first launch, we have implemented advanced concepts such as the airbrakes, advanced additive manufacturing technique, and so on to Darwin II. Furthermore, we will be able to use the data collected from EuRoC for an outreach workshop in the local high school. Overall, this year has been successful in giving students and younger pupils more experience in aerospace and STEM. This would not have been possible without the dedication from the team members.

While it has been a productive year, there were some aspects that did not go as well. As a young team, we were inexperienced in some rocketry-specific aspects and had to go through many iterations before we could finalise the design. As a result, manufacturing and testing was delayed. We didn't realise there was a gap between the engineering we've learned in university and the detail required for a good rocket design. In addition, connections to supports and advice had to be an on-going task as we were not as well-known as other student teams. However, as the years go by and the more events and launches endeavour participates in, the more well-connected the team will be.

We've learned a lot of lessons by building Darwin II. We now know how to construct a more realistic timeline as we understand the effects of lead times of manufacturing, iterations, and testing. In particular, we realised that PCB requires multiple iterations (starting from a breadboard) and smaller testing in between to successfully complete the avionics system and test it with recovery and rest of the hardware. In addition, we have gained more experience in utilising more materials and processes such as HDPE, wood, continuous fibre additive manufacturing, and utilising header pins that allows easier removal of PCB components. We've also learned the importance of team identity and culture in increasing productivity. Because of COVID-19, team socials had to be something that needed to be organised instead of something that naturally happens after a meeting. These socials helped team members to get to know each other and increased productivity and dedication.

For next year, we would like to dedicate more time in the logistics of designing a rocket. Creating a feasible timeline and altering it as necessary, updating databases of parts more rigorously, and ensure that handovers are done more systematically to ensure that the future years that join endeavour do not have to re-invent the wheel. We would also focus more on social media promotion of our work for better documentation and publicity. In the technical aspect of things, we would like to allow more time to test and do multiple iterations of the rocket. This will create a more robust and well thought out rocket. Even more quantitative and qualitative testing will be planned and carried out, and we'll take the lesson learnt to improve upon each iteration. In a similar argument, more simulations is something that we will aim for for next year. It will help us predict the behaviour of the rocket where testing cannot show us and ensure that the rocket will be safe. In addition, it will give endeavour more knowledge in FEA and CFD that can be used for years to come.

For next year's rocket, Darwin III, we would like to improve upon the concepts that we have implemented in Darwin II. A more advanced airbrake control system to improve the controller response and better manipulate the apogee, better bonding between composites and metal components, more in-house composite manufacturing, and advanced data communication between the flight computer and the ground station such as video live streams of flight footage.

A. System Data

Table A.1: Structural system data of Darwin II.

Parameter	**Value**	**Units**
Length	2.74	m
Vehicle & payload mass with propellant	34.5	kg
Propellant mass	10.93	kg
Payload mass	2.4	kg
Number of stages	1	-
Inner diameter	152.4	mm
Outer diameter	156.4	mm
Number of fins	3	-
Fin span	190	mm
Fin root length	360	mm
Fin tip length	70	mm
Target apogee	9000	m
Maximum velocity	575	m/s
Maximum acceleration	141	m/s^2
Flight duration	500	s
Motor burn time	6.4	s
Time from launch to apogee	40	s

Table A.2: Recovery system data of Darwin II.

Assembly	**Parameter**	**Value**	**Units**
Drogue	Coefficient of drag	1.6	-
	Diameter	24	inch
	Mass of CO_2 separation charge	23	g
	Mass of black powder used	0.24	g
	Deployment altitude	9000	m
	Descent rate	28	m/s
Main	Chute coefficient of drag	2.2	-
	Diameter	96	inch
	Mass of CO_2 separation charge	0	g
	Mass of black powder used	0.2	g
	Chute deployment altitude	500	m
	Chute descent rate	6	m/s

Table A.3: Telemetry system data of Darwin II.

Assembly	**Parameter**	**Value**	**Units**
Vehicle	Power duration	1.8	hours
	Communication frequency	433	MHz
	Output power (max.)	100	mW
	Communication range (w/ Yagi RX)	20000	m
Payload	Power duration	>1	hour
	Communication frequency	868	MHz
	Output power	100	mW
	Communication range (w/ Yagi RX)	15000	m
Ground station	Power duration	>2	hours
	Transceiver sensitivity (max.)	-120	dBm
	Communication range (uni-directional)	20000	m
	Communication range (omni-directional)	3000	m

B. Detailed Test Reports

B.1 Recovery testing

TO BE CONDUCTED SHORTLY

B.2 SRAD propulsion system testing

THIS PAGE IS INTENTIONALLY LEFT BLANK

B.3 SRAD pressure system testing

TO BE CONDUCTED SHORTLY

B.4 SRAD Flight computer testing

B.4.1 GPS Module Testing

Testing of the GPS module ensures that we can, without relying on the COTS FC, perform a successful recovery of the rocket once it has completed its flight.

To do so, the following tests were conducted:

Initial Breadboard Test:

This test comprised of building up the GPS circuit on a breadboard, supplying the BigRedBee with its required 5V power supply. Thereafter it could be moved independently around a local park in order to gauge the following:

- Whether it could achieve a firm satellite connection
- If it could sustain this connection
- How accurately it could pinpoint its location

After moving the setup around for roughly 1 hour, the setup was powered off and the results checked through a plug-in on Google Maps.

The results of the test indicated that although the module was slow to establish a satellite link, once it did it never disconnected. It should be noted that this was on a clear day with minimal cloud cover and few natural or man-made obstructions such as trees or buildings. As well as this, the data gathered was plotted and accurately portrayed the route taken during the testing period.

The test was deemed successful and the next stage could be explored.

First PCB Implemented Test:

After the success of the first breadboard test, the GPS module was then connected to the PCB designed to represent its circuit, the telemetry board. Connecting this up to the main controller board, the data from the GPS would be transmitted to our micro-controller and thereafter displayed on its serial monitor on a computer. This would allow us to observe if it satisfied the conditions outlined in the previous test.

Powering on the controller board and placing the setup next to an open window, the output from the micro-controller was observed.

The results indicated that the module now struggled to establish a connection, and when it did it quickly lost it. This was most likely a result of a lack of clear line-of-sight due to obstructions and cloud cover.

This test was repeated many times over the course of several weeks, with varying but unsatisfying results.

Testing Summary:

Over the course of testing the BigRedBee GPS module, the following observations were noteworthy:

- The module struggled with obtaining a satellite lock on cloudy days or when in the presence of obstructions

- When neither of these were hindrances were present, it still took longer than was permissible to establish a connection
- The data transmission to the micro-controller bottle-necked readings from other components as it transmits at only 1Hz

As a result of these findings, it was decided that a new module would be implemented to replace the BigRedBee. The module chosen was an Adafruit Ultimate GPS Breakout. It was chosen because it operated on the same transmission protocol as the BigRedBee, used the same pins to communicate with the controller board, had a faster transmission rate of 10Hz, and was recommended by our Payload sub-team.

Once acquired, it was subjected to the same tests as the previous module and proved to be faster at acquiring satellite connection, even indoors.

Therefore, this will be the module implemented in the final iteration of our FC PCB's.

B.4.2 Battery Testing

In order to guarantee sufficient flight time for the FC, testing how long the batteries would take to discharge was essential. Given that the threshold for full operation is 5V, this meant we were testing a discharge range of 2.4V. This threshold is defined by the components that operate on a 5V supply, e.g.: the Teensy micro-controller. If the battery's voltage drops below 5V, these components will no longer be able to operate at full functionality or in some cases, they won't operate at all.

To confirm how long our FC would function fully for, the following tests were conducted:

Controller Board Drain Test:

The first board to test was the controller board. This contains components such as the IMU's, barometers, and micro-controller. It is a relatively low impact load on the battery supply as all of the components have a current draw in the order of 10's of microamps up to a few milliamps.

A simple test setup consisting of an Arduino Uno and a potential divider breadboard circuit was used to monitor the voltage supplied to the PCB by the battery. The Adruino acted as an analogue voltage sensor, and the potential divider stepped down the voltage to within the Arduino's voltage range of 0-5V.

The board was then connected to the 7.4V battery and powered on. The Arduino's output was confirmed to be approximately 3.7V (which correlated to 7.4V before it was stepped down), and the setup was then left to run. It should be noted that the script controlling the voltage measurement printed the value every second, with the number of elapsed seconds displayed too.

After roughly 2.5 hours, the battery's voltage had dropped by only 0.44V, so the setup was powered down and disconnected as this showed ample running time.

The test was deemed successful and the next stage could be explored.

Testing Summary:

At the time of writing, not all of the tests could be completed for this section.

As it stands, the controller board can operate on battery supply for ample time to encompass standby on the launch pad, flight, and recovery.

Going forward, the telemetry and peripheral board, which contain the components that draw the most current and therefore use the most power, will be subjected to a battery drain test.

B.4.3 Barometer and Temperature Testing

A brief confirmation of the sensor module's temperature stimulus response had been conducted by simply heating the air around the module and observing the temperature rise in the data output. For the pressure, no testing has been conducted thus far.

At the time of writing however, not all of the tests could be completed for this section.

B.4.4 IMU Testing

As with the previous section, this sensor module's stimulus response was tested initially by rotating the board on different axes whilst observing the output. The response was registered, but further thorough testing needs to be conducted to gauge accuracy.

At the time of writing however, not all of the tests could be completed for this section.

B.4.5 RF Testing

Reading data successfully is one thing, but being able to observe these readings is even more so. As a result, it was vital to ensure that our transmission system would be sufficient when our rocket reached apogee. Initially, the idea was to use an amplifier on the telemetry board to boost the transceiver's signal to ground, but this proved to be a bad implementation as it would attenuate our signal significantly. As a result, we decided to implement a more sensitive ground station receiver instead.

This meant testing how well our FC and ground station communicated at increasingly further distances. Since our system now consists of two different types of antennas, uni-directional and omni-directional, these had to both be tested.

The following were tests conducted on these antennas:

Omni-directional Short Range RF Test:

To begin with, a simple breadboard implementation of the transceiver for our FC was connected alongside our ground station breadboard setup; both programmed on an Arduino Uno. They were then placed side-by-side, at a distance of a few inches, and the FC transceiver was set to transmit a simple data packet.

This proved successful and there were no issues reading the packet sent by the FC transceiver.

This meant we could increase the testing distance.

Omni-directional Mid Range RF Test:

Thereafter, the setup was taken outside where they were placed at each end of a street approximately 300m in length.

The same data packet transmission was sent from the FC transceiver and it was received successfully by the ground station transceiver.

Now the setup was ready for a long distance test.

Omni-directional Long Range RF Test:

Lastly, the same setup was taken to two local high points in the city, where the transceivers would be above most obstructions with clear line-of-sight of one another. These points where approximately 2.7km apart.

Following the same procedure, data was successfully transmitted across this distance with very few disruptions to the data stream.

The testing of the transceivers with the omni-directional antennas was deemed a success and the uni-directional antennas could now be tested.

Testing Summary:

At the time of writing, not all of the tests could be completed for this section.

However, we have confirmed that the omni-directional antenna functions appropriately and can be used for recovery in the final stages on the rockets descent.

Going forward, the uni-directional YAGI antenna will be tested under similar conditions to those outlined above. Thereafter, both antennas will be connected simultaneously to the ground station and tested in parallel with the Payload system.

B.4.6 Output Testing

The main controller board contains outputs that control other aspects of the rocket, i.e.: the air-brake system and the recovery initialisation. As a result, it is vital to ensure that these events are triggered appropriately.

In order to confirm this, the following tests were conducted:

Servo Motor Test:

The servo motor controls the extension of the air-brake blades in order to control the speed of the rocket in its cruising state. This means that the servo needs to rotate when supplied a signal from the micro-controller.

In order to test this, a simple script was written on an Arduino to open and close the air-brakes by rotating the servo between two limits. This had proved troublesome at first, but was easily remedied when the Arduino and the servo were connected to the same ground.

After this, it was just a matter of finding appropriate limits for the servo so that it will not stall or extend too far during nominal operation.

This test was deemed successful and so the next stage would be to test it directly from the controller board.

At the time of writing however, not all of the tests could be completed for this section.

E-match Ignition Test:

In order to deploy the parachutes to slow the descent of the rocket after it has achieved its apogee goal and begins its descent back to ground, e-matches are used to ignite a charge that will eject them from the rocket body. These e-matches require an electrical current in order to ignite. This therefore, needed to be tested.

In order to do this, initially, the e-matches were simply connected to a power supply and supplied with a current. This proved successful and they ignited without issue.

The next stage of testing would be to ignite them via the main FC controller board.

At the time of writing however, not all of the tests could be completed for this section.

B.4.7 Miscellaneous Testing

Iteration testing

When each iteration of the FC PCB's arrived, they needed to be tested thoroughly to ensure all electrical connections and supplies were correct in order for the FC to operate fully.

The electrical architecture has undergone 3 versions thus far, with a 4th version underway for the telemetry board. The main points to note from testing these iterations is as follows:

Version 1:

- Incorrectly placed capacitor creating short circuit
- Surface mount components too small to solder adequately
- Bluetooth breakout board no longer required
- Switch circuit resistor incorrectly connected
- Insufficient off-sheet connectors
- No 5V supply on the telemetry board

Version 2:

- Incorrect power supply for Teensy micro-controller
- Switch circuit transistor drew too much
- Antenna amplifier no longer required
- Servo output required an empty pin for PWM control
- Some diodes redundant

Version 3:

- Old GPS module (BigRedBee) to be replaced by Adafruit module
- Eggtimer COTS to be implemented

B.4.8 Future Tests:

Having been unable to complete all the necessary tests at the time of this submission, the following is a summary of what still needs to be tested before the competition:

- Telemetry and peripheral PCB battery drain test
- Pressure, temperature, and IMU data variation
- Uni-directional YAGI antenna range test tests
- E-match ignition PCB test
- Servo control PCB test

C. Hazard Analysis Report

Propellant Hazard Analysis

The most dangerous of all the hazardous material in the rocket is the motor propellant. It is a highly explosive material and must be treated with extreme care. As a COTS solid motor team, EuRoC will be handling and transporting the motor to the competition. We will receive the motor on the launch date and will prepare accordingly.

The motor will not be taken out of its packaging until we are absolutely sure that the vehicle is ready to go on the launch pad and the assembly checklist has been completed. All personnel handling the motor will be wearing safety goggle and the motor will be assembled horizontally to prevent any falls. Members assembling the motor will be extremely familiar and will follow the motor installation procedure and checklist very closely to ensure that the motor is secured. The vehicle will then be transported to the launch pad very carefully. Tasks that has to be done on the launch pad will be minimised and done so in a gentle manner for safety. If the launch is unsuccessful, the members will follow the mishap launch checklist to disassemble the motor assembly and deactivate it accordingly if deemed to be safe.

Separation Charge (CO_2 Canister and Black powder) Hazard Analysis

While vital for recovery, CO_2 canisters and black powder can be dangerous if handled incorrectly. Our main separation charges are the CO_2 canisters, one main and one redundant. These require a small amount of black powder and an e-match to pressurise and separate the vehicle. Our main chute deployment system, the tender descender, also requires a small amount of black powder to actuate. Recovery testing will allow us to know the exact amount of black powder we need, and precise measurement will ensure that we use the minimum that we need for safety and efficiency.

Both the black powder and the CO_2 canisters will be available through the EuRoC pyrotechnical shop and will be transported and handled correctly until the launch date.

Once the black powder and CO_2 canisters are in our possession, we would have to ensure that it is handled safely. All members that will handle black powder will be wearing gloves and all members working in the recovery assembly will be wearing safety goggles. No naked flames or sparks will be near the black powder to prevent any accidental ignition.

D. Risk Assessment

Table D.1: Risk assessment matrix of Darwin II.

Failure mode	Mission Phase	Failure probability	Mishap severity	Criticality ranking	Comment and justification
Insufficient pressurisation during recovery	Apogee	1	3	3	Check seal during assembly and apply additional adhesives as needed
Shear pins not breaking	Apogee	1	3	3	Design according to rocketry standard Test by previous designers
Payload detached from nose cone after separation	Apogee and shortly after	1	3	3	Apply adhesives during final assembly
Detachment of metal tip of nose cone	All	1	1	1	Minor effect on aerodynamic performance
Drogue chute deployment failure	Apogee	2	3	6	Receive advice from expert rocketeer in UK in folding and storage of drogue chute
Battery disconnected during flight	All	1	3	3	Tape/hot glue on connection
Connection from vehicle/payload to ground control lost	All	2	3	6	All members focused on tracking vehicle for yagi direction with binoculars
Avionics fuselage connection failure during flight	All	1	2	2	Fuselage is non-structural component of section & components are securely attached
Airbrake gear failure (seizing/breaking)	Motor burnout to apogee	2	1	2	Airbrake actuates radially and therefore no aerodynamic force will be applied if failed
Detachment of motor sleeve from motor bulkhead	All	2	2	4	Redesign motor bulkhead to increase interference between bulkhead and motor sleeve
Fin connection failure	All	2	3	6	Increased attachment area & additional GFRP fillet on fin
Leading and trailing edge falling out	All	2	1	2	Minor performance deterioration
Aft cone failure due to motor thrust	Powered ascent	2	3	6	Additional metal reinforcement on area above motor thrust ring
Electronics bay rods buckling	Powered ascent	1	3	3	Rod made from steel & increased thickness Analytical and numerical analysis
Motor sleeve buckling	Powered ascent	1	3	3	Increased thickness of the sleeve & Load carried also by fuselage and motor bulkhead
Airframe buckling	Powered ascent	1	3	3	Increased of the wall thickness and general strength
Shearing of airframe joint bolts	All	1	3	3	Increased number of bolts & Glued connections
Failure of joints under bending	Powered ascent	1	3	3	At least one body diameter in the interfaces
Rocket becomes unstable at supersonic velocities	Powered ascent	1	3	3	OpenRocket, RasAero and Star CCM+ analysis
Motor failed ignition	Launch	2	2	4	Checklist and inspection of mortor and e-matches
Entanglement of the parachutes	All	1	3	3	Proper folding of the parachutes
Shock cord breaking	Recovery	1	3	3	Analytical calculation and safety factor when selecting the diameter
Tender descender not working properly	Recovery	2	3	6	Use of the device according to manufacture
Run out of battery	All	1	2	2	Analytical analysis of the battery duration Plus 1h of total battery
Poor wire connection	All	1	3	3	Use of block terminal to secure the wires Thoroughly test of the wires connection prior to launch
Improper alignment of the fins	Powered ascent	2	2	4	Correct assembly of the fins Aligment with laser system
Radio frequency interference	Recovery	2	2	4	Two body diameters of RF transparency around the emitters Use of different frequency Use of Yagi and onmidirectional antennas in ground station

E. Checklists & Procedures

E.1 Shipment & Edinburgh departure

Shipment checklist:

- Toolbox
  - Screwdriver, allen key, spanners
  - Nippers, tweezers, pliers
  - Soldering iron, solder, soldering tape, solder sucker, wire
  - Epoxy, superglue, masking tape, duct tape, hot glue
  - Knife, scissors
  - Dremel, Dremel bits
  - Electrical adapters
- Fasteners
  - Avionics Bay:
    - 11x M3's for PCB mounting
    - 7x M2's for securing SD card reader and barometers
    - 12x M3's for securing IMU's
    - 4x M3's for securing COTS FC
    - 8x M2.5's for securing Raspberry Pi Zero's
    - 2x M2.5's for securing GPS module
    - 4x M2.5's fr mounting Raspberry Pi camera module
    - 4x M3's for mounting the antenna support
- Main vehicle
  - Nose Cone
  - Nose cone tip
  - Shear pins
  - Electronics bay assembly and recovery bay
  - Lower body fuselage
  - Motor bulkhead
  - Motor sleeve
  - Aft cone
- Recovery system
  - Main Parachute
  - Drogue Parachute
  - Tinder Rocketry RAPTOR CO2 Ejection System, 2x
  - Rocketman Shock Cord
  - 3 Rocketman Y-harness

  - 2 Eye Bolt M8 x 18mm
  - 25 x 0.3m E-match
  - 2 23g CO2 Canister
  - Fruity Chutes L2 Recovery Tether
- Aerials
- Banner (pop up and stand)
- Technical poster
- PPE Boots & goggles
- Binoculars
- Spare 3D print parts and sensors

Edinburgh departure:

- First-aid kit
- Masks
- Hard copy of documents
  - Technical report
  - Checklist & procedures
  - Other logistics related documents
- Avionics & ground control
  - Completed avionics bay and ground control
    - 3 PCB's
    - 3 Batteries
    - COTS flight computer
    - Antennas
    - SD card
    - Independent camera module
  - Cables for antenna (uFL to SMA), inter-PCB connection (jumpers), and micro-controller (USB-A to micro-USB)
  - Battery charger
  - SD card reader
- Payload
  - CanSat
  - CubeSat
  - Batteries
  - COTS flight computer
  - Antennas
  - Recovery system
  - Fasteners

E.2 Pre-launch assembly checklist & procedure

E.2.1 Lower section

- Motor sleeve attached
- Fin attachment bonded
- Fin inserted
  - Fin edges inserted and attached
- Aft cone ring interested
- Full lower assembly glued and assembled
- Motor inserted
- Aft. bolted to the lower assembly
- Motor bolted to motor bulkhead
- motor bulkhead attached to lower assembly fuselage

E.2.2 Airbrake

- Rack & gear meshed and secured
- Check correct actuation of the fins
- Check correct and successful actuation of the servo
- Avionics rod secured to the motor bulkhead

E.2.3 Avionics bay

Assembly procedure:

1.  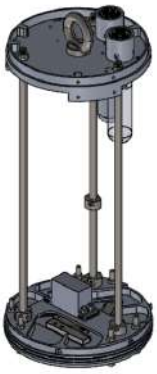

   Position and secure the rod clasps at the right location on the rods with M3 screws. Slide into airbrake and recovery bulkhead assembly and secure with M6 nuts.

2. 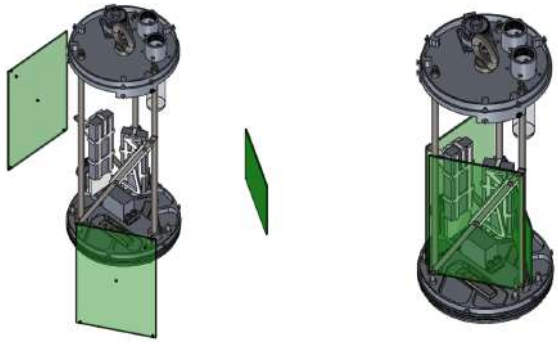

   Mount cross-rods and PCB assemblies; including battery, camera and GPS mounts, and align with cross rods using hole positions. Then, attach assembly to the 3 structural rods via the pre-positioned clamps.

3. 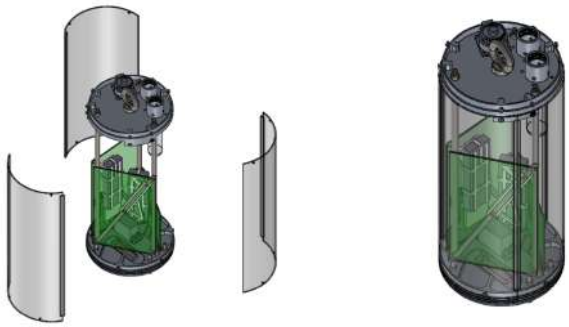

   Position the 3 outer "skin" sections and attach to recovery bulkhead assembly and airbrakes via. 6x M3 bolts at top and bottom.

Checklist:

- recovery bulkhead is assembled
- Collar secured
- PCB secured
- PCB is working
- Connections between boards and to e-match and servo outputs
- Side panel attached

E.2.4 Recovery section - INCOMPLETE CHECKLIST & PROCEDURE

Hardware assembly procedure:

1. 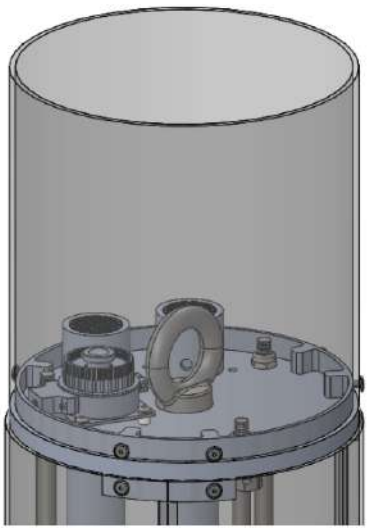

   Assemble recovery bulkhead by securing camera, canisters and eyebolt. Slide bulkhead onto electronics bay rods and secure with nuts.

2. 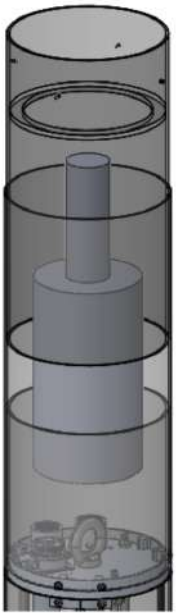

   Connect shock cord to eyebolt. Position and secure coupling tube and recovery bay body tube. Insert and organise parachutes and cords.

Recovery procedure: linking parachutes

Checklist:

- try to see if recovery section is sealed by pushing air into it or something through one shear pin hole?
- all recovery connections are secure
- no tangles in shock cords
- black powder in tender descender and CO_2 canister
- avionics rod secured

E.2.5 Nose cone - INCOMPLETE CHECKLIST

Assembly procedure

1.  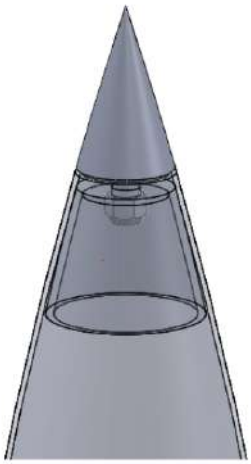

   Secure metal tip using threaded end and M10 nut.

2. 

   Apply adhesive to payload spring plate and payload rail guides, and position in nose cone.

3.

Compress spring by inserting payload and payload separator plate.

checklist

- Payload secured to nose cone
- Tip secured

Payload - INCOMPLETE CHECKLIST

- Cube and Can connected
- recovery all inside
- sensors are on and connected

E.2.6 Entire vehicle without motor - INCOMPLETE CHECKLIST

Assembly procedure:

1.

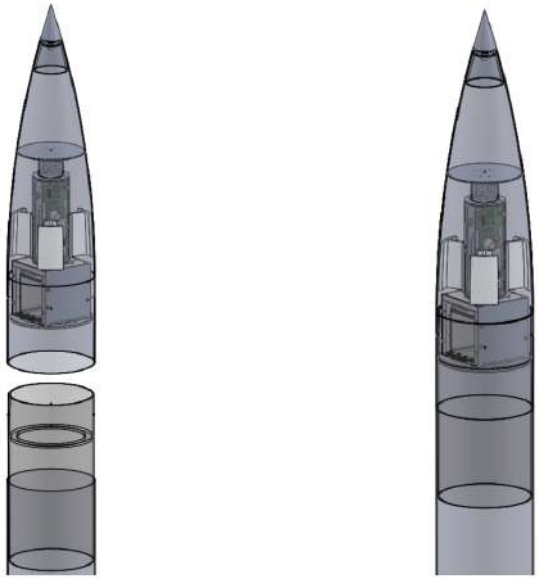

Slide nose cone assembly over upper coupler tube and secure in place with shear pins.

Checklist:

- Shear pins inserted

E.3 Launch day

E.3.1 Motor installation Procedure

1.

Slide the motor into the motor sleeve assembly.

2. 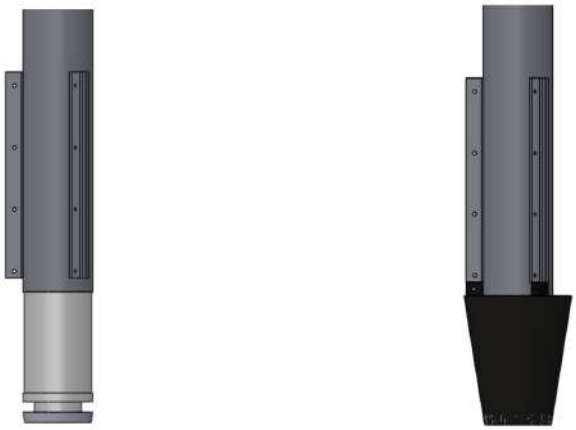

Slide on aft cone and align tab on aft cone with tab on fin attachment.

3. 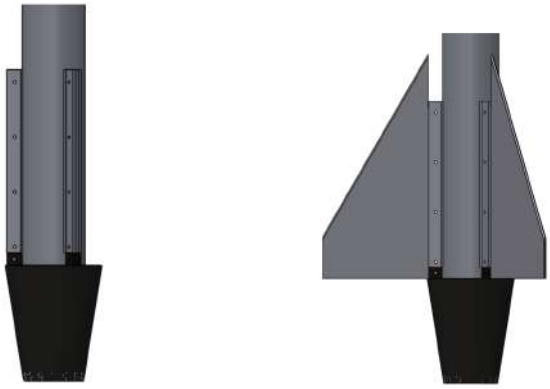

Insert fins into aligned tabs and secure with M5 bolts and nuts.

4. 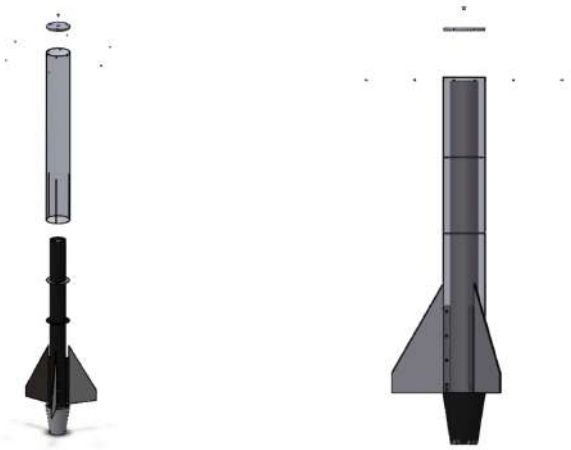

Slide in the assembly from step 4 to lower body fuselage.

5.

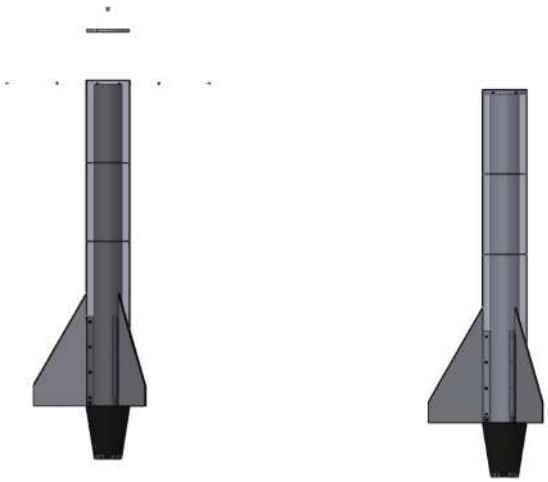

Insert motor bulkhead on top and secure with 6 M3 screws and screw in motor from top with 3/8x1/2 bolt.

E.3.2 Launch checklist

- sensor calibration
- avionics initialisation
- filming setup for recording & recovery

E.3.3 motor mishap disassembly PROCEDURE & CHECKLIST

- Remove rocket from the launch pad
- Cut current from e-matches Remove e-matches and any other activation device
- Move rocket to a safe working location
- Inspect the motor

E.3.4 motor disassembly after recovery PROCEDURE

- Remove Avionics bay from Airbrakes
- Unscrew rods from motor bulkhead
- Remove airbrakes
- Remove motor retention bolt
- Remove Aft cone bolts
- Slide out motor

F. Engineering Drawings

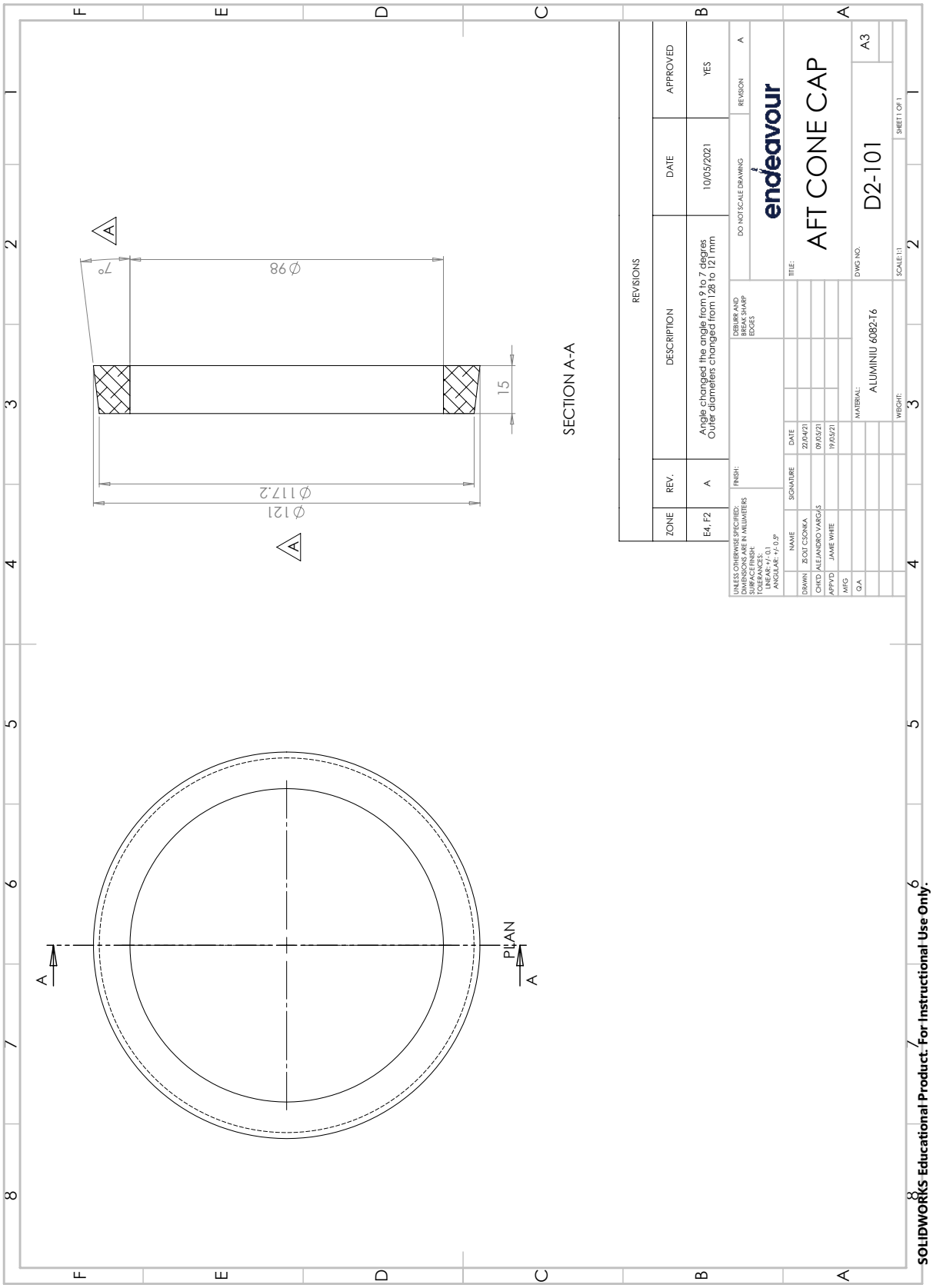

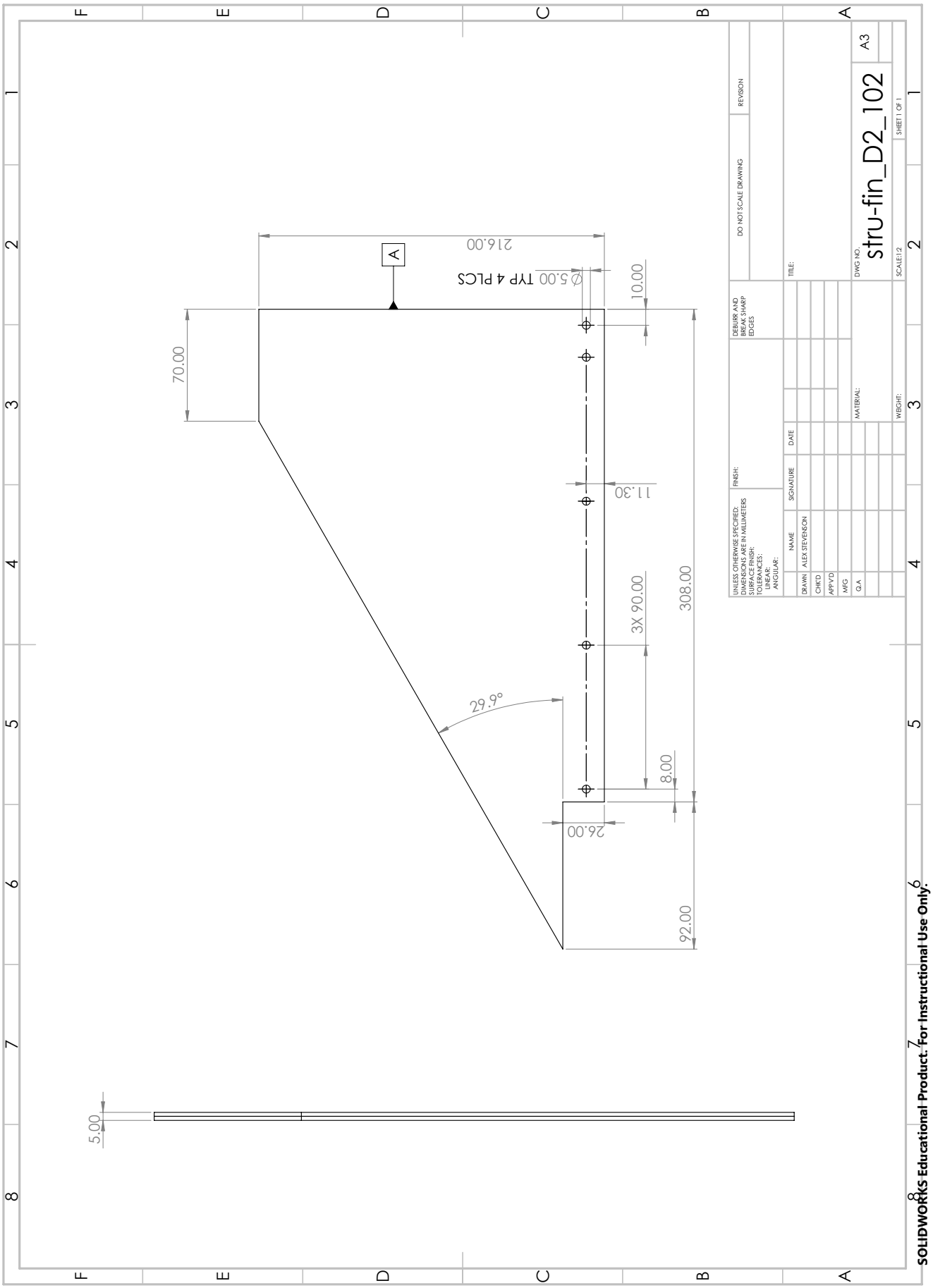

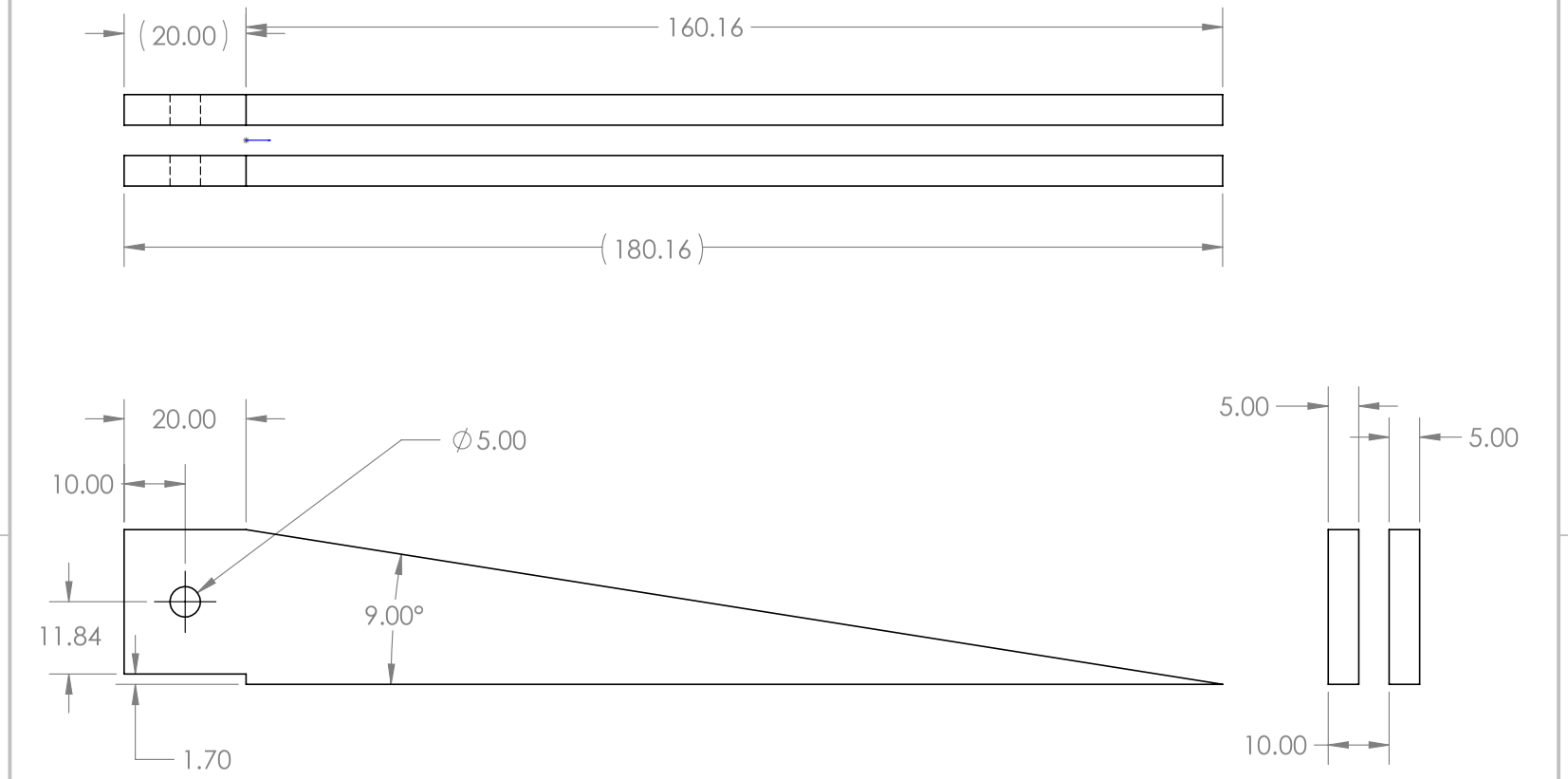

		UNLESS OTHERWISE SPECIFIED:		NAME	DATE
		DIMENSIONS ARE IN MILIMMITERS TOLERANCES: ±0.125MM FRACTIONAL ± ANGULAR: MACH ± BEND ± TWO PLACE DECIMAL ± THREE PLACE DECIMAL ±	DRAWN	BCM	
			CHECKED		
			ENG APPR.		
			MFG APPR.		
			Q.A.		
		INTERPRET GEOMETRIC TOLERANCING PER:	COMMENTS:		
		MATERIAL THORNEL MAT VMA			
NEXT ASSY	USED ON	FINISH			
APPLICATION		DO NOT SCALE DRAWING			

ENDEAVOUR

TITLE:

AFT CONE CONNECTOR

SIZE	DWG. NO.	REV
A	D2-103	A

SCALE: 1:1 | SHEET 1 OF 1

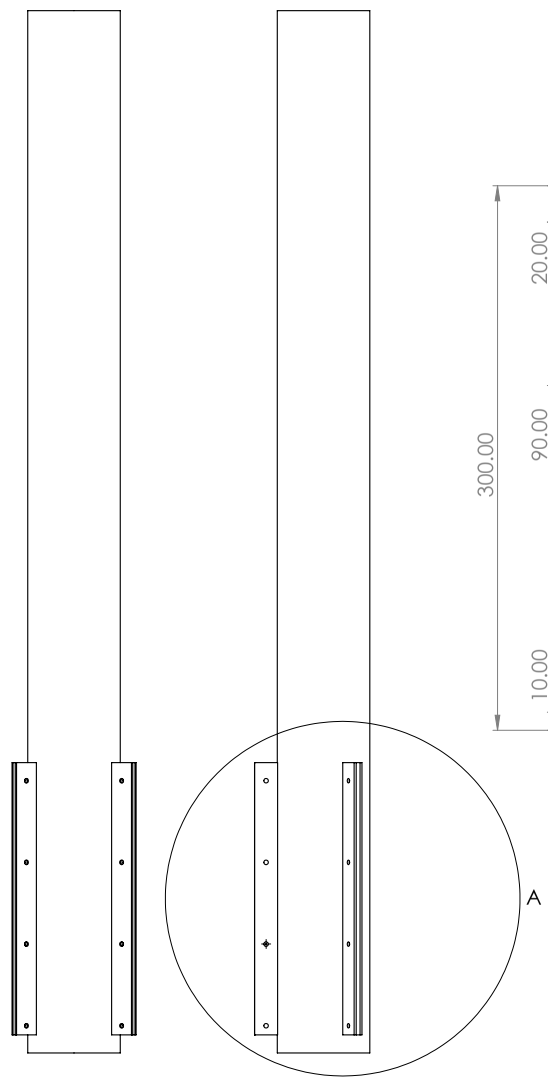

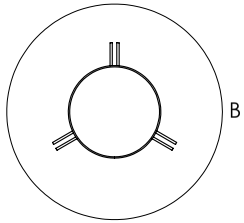

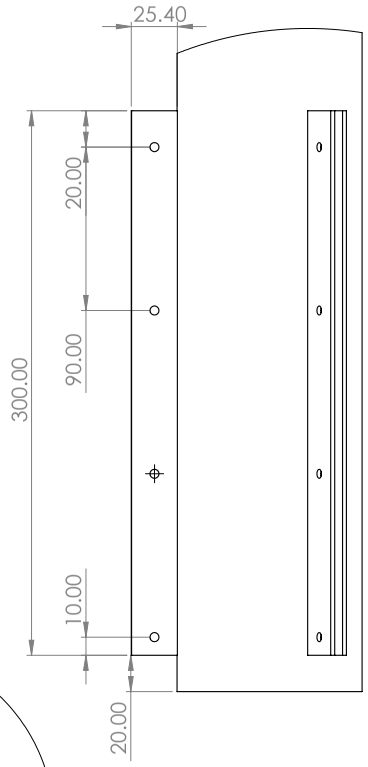

DETAIL A
SCALE 2 : 5

DETAIL B
SCALE 1 : 1

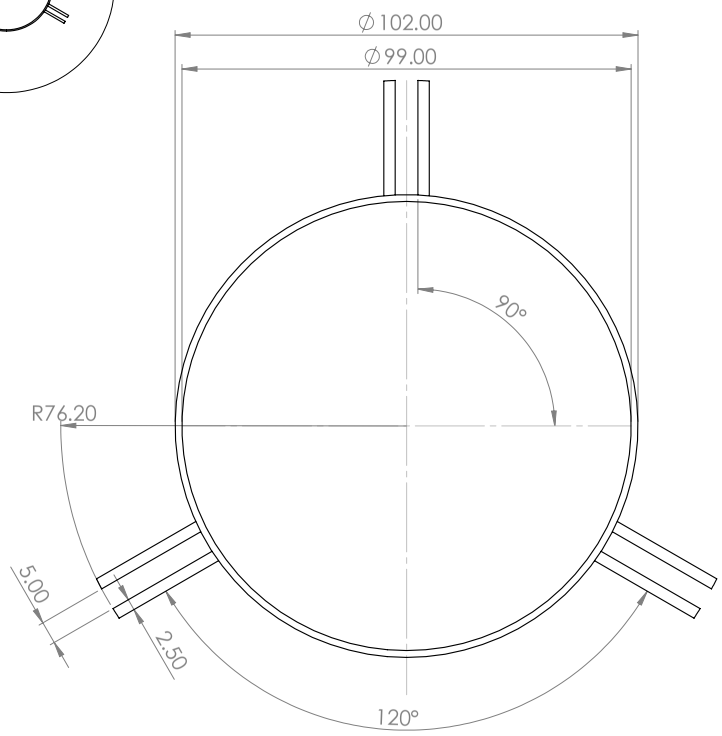

UNLESS OTHERWISE SPECIFIED: DIMENSIONS ARE IN MILLIMETERS SURFACE FINISH: TOLERANCES: LINEAR: ANGULAR:		FINISH:		DEBURR AND BREAK SHARP EDGES	DO NOT SCALE DRAWING	REVISION
	NAME	SIGNATURE	DATE		TITLE:	
DRAWN						
CHK'D						
APP'V'D						
MFG						
Q.A				MATERIAL:	DWG NO.	A3
					main part of fin attachment_D2_	
				WEIGHT:	SCALE:1:10	SHEET 1 OF 1

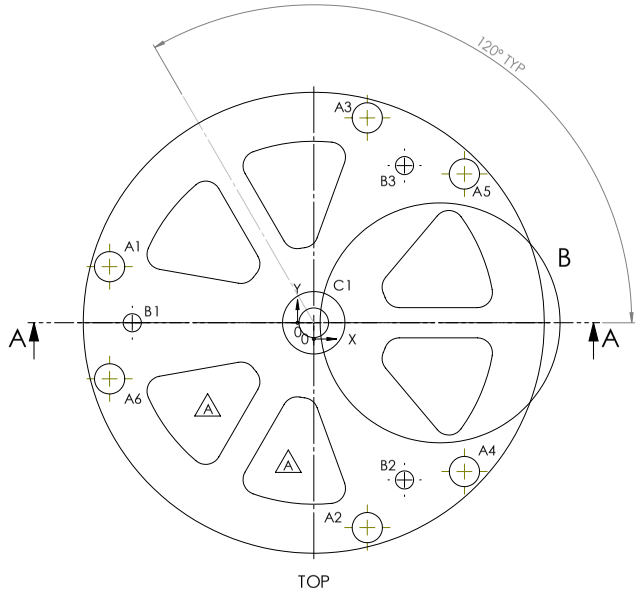

TOP

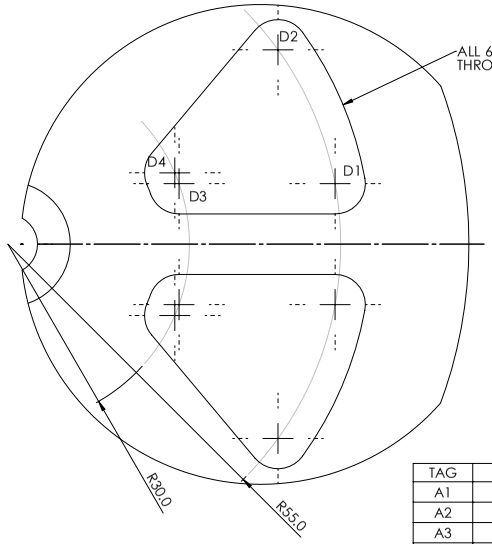

DETAIL B

SCALE 2 : 1

TAG	X LOC	Y LOC	SIZE
A1	-67.5	18.54	⌴ Ø10.0↧5.0
A2	17.7	-67.73	⌴ Ø10.0↧5.0
A3	17.7	67.73	⌴ Ø10.0↧5.0
A4	49.8	-49.19	⌴ Ø10.0↧5.0
A5	49.8	49.19	⌴ Ø10.0↧5.0
A6	-67.5	-18.5	⌴ Ø10.0↧5.0
B1	-60	0	M6x1-H6 THRU
B2	30	-51.96	M6x1-H6 THRU
B3	30	51.96	M6x1-H6 THRU
C1	0	0	Ø 9.8 THRU ALL ⌴ Ø 20.6 ↧ 6.4
D1	54.1	10.0	Ø10.0 THRU
D2	44.6	32.1	Ø10.0 THRU
D3	28.3	10.0	Ø10.0 THRU
D4	27.6	11.8	Ø10.0 THRU

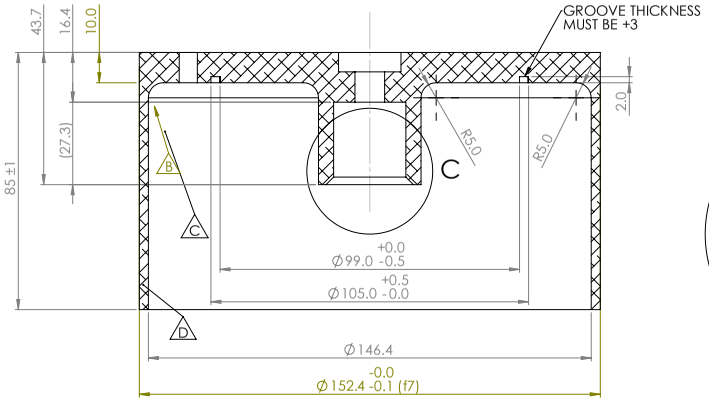

SECTION A-A

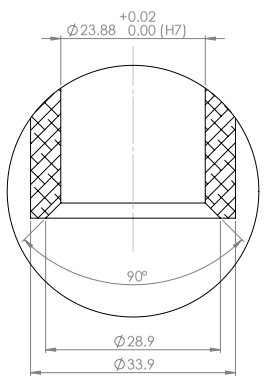

DETAIL C

SCALE 2 : 1

REVISIONS				
ZONE	REV.	DESCRIPTION	DATE	APPROVED
E9, F10	A	Milled holes added.	18/05/2021	Yes
C10	B	Addition of the external flange	17/08/2021	Yes
C10	C	External flange added in rev B is changed to a shoulder with an outer diameter 5mm smaller than the bulkhead's.	23/08/2021	Yes
B10	D	Shoulder added in rev C is replaced to a flange similar to rev B, but longer.	24/08/2021	

UNLESS OTHERWISE SPECIFIED:
DIMENSIONS ARE IN MILLIMETERS
SURFACE FINISH:
TOLERANCES:
LINEAR: ±0.1 mm
ANGULAR: ±0.5°

FINISH:

DEBURR AND BREAK SHARP EDGES

DO NOT SCALE DRAWING | REVISION D

endeavour

	NAME	SIGNATURE	DATE
DRAWN	ZSOLT CSONKA		31/08/21
CHK'D			
APPV'D			
MFG			
Q.A			

TITLE: MOTOR BULKHEAD

MATERIAL: ALUMINUM 6082-T6

WEIGHT: 685.9 g

DWG NO. D2-111

A2

SCALE:1:1 | SHEET 1 OF 1

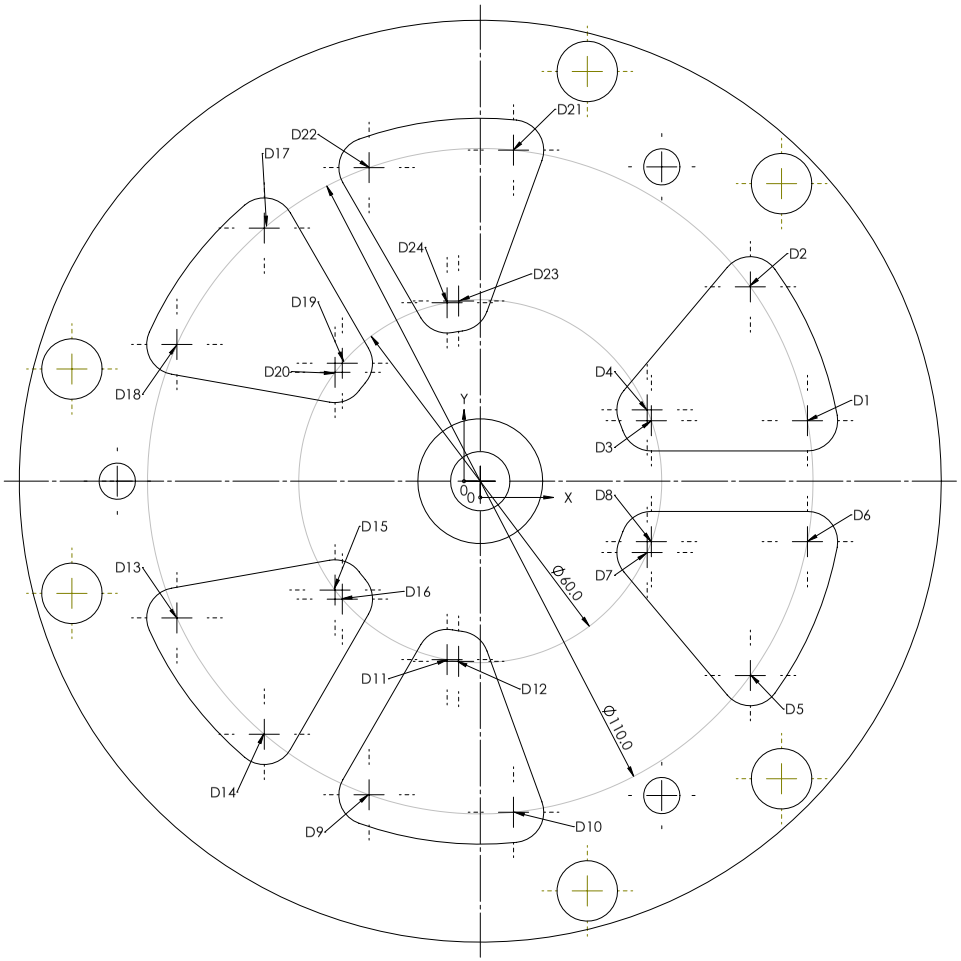

TAG	X LOC	Y LOC	SIZE
A6	-67.50	-18.54	⌴ Ø10.0↧5.0
D1	54.08	10.0	Ø10.0 THRU
D2	44.64	32.12	Ø10.0 THRU
D3	28.28	10.0	Ø10.0 THRU
D4	27.58	11.79	Ø10.0 THRU

REVISIONS				
ZONE	REV.	DESCRIPTION	DATE	APPROVED
	B	Addition of the external flange	17/08/2021	Yes
	C	External flange added in rev B is changed to a shoulder with an outer diameter 5mm smaller than the bulkhead's.	23/08/2021	Yes
	D	Shoulder added in rev C is replaced to a flange similar to rev B, but longer.	24/08/2021	

UNLESS OTHERWISE SPECIFIED:
DIMENSIONS ARE IN MILLIMETERS
SURFACE FINISH:
TOLERANCES:
LINEAR: ±0.1 mm
ANGULAR: ±0.5°

FINISH:

DEBURR AND BREAK SHARP EDGES

DO NOT SCALE DRAWING | REVISION D

endeavour

	NAME	SIGNATURE	DATE
DRAWN	ZSOLT CSONKA		24/08/21
CHK'D			
APP'D			
MFG			
Q.A			

TITLE: MOTOR BULKHEAD

MATERIAL: ALUMINUM 6082-T6

DWG NO. D2-111 | A2

WEIGHT: 679.4 g | SCALE:1:1 | SHEET 1 OF 1

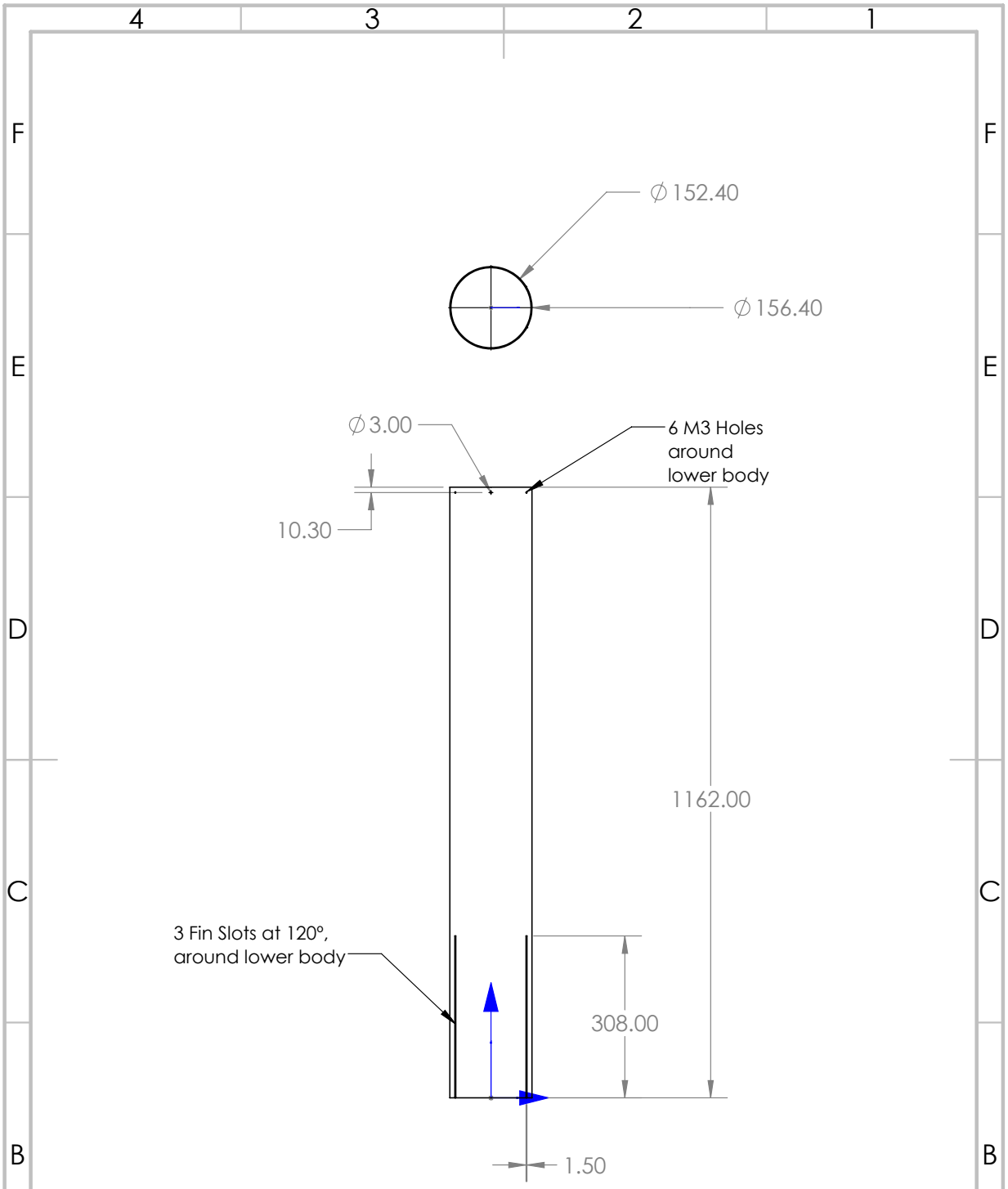

UNLESS OTHERWISE SPECIFIED: DIMENSIONS ARE IN MILLIMETERS SURFACE FINISH: TOLERANCES: +-0.125mm LINEAR: ANGULAR:	FINISH:		DEBURR AND BREAK SHARP EDGES	DO NOT SCALE DRAWING	REVISION	A
				ENDEAVOUR		
	NAME	SIGNATURE	DATE	TITLE:		
DRAWN	BCM			Lower Body		
CHK'D						
APPV'D						
MFG						
Q.A				DWG NO.		A4
				D2-112		
				WEIGHT:	SCALE:1:10	SHEET 1 OF 1

MATERIAL: Hexcel AS4C (3000 Filaments)

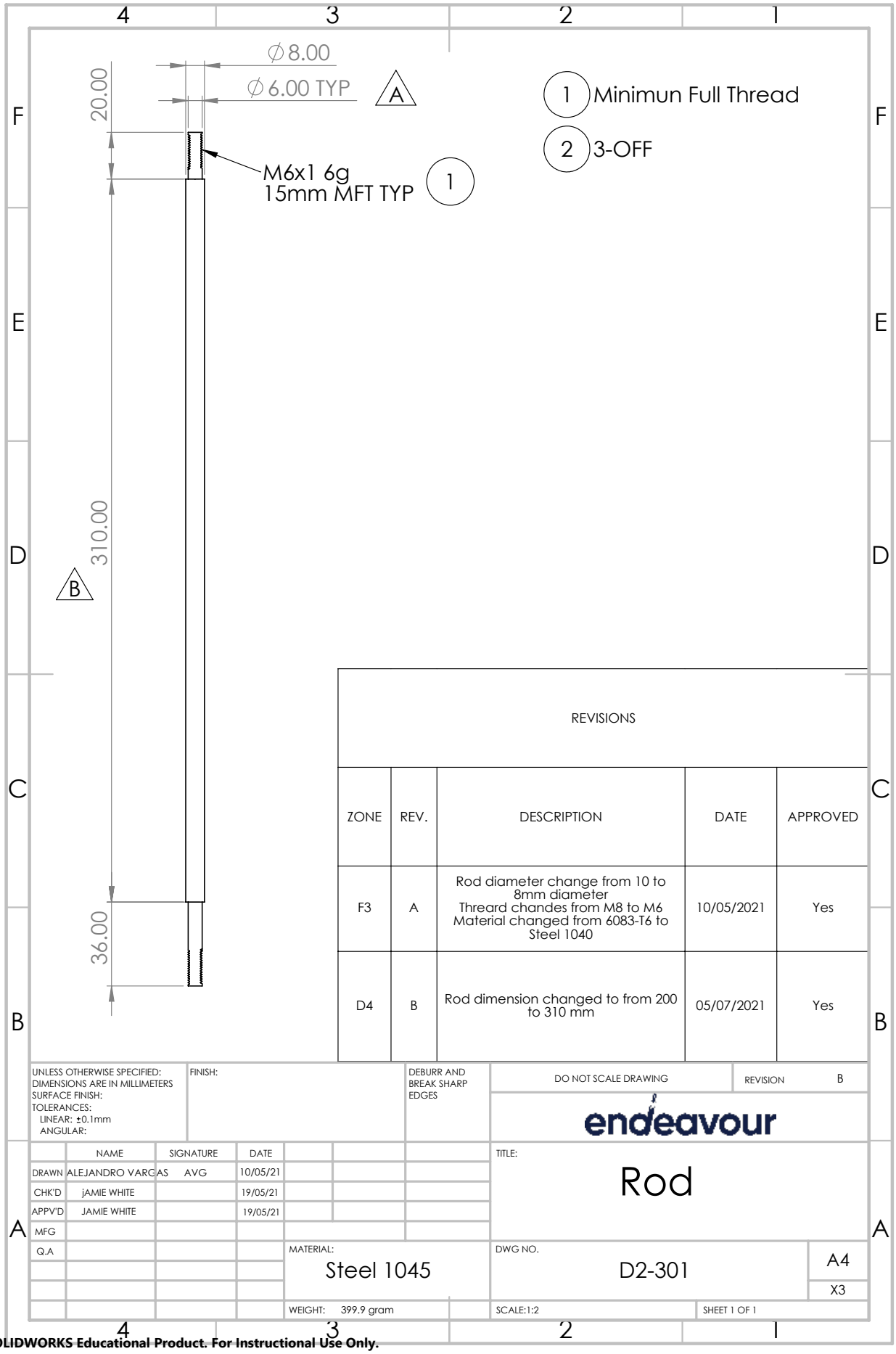

REVISIONS				
ZONE	REV.	DESCRIPTION	DATE	APPROVED
F3	A	Rod diameter change from 10 to 8mm diameter Threard chandes from M8 to M6 Material changed from 6083-T6 to Steel 1040	10/05/2021	Yes
D4	B	Rod dimension changed to from 200 to 310 mm	05/07/2021	Yes

UNLESS OTHERWISE SPECIFIED: DIMENSIONS ARE IN MILLIMETERS SURFACE FINISH: TOLERANCES: LINEAR: ±0.1mm ANGULAR:		FINISH:		DEBURR AND BREAK SHARP EDGES		DO NOT SCALE DRAWING	REVISION B
	NAME	SIGNATURE	DATE			TITLE:	
DRAWN	ALEJANDRO VARGAS	AVG	10/05/21			Rod	
CHK'D	jAMIE WHITE		19/05/21				
APPV'D	JAMIE WHITE		19/05/21				
MFG							
Q.A				MATERIAL: Steel 1045		DWG NO. D2-301	A4
							X3
				WEIGHT: 399.9 gram		SCALE:1:2	SHEET 1 OF 1

TAG	X LOC	Y LOC	SIZE
A1	-51.96	30	Ø6.5 THRU
A2	0	-60	Ø6.5 THRU
A3	51.96	30	Ø6.5 THRU
B1	-45	-2	Ø29.5 THRU
B2	-23.14	-40.91	Ø29.5 THRU
C1	0	0	Ø10.0 THRU

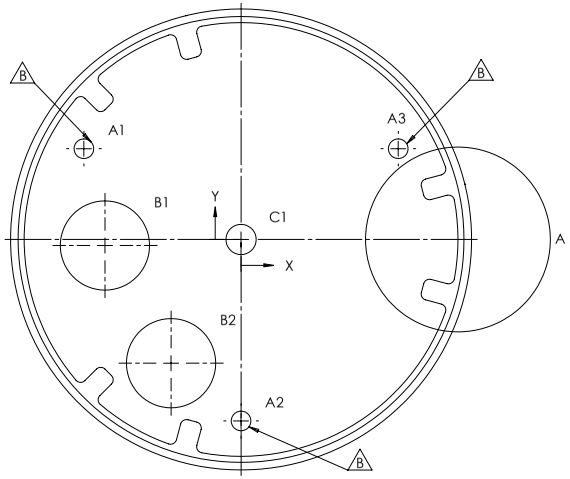

TOP PLAN

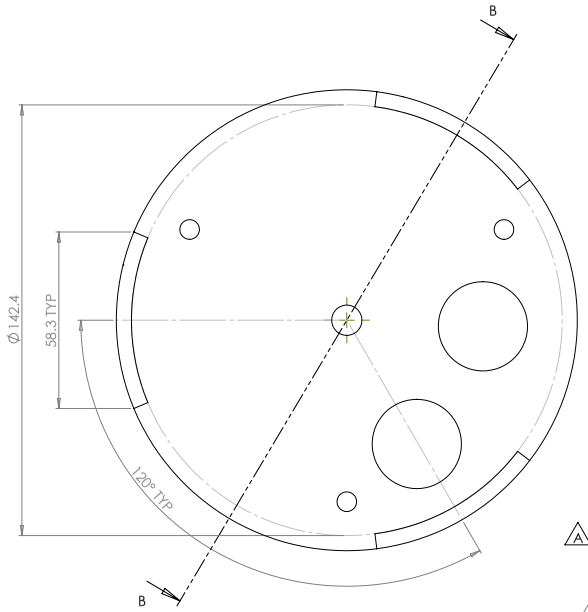

BOTTOM

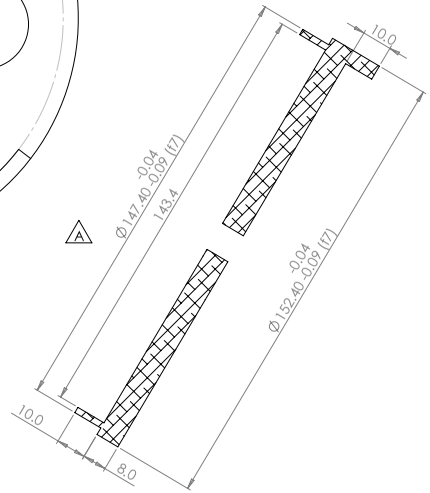

SECTION B-B

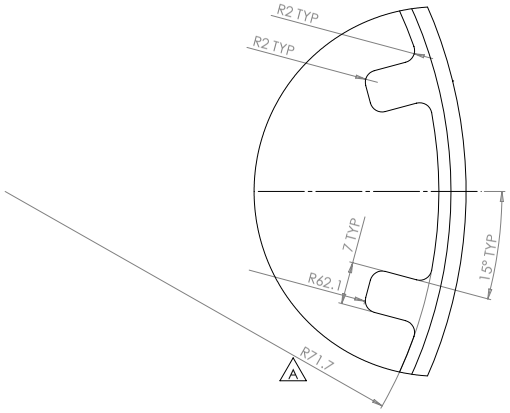

DETAIL A
SCALE 2 : 1

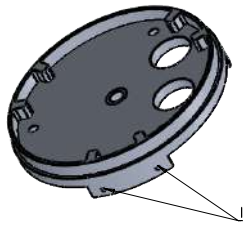

ISOMETRIC

REVISIONS				
ZONE	REV.	DESCRIPTION	DATE	APPROVED
A10, E3	A	Outer diameter change from 152.4 to 147.4 mm	15/05/2021	Yes
D9, G11, G8	B	Holes changed from 8mm to 6.5mm	15/05/2021	Yes

UNLESS OTHERWISE SPECIFIED: DIMENSIONS ARE IN MILLIMETERS SURFACE FINISH: TOLERANCES: LINEAR: +/- 0.1 ANGULAR: +/- 0.5
FINISH:
DEBURR AND BREAK SHARP EDGES
DO NOT SCALE DRAWING
REVISION B

endeavour

	NAME	SIGNATURE	DATE
DRAWN	JO SHEPTON		05/04/21
CHK'D	JAIME WHITE		05/04/21
APP'V'D	LUIS JAVIER VARGAS		15/05/21
MFG			
Q.A			

TITLE: RECOVERY BULKHEAD
MATERIAL: ALUMINIUM 6082-T6
DWG NO. D2 - 401
A2
WEIGHT: 418.3 g
SCALE:1:1
SHEET 1 OF 1

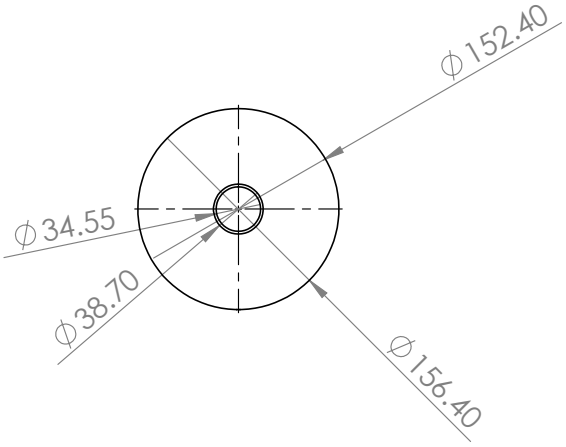

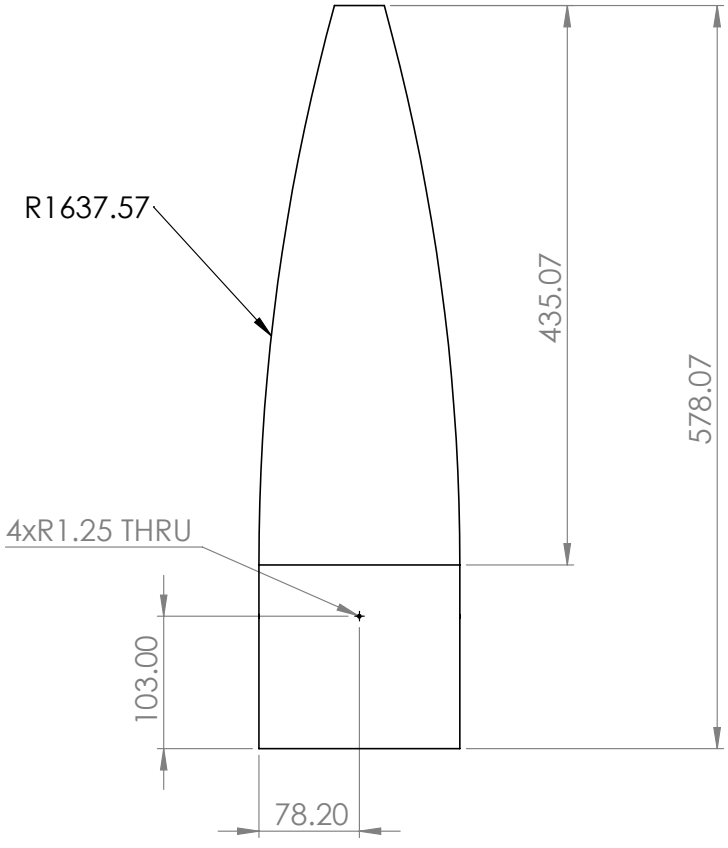

		DIMENSIONS ARE IN MILIMMETERS TOLERANCES: ±0.125MM FRACTIONAL ± ANGULAR: MACH ± BEND ± TWO PLACE DECIMAL ± THREE PLACE DECIMAL ±		NAME	DATE
			DRAWN	BCM	
			CHECKED		
			ENG APPR.		
			MFG APPR.		
		MATERIAL GFRP	Q.A.		
			COMMENTS:		
NEXT ASSY	USED ON	FINISH			
APPLICATION		DO NOT SCALE DRAWING			

ENDEAVOUR

Nose Cone

SIZE	DWG. NO.	REV.
A	D2-501 Nose Cone	A
SCALE:1:5	WEIGHT:	SHEET 1 OF 1

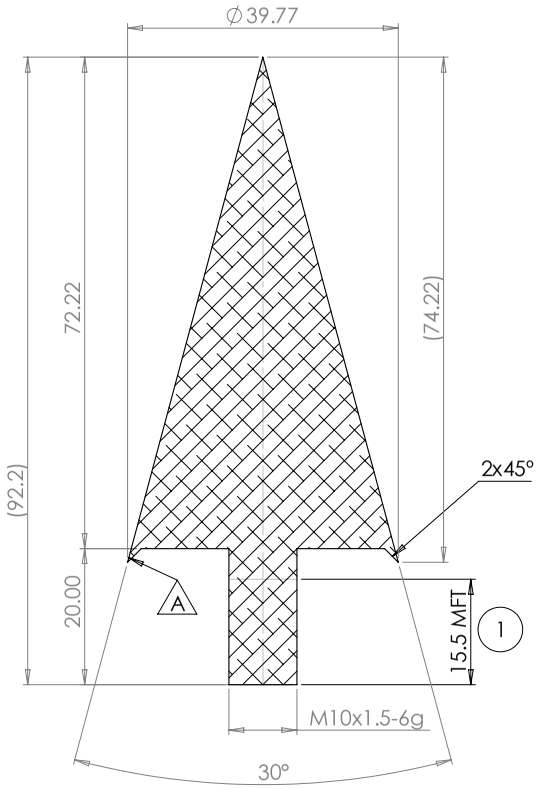

SECTION A-A

1 MINIMUN FULL THREAD

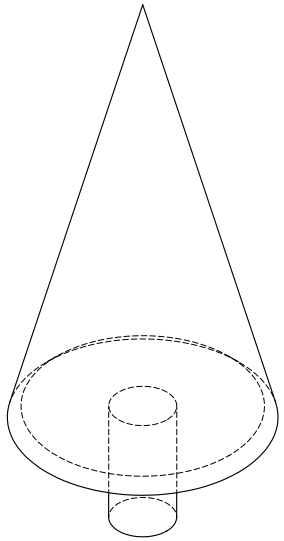

ISOMETRIC

REVISIONS				
ZONE	REV.	DESCRIPTION	DATE	APPROVED
D7	A	2x45° internal flange added	18/05/2021	Yes

UNLESS OTHERWISE SPECIFIED: DIMENSIONS ARE IN MILLIMETERS SURFACE FINISH: TOLERANCES: LINEAR: +/-0.1 ANGULAR:+/-0.5°		FINISH:		DEBURR AND BREAK SHARP EDGES	DO NOT SCALE DRAWING		REVISION A
	NAME	SIGNATURE	DATE		TITLE:		
DRAWN	ZSOLT CSONKA		22/04/21		Metal Tip		
CHK'D	ALEJANDRO VARGAS		09/05/21				
APP'V'D	JAMIE WHITE		19/05/21				
MFG							
Q.A				MATERIAL: ALUMINIUM 6082-T6	DWG NO. D2-504		A3
				WEIGHT:	SCALE:3:2	SHEET 1 OF 1	

endeavour

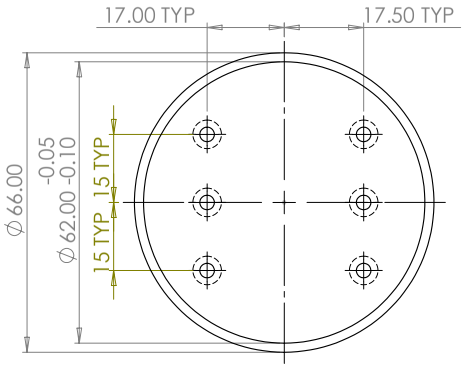

TOP

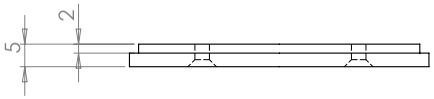

FRONT

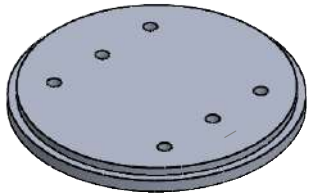

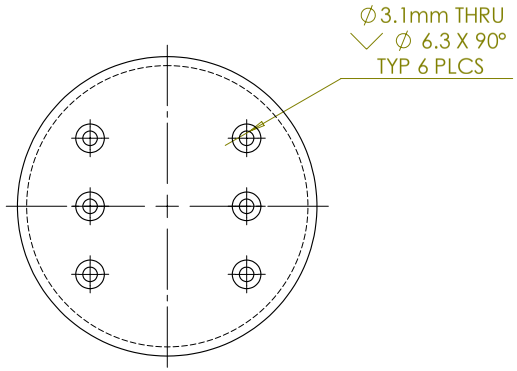

BOTTOM

UNLESS OTHERWISE SPECIFIED: DIMENSIONS ARE IN MILLIMETERS SURFACE FINISH: TOLERANCES: LINEAR: +/-0.1mm ANGULAR: +/-1 deg	FINISH:				DEBURR AND BREAK SHARP EDGES	DO NOT SCALE DRAWING / REVISION
	NAME	SIGNATURE	DATE			endeavour
DRAWN	Calum Arnott	C.A.	14.04			TITLE: PLD_Bottom_Plate
CHK'D	Alberto Pragida	A.P.	15.04			
APP'V'D						
MFG						
Q.A				MATERIAL: Alumininium 6063		DWG NO. D2-608 / A3
				WEIGHT:		SCALE:1:1 / SHEET 1 OF 1

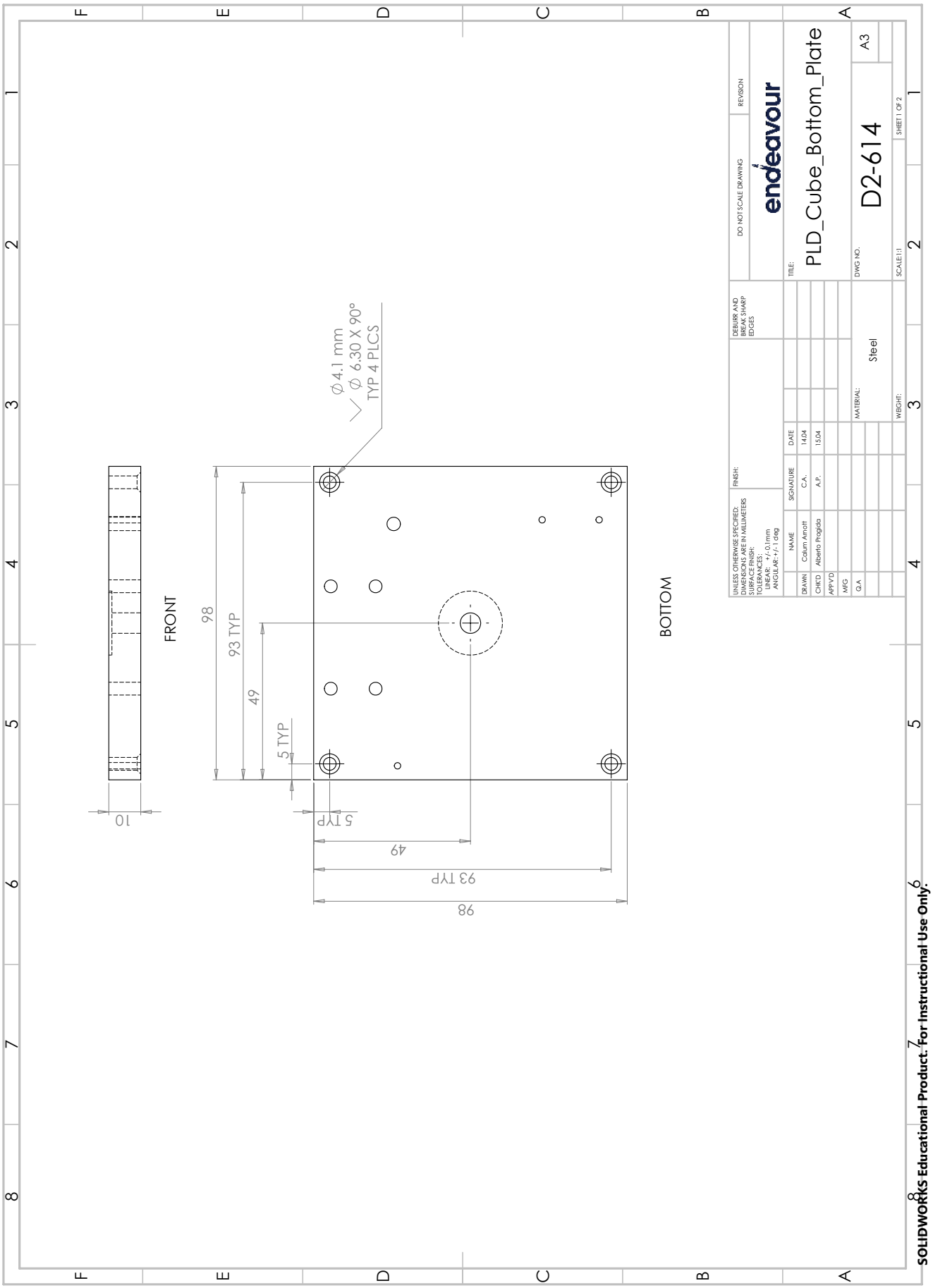

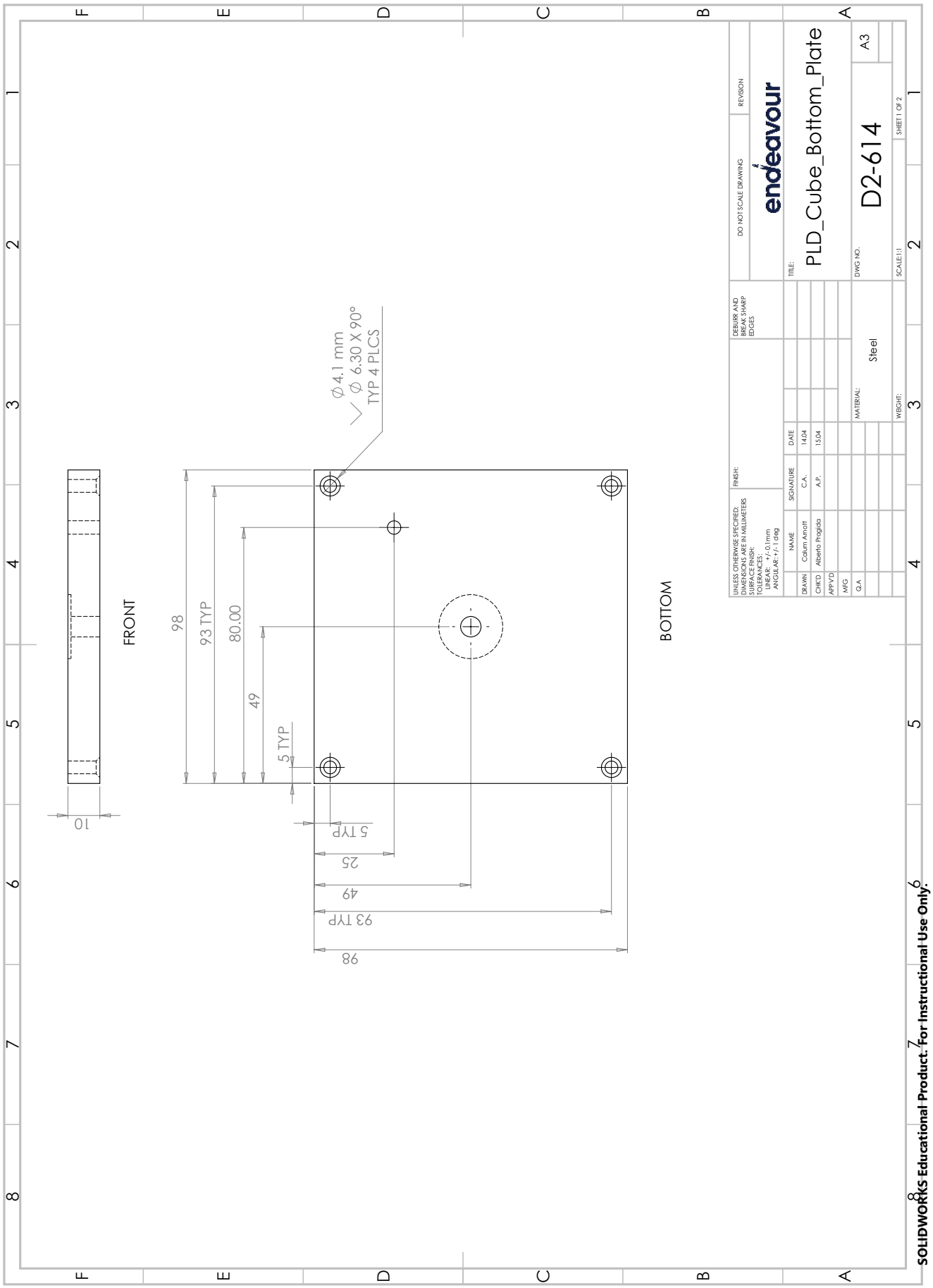

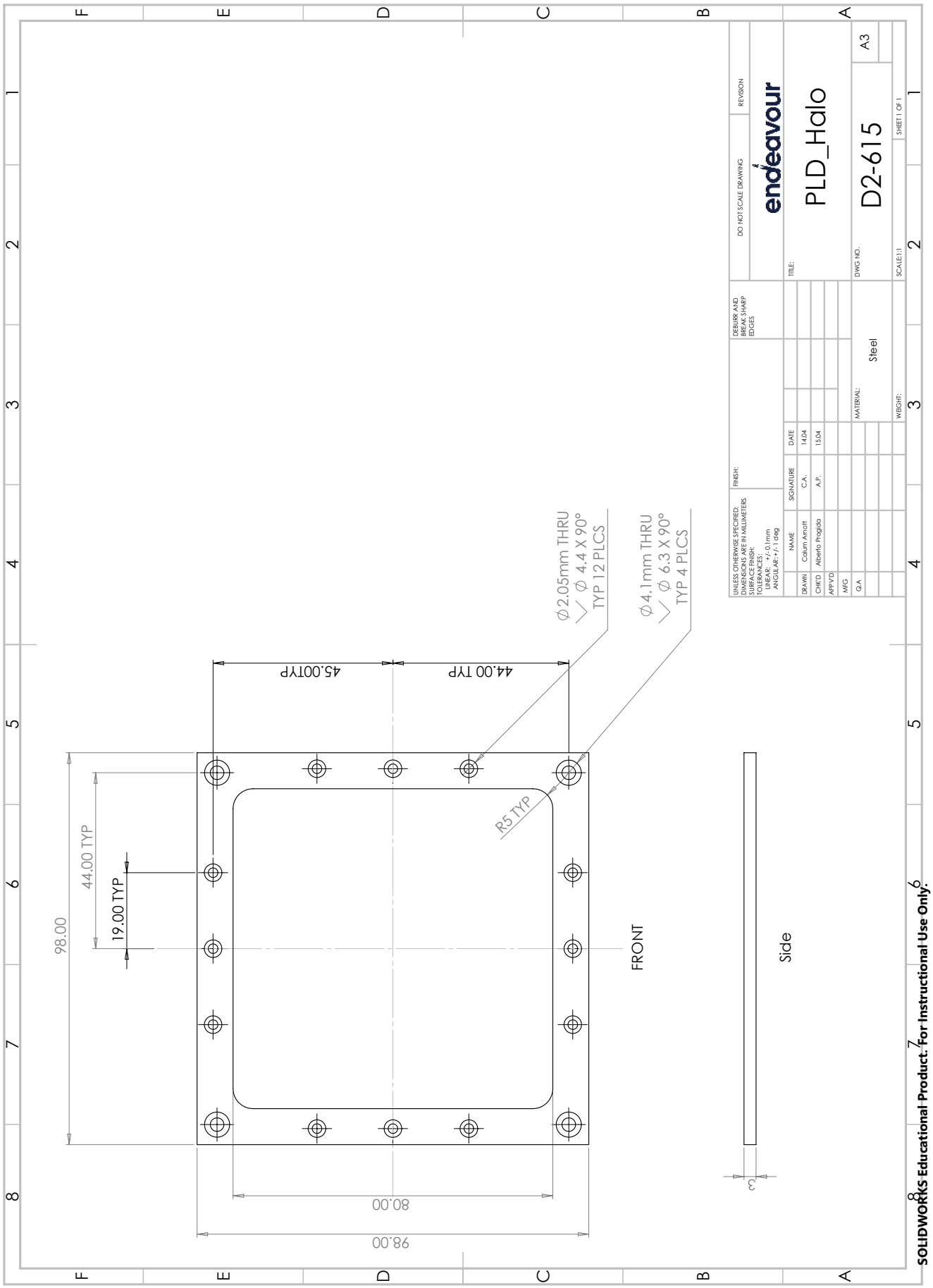

TOP

(1) 4 - OFF

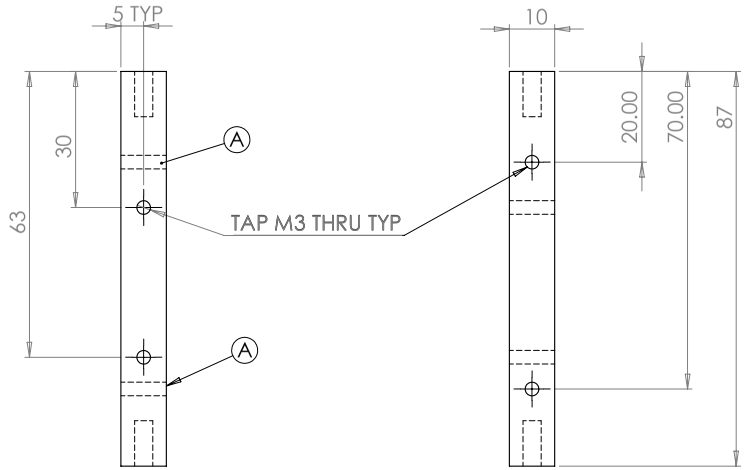

SIDE

FRONT

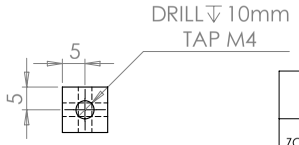

BOTTOM

REVISIONS				
ZONE	REV.	DESCRIPTION	DATE	APPROVED
D6, E6	A	M3 added	19/05/2021	Yes

UNLESS OTHERWISE SPECIFIED: DIMENSIONS ARE IN MILLIMETERS SURFACE FINISH: TOLERANCES: LINEAR: +/- 0.1mm ANGULAR: +/- 0.5 deg		FINISH:		DEBURR AND BREAK SHARP EDGES		DO NOT SCALE DRAWING	REVISION B A
	NAME	SIGNATURE	DATE			endeavour	
DRAWN	Alberto Progida	A.P.	29.04			TITLE: PLD_Rail	
CHK'D	Alberto Progida	A.P.	29.04				
APP'V'D	LEJANDRO VARGAS	A.V.G.	15.05				
MFG							
Q.A				MATERIAL: Steel		DWG NO. D2-616	A3
				WEIGHT:		SCALE:1:1	SHEET 1 OF 1

Note: see Sheet 2 for further hole details on FRONT view

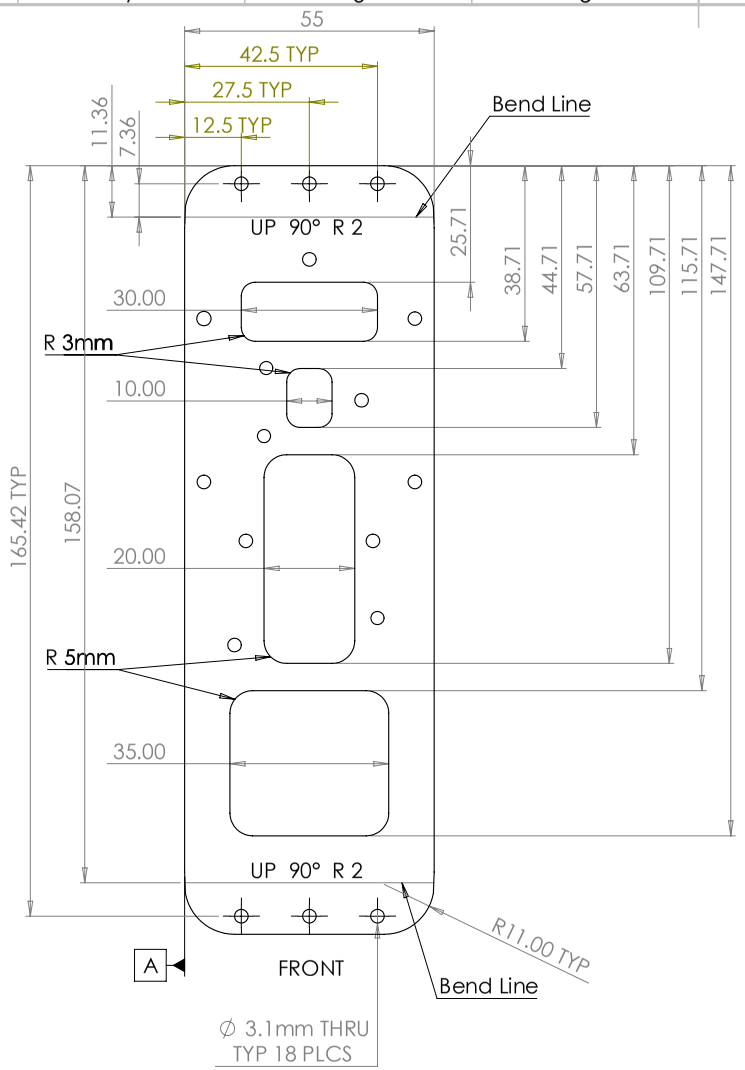

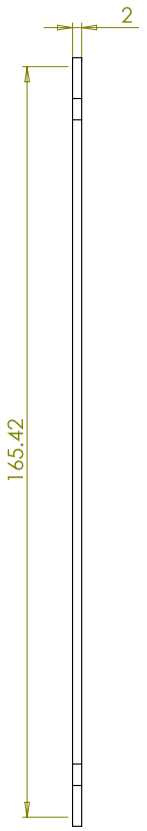

SIDE

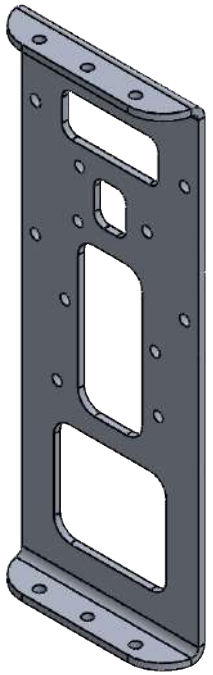

UNLESS OTHERWISE SPECIFIED: DIMENSIONS ARE IN MILLIMETERS SURFACE FINISH: TOLERANCES: LINEAR: +/- 0.1mm ANGULAR: +/- 1 deg	FINISH:				DEBURR AND BREAK SHARP EDGES	DO NOT SCALE DRAWING / REVISION
	NAME	SIGNATURE	DATE			endeavour
DRAWN	Calum Arnott	C.A.	14.04			TITLE: PLD_RASPix_Plate
CHK'D	Alberto Pragida	A.P.	15.04			
APP'V'D						
MFG						
Q.A				MATERIAL: Alumininium 6063		DWG NO. D2-607a / A3
				WEIGHT:		SCALE:1:1 / SHEET 1 OF 2

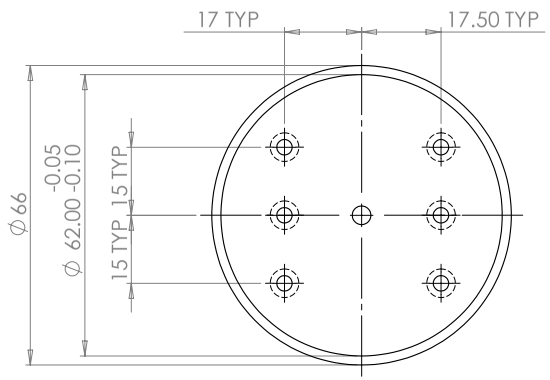

Top

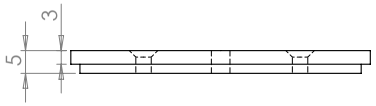

Front

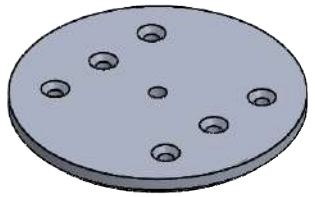

Isometric

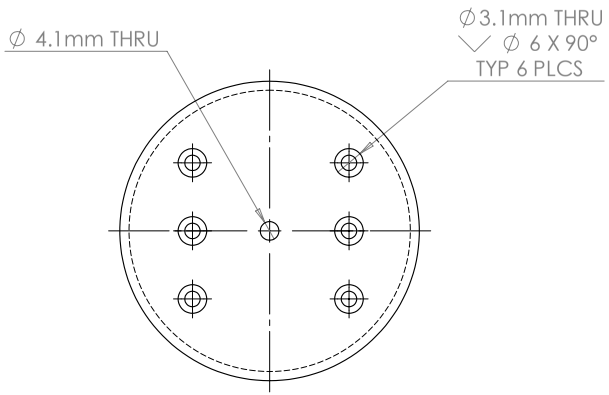

Bottom

UNLESS OTHERWISE SPECIFIED: DIMENSIONS ARE IN MILLIMETERS SURFACE FINISH: TOLERANCES: LINEAR: +/- 0.1mm ANGULAR: +/- 1 deg		FINISH:			DEBURR AND BREAK SHARP EDGES	DO NOT SCALE DRAWING / REVISION
	NAME	SIGNATURE	DATE			endeavour
DRAWN	Calum Arnott	C.A.	14.04			TITLE: PLD_Upper_Plate
CHK'D	Alberto Pragida	A.P.	15.04			
APP'V'D						
MFG						
Q.A				MATERIAL: Polycarbonate		DWG NO. D2-608b / A3
				WEIGHT:		SCALE:1:1 / SHEET 1 OF 1

G. Subsystem Details

G.1 Payload Mass Budget

CANSat Mass Budget (EuRoC Configuration)

	Component	Details	Mass (g)	Uncertainty (g)	Quantity	Total Mass (g)	Total Uncertainty (g)	Source
Electronics	Arduino Nano	Includes headers	6	± 1.0	1	6	± 1	Measured with scale (1g accuracy)
	Raspberry PI	2B	30	± 1.0	1	30	± 1	
	Detector	Raspix 2.4	59	± 1.0	1	59	± 1	
	SD Card Module	DFR0229	4	± 1.0	1	4	± 1	
	UV Sensor	Adafruit 1918						
	Pressure/Temp Sensor	Adafruit DPS310						
	Humidity/Temp Sensor	DHT22						
	TVOC/CO2 Sensor	SGP30						
	Ozone Sensor	MQ-7	2	± 1.0	1	2	± 1	
	Resistive Patch	RSPro	2	± 1.0	1	2	± 1	
Power	Battery	Energizer 6LR61	34	± 1.0	2	68	± 2	
Structure	Battery Clip	PETG	3.1	± 0.2	1	3.1	± 0.2	SolidWorks Mass Properties Database (10% uncertainty)
	Sensor Mount	PETG	9.8	± 0.5	1	9.8	± 0	
	Vertical Plates	Aluminium 6063	34.5	± 1.7	2	69	± 3	
	Bulkheads	Polycarbonate	17	± 1.0	2	34	± 1	Measured with scale (1g sensitivity)
	Outer Tube	SRBF	64	± 1.0	1	64	± 1	
	Eye Nut	M3 - Stainless Steel	7	± 1.0	1	7	± 1.0	
	Bolt + Washer	M3x12mm - SS						
Misc.	Fasteners (Bolts)	M3x10mm - SS	0.8	(-)	22	17.6	(-)	Datasheets
	Fastners (Nuts)	M3 Nylock	0.3	(-)	22	6.6	(-)	

Total Mass (g)	382.1	± 15.1

High End Estimate (g)	397.20
Low End Estimate (g)	367.01

Figure G.1: CANSat Section Mass

CUBESat Mass Budget (EuRoC Configuration)

	Component	Details	Mass (g)	Uncertainty (g)	Quantity	Total Mass (g)	Total Uncertainty (g)	Source
Electronics	Teensy 4.0	Includes headers	3	± 1.0	1	3	± 1	Measured with scale (1g accuracy)
	EasyMini	COTS flight Computer	6.5		1	6.5	± 1	
	Pressure Sensor	BMP388	59		1	59	± 1	
	Transceiver	RFM95W	5		1	5	± 1	
	GPS Receiver	Adafruit Ultimate GPS	3		1	3	± 1	
	Antenna	RSPro Stock Rubber Point	10		1	10	± 1	
	SMA Extension	150mm	5		1	5	± 1	
	PCB	1.6mm FR4 Construction	3		1	3	± 1	
	Passive Components	Capacitors, Terminal Blocks, Resistors	3		1	3	± 1	
Power	Battery	Energizer 6LR61	34	± 1.0	3	102	± 3	
Structure	Battery Holder	Printed ABS	15	± 0.8	1	15	± 0.8	SolidWorks Mass Properties Database (5% uncertainty)
	Antenna Holder	Printed ABS	12	± 0.6				
	Structure	Upper and Lower Bulkheads, Vertical Struts	634	± 31.7	1	634	± 32	
	Side Panels	GFRP	26	± 1.3	4	104	± 5	
	Recvery Bay	GFRP monocoque	96	± 4.8	2	192	± 1	
	Eye Nut	M6, Stainless Steel	15	± 0.8	1	15	± 1	
	Eye Nut	M4, Stainless Steel	7	± 0.4	1	7	± 0	
Recovery	Quicklinks and Swivels	Stainless Steel	15	± 3.0	2	30	± 6	Measured with scales (1g accuracy)
	Shock Cords	3/8" Nylon	10	± 1.0	2	20	± 2	
	L2 Tender Descender	Aluminium 6063	52	± 1.0	1	52	± 1	
	Deployment Bag	Neoprene	20	± 1.0	1	20	± 1	
	Main Chute	Rip-Stop Nylon	60	± 1.0	1	60	± 1	
	Drogue Chute	Rip-Stop Nylon	21	± 1.0	1	21	± 1	
Misc.	Fasteners (Bolts)	CSK M4x20, M4x20, M2x10, M6x25, M3x10, M2x8, M4x10	0.8	(-)	49	39.2	(-)	Datasheets
	Fastners (Nuts)	M3 Nylock	0.3	(-)	24	7.2	(-)	
					Total Mass (g)	1415.9	± 63.8	
				High End Estimate (g)		1,479.65		
				Low End Estimate (g)		1,352.15		

Figure G.2: CUBESat Section Mass

H. Detailed Structural and Mechanical Calculation

During the calculation of the expected loading on the rocket's airframe, described in Section 2.3.3 Darwin II was split into a number of body elements, along the length of which the axial and shear forces, and bending moments were to be calculated. Table H.1 provides more detail on the exact values used in the calculation of these forces, where C_D is drag coefficient and C_N is normal force coefficient.

Table H.1: Structural system data of Darwin II.

Parameter	**Body station**	**Value**	**Units**
Nose cone	Length	0.55	m
	Mass	1.05	kg
	C_D	0.03	-
	C_N	0.08	-
Recovery bay	Length	0.38	m
	Mass	7.4	kg
	C_D	0.05	-
	C_N	0.02	-
Electronics bay	Length	0.31	m
	Mass	4.2	kg
	C_D	0.03	-
	C_N	0.01	-
Lower body	Length	0.81	m
	Mass	12.4	kg
	C_D	0.16	-
	C_N	0.21	-
Lower body + fins	Length	0.63	m
	Mass	7.5	kg
	C_D	0.07	-
	C_N	0.09	-

I. Detailed Software Architecture

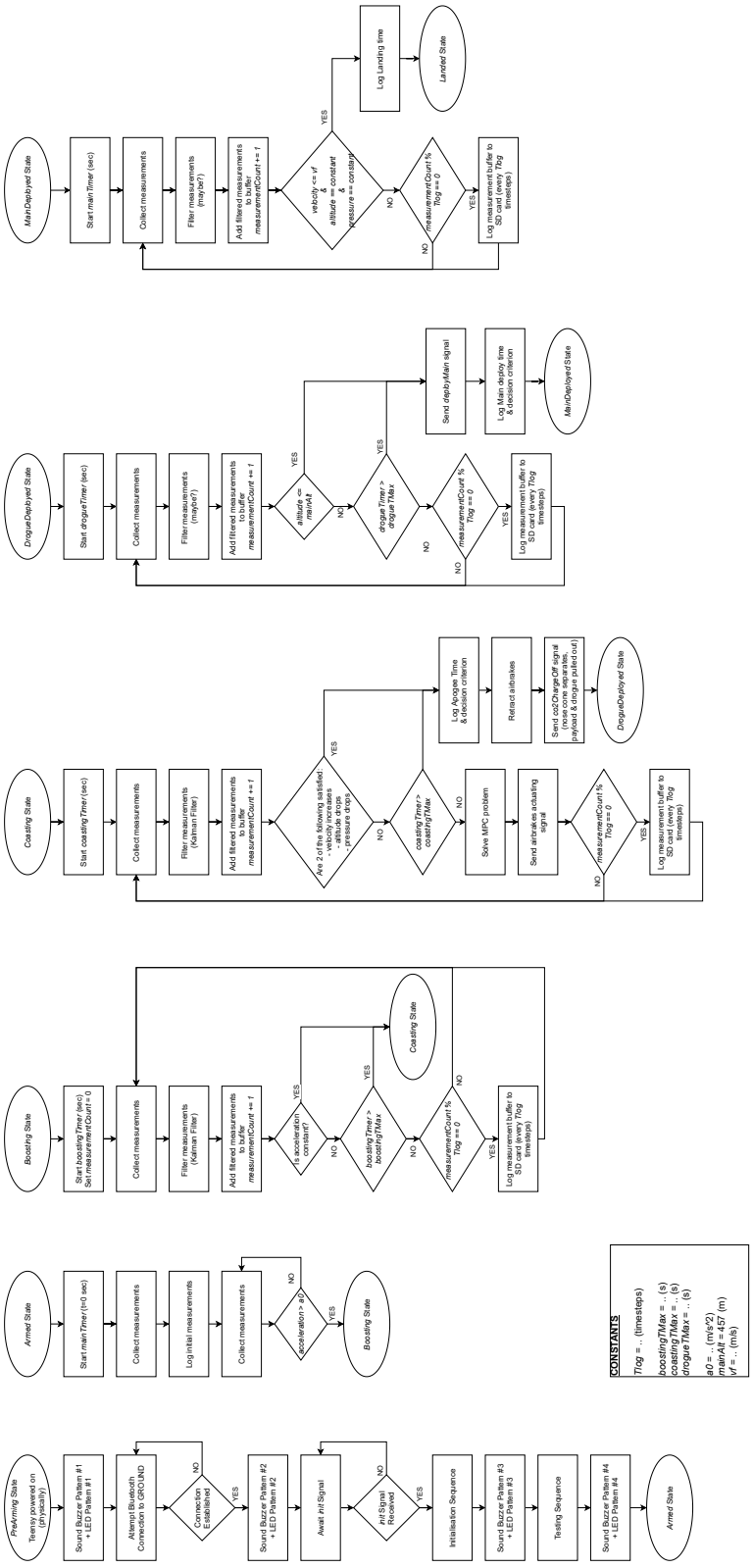

Figure I.1: Software logic for SRAD FC.

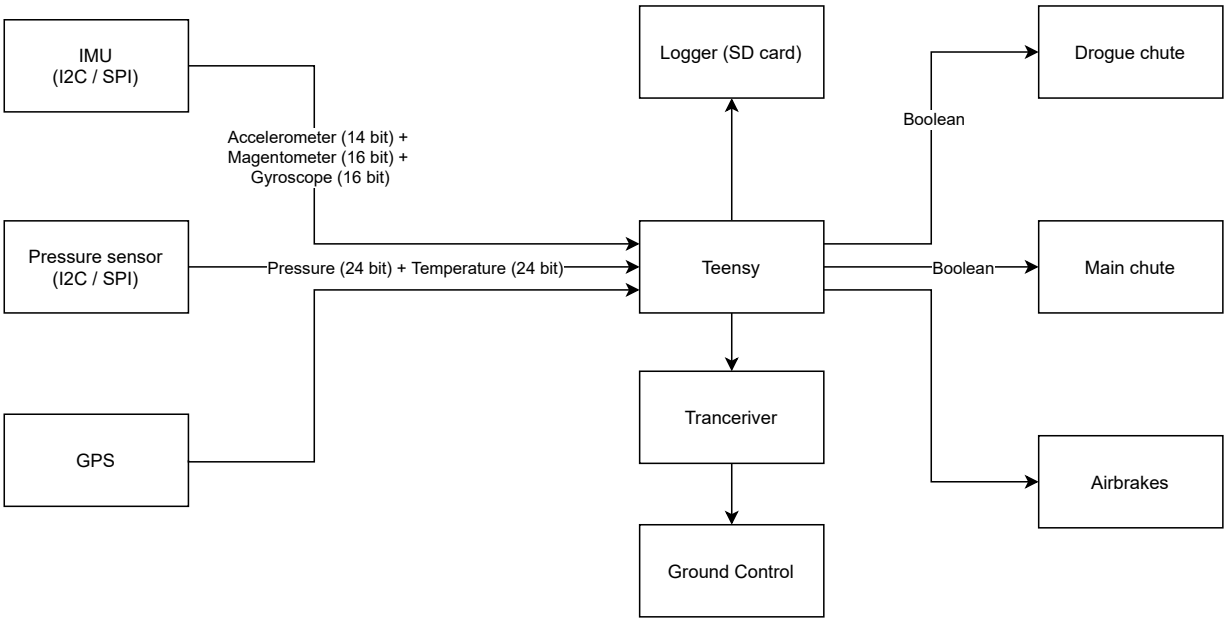

Figure I.2: DATA Flow Teensy

J. Detailed Electrical Architecture

J.1 Overview

The Darwin II FC is composed of three PCBs purposely designed with modularity and easy integration in mind. The three boards and the COTS FC are powered in parallel from the 7.4V LiPo battery power supply, which is stepped down primarily to 5V and 3.3V for its components. The COTS flight computer is completely isolated from the SRAD flight computer, and conncects in parallel with the outputs.

The following diagram demonstrates the connections between each of the PCB's:

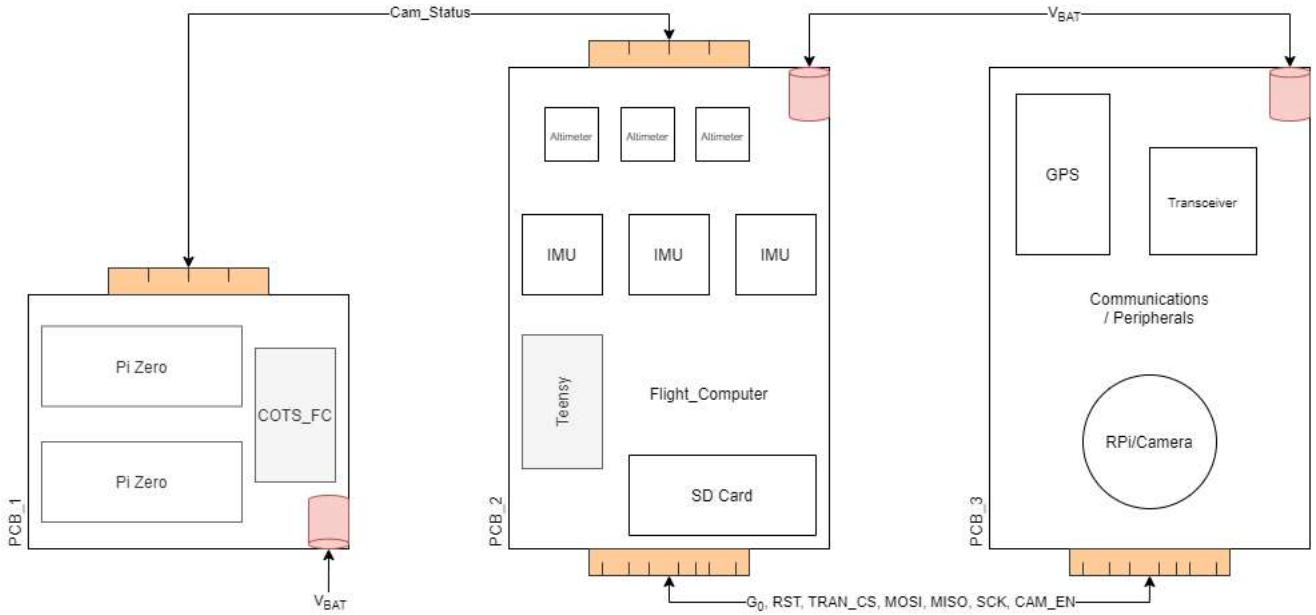

Figure J.1: PCB Integration

Processing:

Our FC is controlled by a PJRC Teensy 4.0 micro-controller situated on our 2nd PCB, the controller board (see Figure J.3). It operates on an ARM Cortex-M7 running at a maximum clock speed of 600MHz.

It contains 40 digital I/O pins, 31 of which can produce Pulse Width Modulation (PWM) outputs. These pins are are used to facilitate data flow and system control in the FC. These functions include, but are not necessarily limited to:

- Reading from our sensor modules
- Performing calculations on the data read from the sensors
- Igniting the e-matches to initiate the recovery sequence
- Rotating the servo motor to control the airbrakes system
- Transmitting the data through the transceiver module to the ground station
- Activating the camera system

- Log flight data to the on-board SD card

Communication:

In order to relay flight data from the vehicle to the ground station, our FC utilises an Adarfuit RFM96W LoRa Radio transceiver breakout situated on our telemetry board (see Figure J.4). It operates at a frequency of 434MHz, with a maximum power output of 100mW. It can achieve a range of up to 20km with the appropriate antenna and clear line-of-sight.

Our ground station utilises the same transceiver module, connected to an Arduino Uno.

For transmitting down to ground, we will be using an omni-directional antenna to maximise the transmission area. The ground station will have two antennas, the same omni-directional antenna as the FC, and a uni-directional YAGI antenna. These will be used at different stages of the rockets flight:

- From launch and until we deploy the main chute, we will use the YAGI uni-directional antenna as we can guarantee clear line-of-sight. It requires us to aim it straight at the rocket in order to maintain a strong connection.
- When the main chute has has deployed and the vehicle's descent slows, its path could vary significantly. As a result, keeping track of the rockets location will prove more difficult, hence switching to the omni-directional antenna. This means we will have an increased chance of receiving transmissions from the vehicle and this will aid in recovering it.

Measurements:

One of our FC's primary objectives is to obtain data from various sensors throughout its flight. This data is relayed to ground through the communication system described above, as well as stored on a dedicated SD card.

The following sensor modules are present on our FC, situated on the controller board (see Figure J.3):

- Sparkfun LSM9DS1 IMU breakout: contains an accelerometer, magnetometer, and gyroscope, to provide 9 degrees of freedom (DoF), measuring acceleration, angular velocity, and heading.
- Parallax MS5607 Altimeter Module: contains a barometric pressure and temperature sensor to measure altitude and temperature.
- Adafruit Ultimate GPS breakout: a GPS transceiver module that provides accurate geographical positioning outputs

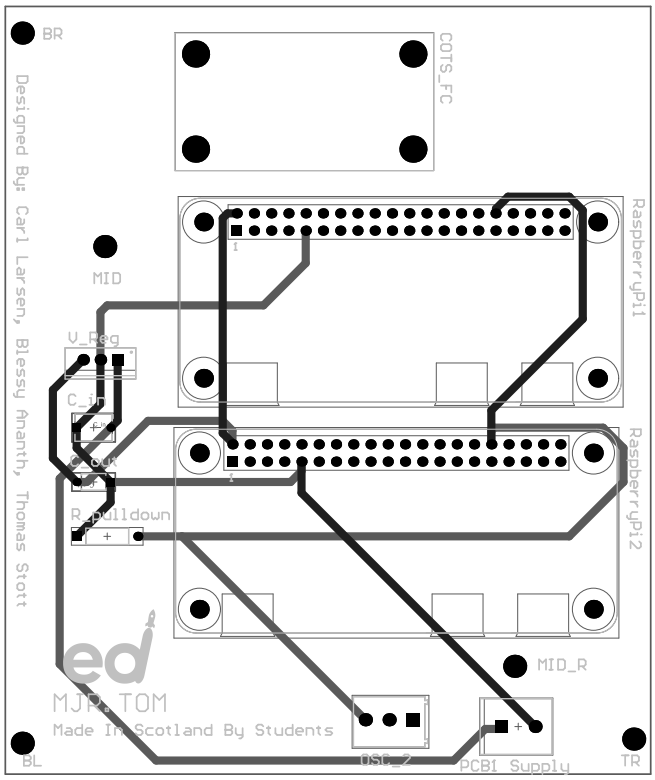

(a) PCB 1 Layout.

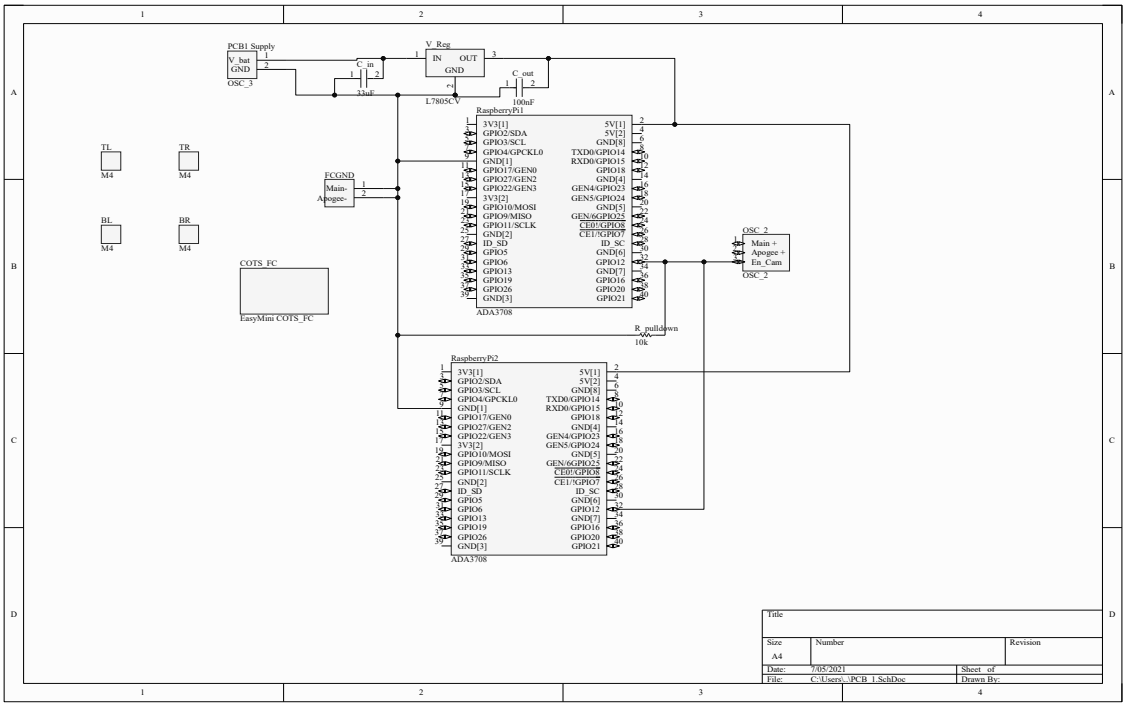

(b) PCB 1 schematic.

Figure J.2: PCB 1 - COTS FC and camera module board.

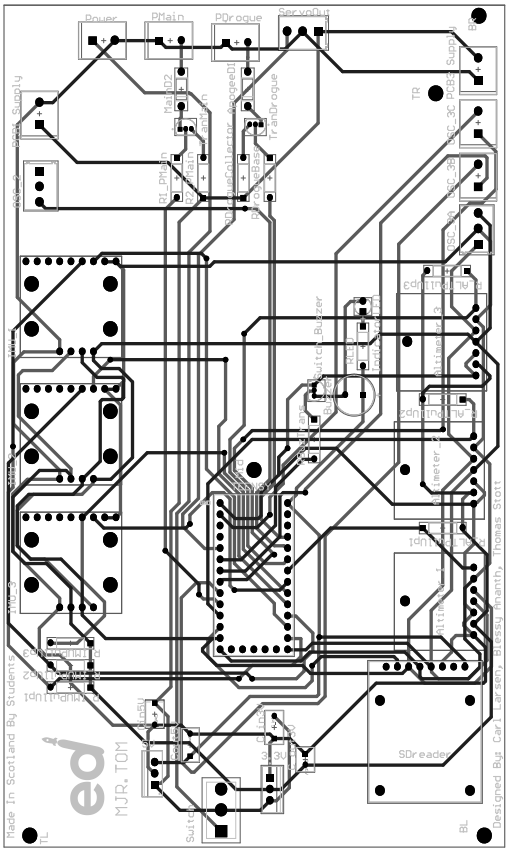

(a) PCB 2 Layout.

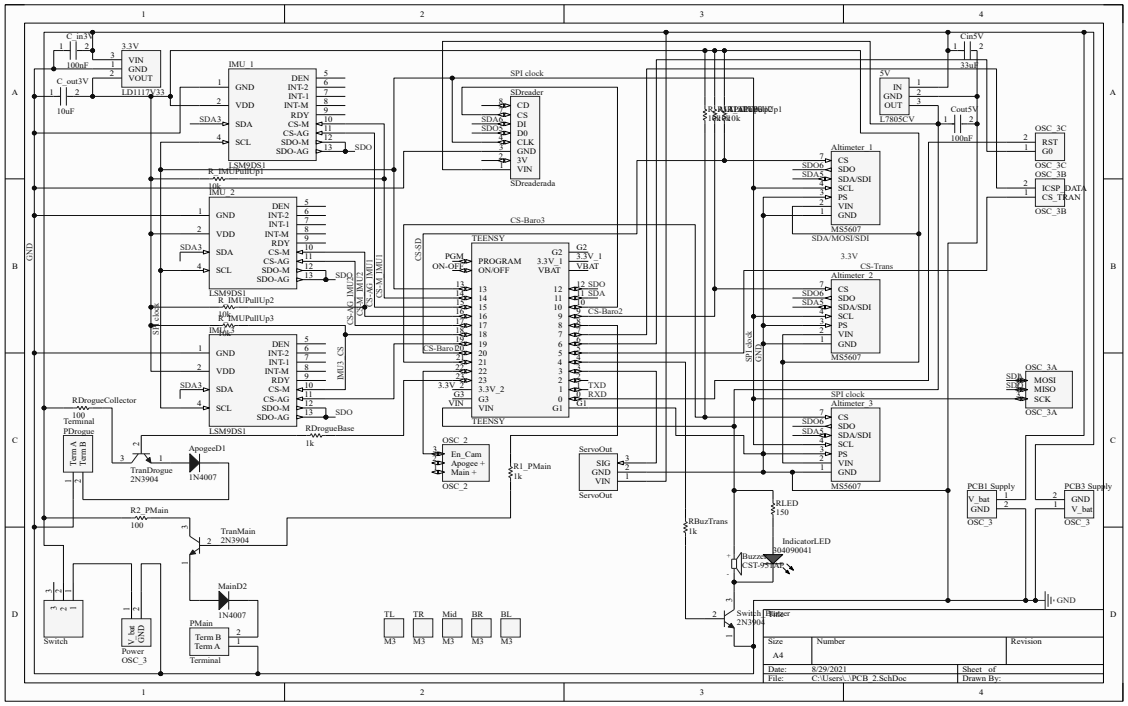

(b) PCB 2 schematic.

Figure J.3: PCB 2 - SRAD FC board with sensors, indicators, and outputs.

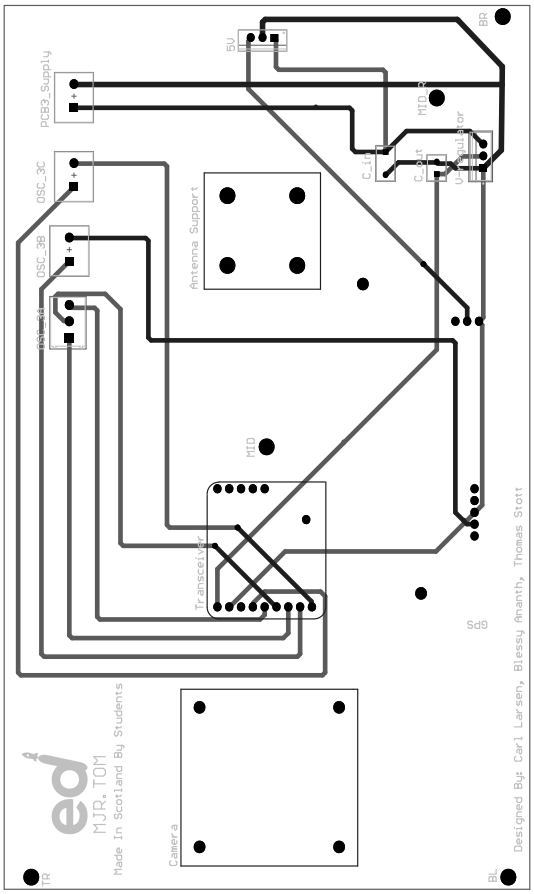

(a) PCB 3 Layout.

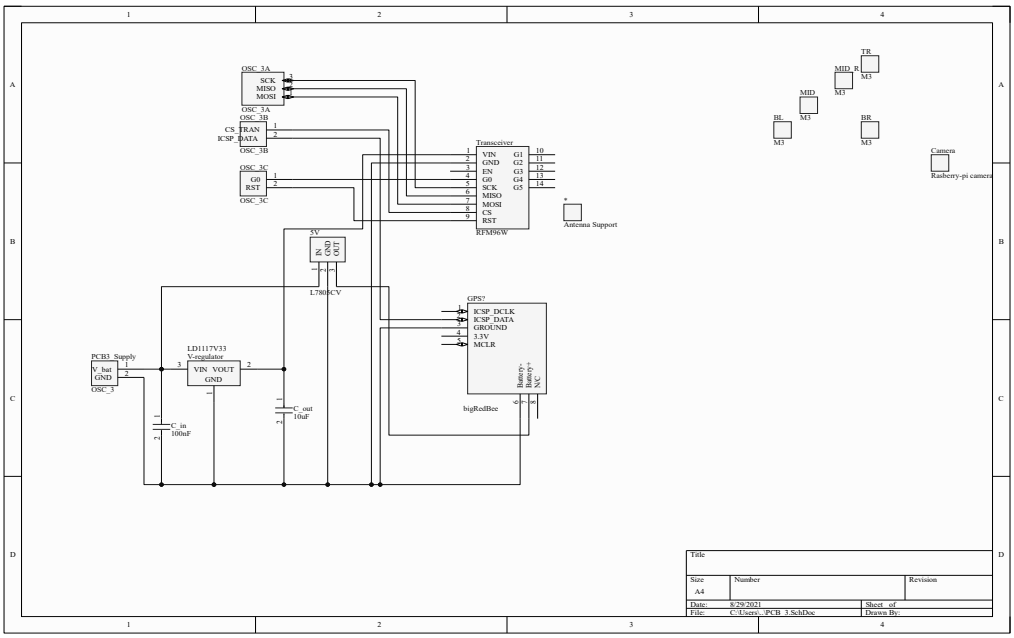

(b) PCB 3 schematic.

Figure J.4: PCB 3 - Telemetry Board.

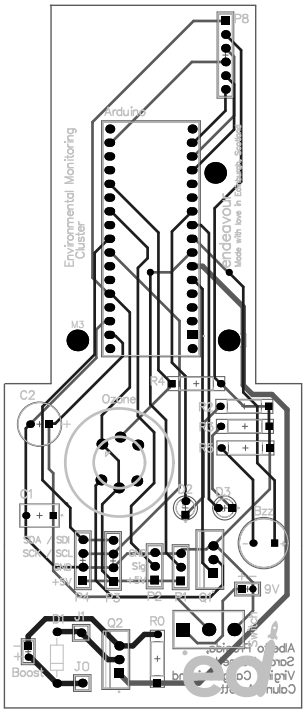

(a) EMC Layout.

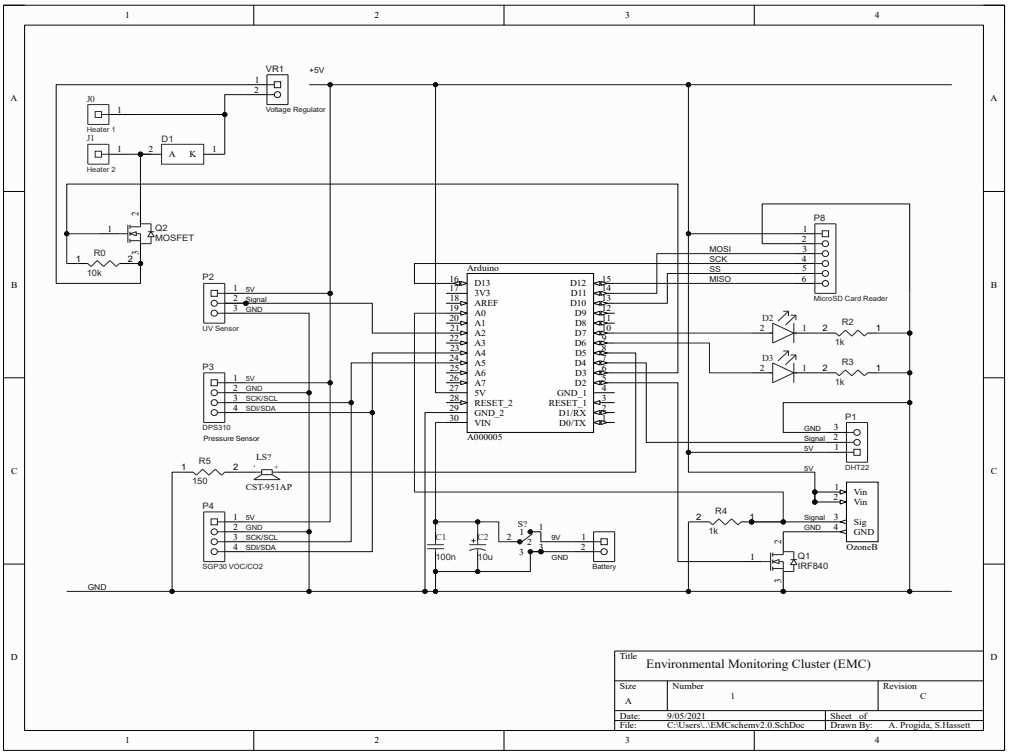

(b) EMC schematic.

Figure J.5: Environmental Monitoring Cluster

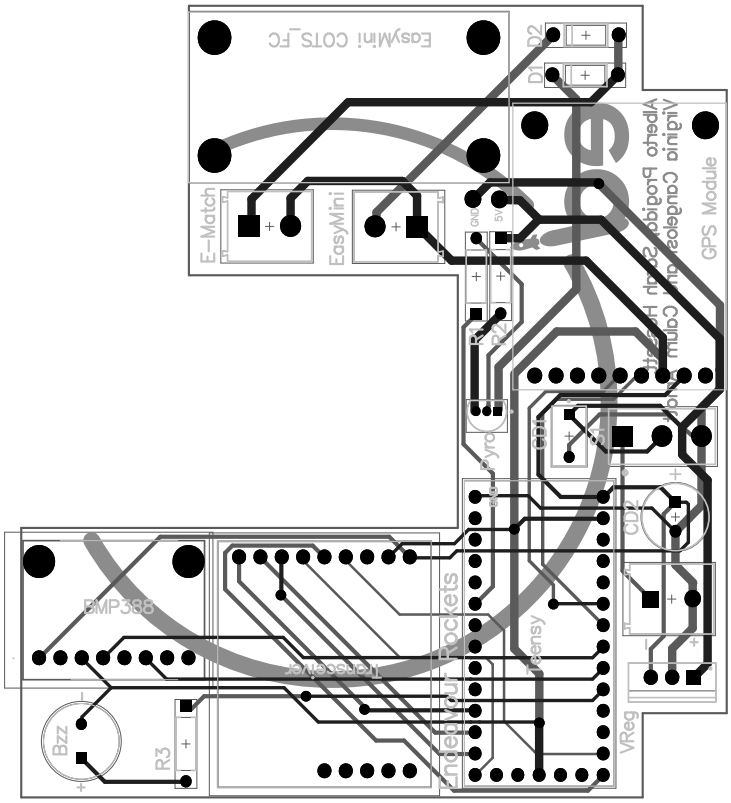

(a) PCB 3 Layout.

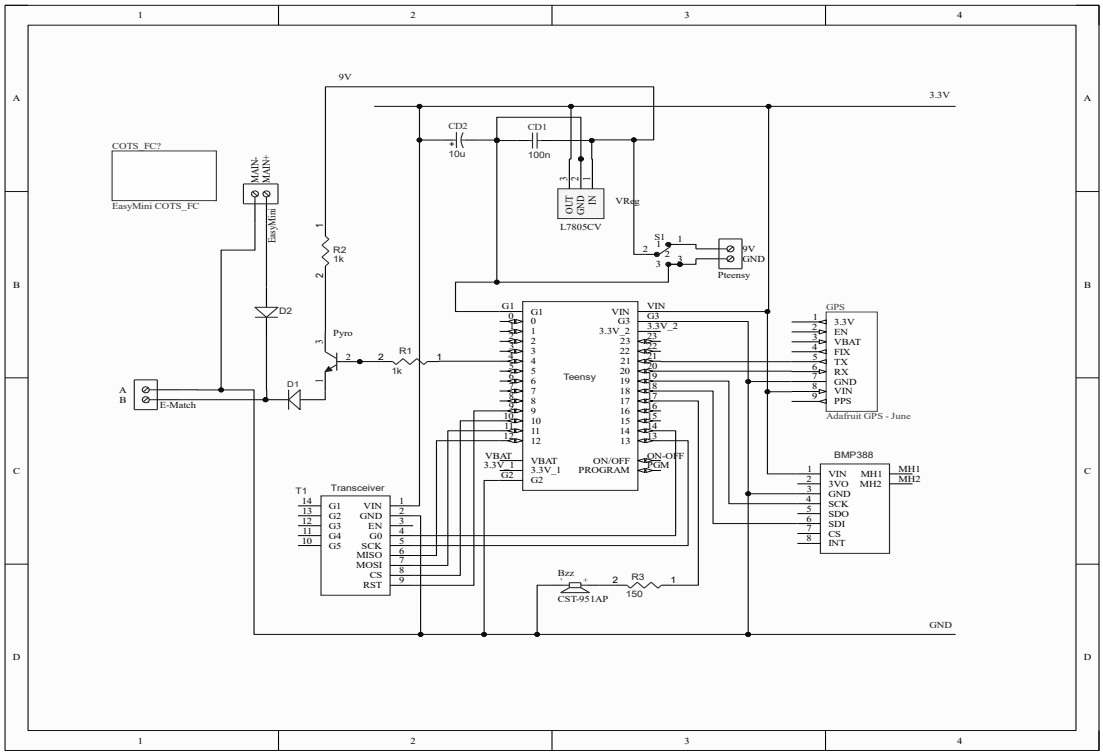

(b) PCB 3 schematic.

Figure J.6: Recovery Flight Computer